

50-280

VEPCO NOMAD CODE AND MODEL SUPPLEMENTAL INFORMATION.

Docket # 50-280
Control # 8407170305
Date 7/6/84 of Document:
REGULATORY DOCKET FILE

— NOTICE —

THE ATTACHED FILES ARE OFFICIAL RECORDS OF THE DIVISION OF DOCUMENT CONTROL. THEY HAVE BEEN CHARGED TO YOU FOR A LIMITED TIME PERIOD AND MUST BE RETURNED TO THE RECORDS FACILITY BRANCH 016. PLEASE DO NOT SEND DOCUMENTS CHARGED OUT THROUGH THE MAIL. REMOVAL OF ANY PAGE(S) FROM DOCUMENT FOR REPRODUCTION MUST BE REFERRED TO FILE PERSONNEL.

DEADLINE RETURN DATE _____

RECORDS FACILITY BRANCH

ATTACHMENT 1

RESPONSE TO QUESTIONS AND COMMENTS ON VEPCO NOMAD CODE AND MODEL (VEP-NFE-1)

Question 1. The NOMAD model represents the fuel by 32 axial regions.

This implies an axial mesh spacing of more than 11 cm which is large for an explicit 2-group, finite difference code, particularly in light of studies of the dependence of finite difference generated results to mesh spacing.

Response

VEPCO has found that 32 axial regions provide axial mesh spacing which is sufficiently small to yield consistently accurate results with NOMAD. NOMAD uses mesh points between each axial region during an inner iteration solution of Equation (2.1-5), and then solves for the flux at the center of each axial region using Equation (2.1-11). In effect, NOMAD uses twice as many mesh points as axial regions to solve for the flux and power distributions.

To demonstrate the accuracy of the 32 axial region model, one of the load follow maneuvers from Section 5.6 (N1C3 Shutdown/Return to Power Case 1) was performed with the 32 axial region model and with a 64 axial region model. Figures 1.1 and 1.2 show virtually identical results for delta-I and critical boron concentration throughout the case. Figures 1.3 through 1.8 show comparisons of axial power distributions calculated at specific

timesteps during the load follow simulation. The 32 region model local power predictions are never more than 0.9% less than the 64 region model results for any of these cases.

Question 2. The treatment of rod insertions which fall between axial zone boundaries is not described nor is its adequacy.

Response

Inadvertently omitted from the NOMAD Topical Report was a section which described the NOMAD control rod model. The following description is extracted from an internal VEPCO report documenting NOMAD:

"NOMAD accounts for the control rod cross sections in the top reflector and any rodded fuel regions. NOMAD adds the control rod macroscopic cross sections to the region macroscopic cross sections. If a particular control rod bank is located at step 225 (top of fuel) or less, then the top reflector is completely rodded with respect to that bank. If the bank is positioned at a higher step, the top reflector is partially rodded, and the rod cross sections are volume-weighted by the fraction of the reflector region which is rodded."

"The code inserts each control rod bank by step (228 steps = completely withdrawn, 0 steps = completely inserted). The distance per rod step is 0.625 inches in NOMAD. The fuel region which is partially rodded (where

the tip of the control rod bank is located) is handled in the same manner as the partially rodded reflector region, by volume-weighting the rod cross sections."

"The NOMAD control rod model includes the modeling of four control banks, two shutdown banks, and one part length bank, and the capability to move all four control banks in overlap."

This method of volume-weighting the control rod cross sections for a partially rodded region is also used in other codes such as the 3-D nodal code SIMULATE.

To demonstrate the adequacy of the model for rod insertions which fall between axial region boundaries, a series of calculations were performed with the 32 axial region model and the 64 axial region model. A control rod bank was inserted to various positions, each position corresponding exactly to a mesh boundary between two axial regions in the 64 region model and to the center of an axial region in the 32 region model. The axial power distributions from these calculations are compared in Figures 2.1 through 2.5. The local power predictions from the 32 region model are never more than 1.6% less than the 64 region results.

Question 3. The functional dependency of the macroscopic cross sections on the independent variables (e.g., exposure, fuel temperature) is not described and its adequacy, therefore, cannot be determined.

Response

The functional dependency of the macroscopic cross sections on the independent variables is expressed as follows:

$$\text{SIGt} = \text{SIGtbase} + (\text{IV1} * \text{COEFt1} + \dots + \text{IVx} * \text{COEFtx})$$

where

SIGt = macroscopic cross section type t for certain set of
independent variables

SIGtbase = base macroscopic cross section type t

IVx = value of independent variable x

COEFtx = coefficient for SIGt versus independent variable x
= $\Delta \text{SIGt} / \Delta \text{IVx}$.

SIGt and COEFtx are calculated by the XSFIT and XSEXP codes at different core average burnups for the particular cycle. NOMAD uses the equation given above to calculate the macroscopic cross sections at the tabulated burnups nearest the burnup of an axial region. The code then linearly interpolates to determine the macroscopic cross section for that region.

After calculating the cross section coefficients, the XSFIT code compares the actual core average cross sections from PDQ to the cross sections obtained using the coefficients in the above equation. The difference between the actual and predicted cross sections is typically less than 0.05%.

Question 4. The use of re-edits which do not involve flux calculations for off-nominal conditions is a feature of other procedures (e.g., ARMP). However, those procedures are usually concerned with long term burnup analyses. The adequacy of this type of treatment for some of the NOMAD applications should be justified.

Response

A series of restart flux and eigenvalue calculations were performed with the PDQ07 One Zone model at one burnup step. The macroscopic cross sections obtained from these calculations were input to the XSFIT and XSEXP codes to calculate the cross section coefficients in accordance with the procedure described in Response to Question No. 3 above. The macroscopic cross sections predicted with these coefficients are compared to similar results using the normal methodology without flux re-calculations for off-nominal conditions in Figures 4.1 through 4.31. The results are virtually identical for most cases, and the maximum difference for all cases is 0.1%.

Question 5. The normalization of NOMAD to FLAME solely on the basis of flux difference and mid-plane power in the buckling search seems too limited. In addition, performing the buckling search for rodded configurations with the xenon distribution "frozen at HFP, ARO equilibrium conditions..." does not sound like the right way to do this.

Response

VEPCO's experience has been that axial offset, midplane power and critical boron are sufficient conditions for normalizing NOMAD to FLAME. This is very similar to the 1-D to 3-D normalization methods used by some vendors. Comparisons of NOMAD and FLAME axial power distributions for every burnup step of S1C7 are presented in Figures 5.1 through 5.11. The maximum difference between NOMAD and FLAME is 2.9% for these cases.

Performing the buckling search for rodded configurations with the xenon distribution "frozen at HFP, ARO equilibrium conditions..." was chosen as a simple method of maintaining consistency between computer code models and not for any theoretical reasons. However, this method is no longer employed, as explained in Response to Question No. 6 below.

Question 6. What is done vis-a-vis the buckling for intermediate rod/power configurations?

Response

The HFP, ARO buckling coefficients B0 and BTILT are automatically adjusted by NOMAD to compensate for intermediate rod/power configurations. VEPCO has found that adjusting the buckling coefficients in this manner provides excellent results compared to 3-D FLAME calculations at intermediate rod/power configurations. Figure 6.1 shows the correlation between NOMAD

and FLAME for a variety of power levels, rod insertions, and xenon conditions when this buckling adjustment is used. These cases were performed for two Surry and two North Anna cycles for the following range of conditions: BOC, MOC, and EOC burnups; 0, 25, 50, 75, and 100% power; no xenon, equilibrium xenon, and xenon frozen at HFP, equilibrium conditions; and control rods inserted from 0 to 67%. Figures 6.2 through 6.7 show the NOMAD results obtained with this new buckling adjustment for the three load follow maneuver simulations previously presented in Section 5.6 and Figures 5-33 through 5-38 of the NOMAD Topical Report. This methodology replaces the deep insertion control rod model described in the NOMAD Topical Report.

Question 7. Is the use of flux squared power sharing for 1-D/2-D synthesis justified?

Response

VEPCO uses the standard power sharing technique for performing its 1-D/2-D synthesis calculations. The flux squared sharing is a separate quantity used for importance-weighting of 2-D control rod bank worths for predicting bank worths measured by rod swap. To clarify this in the topical report, VEPCO proposes certain changes to the text. See Attachment 2, "PROPOSED TEXT CHANGES TO THE NOMAD TOPICAL REPORT".

Question 8. Possible "typos"

- a. The definition for flux difference in Equation 2.7-1 is actually the definition for axial offset.

Response

Equation 2.7-1 defining delta-I, or flux difference, is correct. Axial offset is defined as:

$$\text{Axial offset(\%)} = \text{Delta-I(\%)/PR} = \frac{\text{Power(top)} - \text{Power(bottom)}}{\text{Power(top)} + \text{Power(bottom)}} * 100.$$

- b. KappaSigf2 is dependent on xenon in Table 3-1 but NuSigf2 is not.

Response

NuSigf2 is also dependent on xenon.

- c. In terms of the strict definition of tri-diagonal matrices, only M on page 2-5 is tri-diagonal.

Response

M is the only tridiagonal matrix in the equation on page 2-5.

Question 9. Since the NOMAD model incorporates a depletion calculation, comparisons of predicted and measured axial power distributions as a function of burnup should be presented to validate the depletion model. For example, how do EOC axial power distributions compare with measurement?

Response

Figures 9.1 through 9.5 compare NOMAD predicted axial power distributions to INCORE measurements for MOC and EOC for three different cycles. The axial shapes agree very well. Using a 2.5% grid factor is conservative for 94.5% of the points between 15% and 85% of core height for these shapes.

Figures 9.7 and 9.8 compare EOC axial burnup distributions obtained with NOMAD and FLAME for two cycles. These figures confirm that the NOMAD depletion methodology is consistent with that of FLAME.

Question 10. NOMAD calculated xenon worths are compared to results obtained from the XETRN code. Since XETRN is a point kinetics code and also has not been reviewed and approved by the NRC, justify its use a reference calculation.

Response

Xenon worth results from NOMAD, XETRAN, and PDQ are compared in Figures 10.1 and 10.2. Xenon concentrations for the same cases are shown in Figures 10.3 and 10.4.

Question 11. How do the NOMAD FQ results compare with the quoted vendor results in the FAC analysis, particularly at cases which are close to the Technical Specification limit? Are any of the NOMAD results lower than the vendor results for FQ?

Response

At points close to the Technical Specification limit NOMAD results are within $\pm 1\%$ of vendor results for FQ. The results for the remainder of the core are within $\pm 1\%$ for N2C2 and $+1\%$ to -2.5% for N1C4.

Question 12. The radial buckling distribution requires that adjustments be made to account for control rod insertions. Please describe in more detail how these adjustments are made.

Response

Please see Response to Question No. 6 above.

Question 13. Describe the difference, if any, between Technical Specifications governing CAOC with the VEPCO NOMAD analysis compared to present Technical Specifications using vendor analysis.

Response

There are no differences in the Plant Technical Specifications governing CAOC operation since the VEPCO CAOC analysis is identical to the methodology documented in References 1 and 2. The only differences are the codes used by VEPCO (i.e.; PDQ, FLAME, and NOMAD).

Question 14. Describe the three cases referred to in the FAC analysis and explain how they were selected.

Response

These are identical to the three cases in the Westinghouse 3 Case FAC (CAOC) analysis as documented in Reference 1 and 3. Again there are no methodology differences only the codes used by VEPCO are different (i.e.; PDQ, FLAME, and NOMAD).

REFERENCES

1. F. M. Bordelon et al., "Westinghouse Reload Safety Evaluation Methodology", WCAP 9272, March 1978 (Proprietary).
2. T. Morita et al., "Topical Report Power Distribution Control and Load Following Procedures", WCAP 8385, September 1974 (Proprietary).
3. "Virginia Electric and Power Company, Surry Power Station, 3-Case FAC Analysis Description", John Rolin (Westinghouse) to L. M. Girvin (VEPCO); Attachment 1, "Justification of Peaking Factor Subcase Analysis".

FIGURE 1.1

N1C3 SHUTDOWN/RETURN TO POWER (CASE 1) DELTA-I

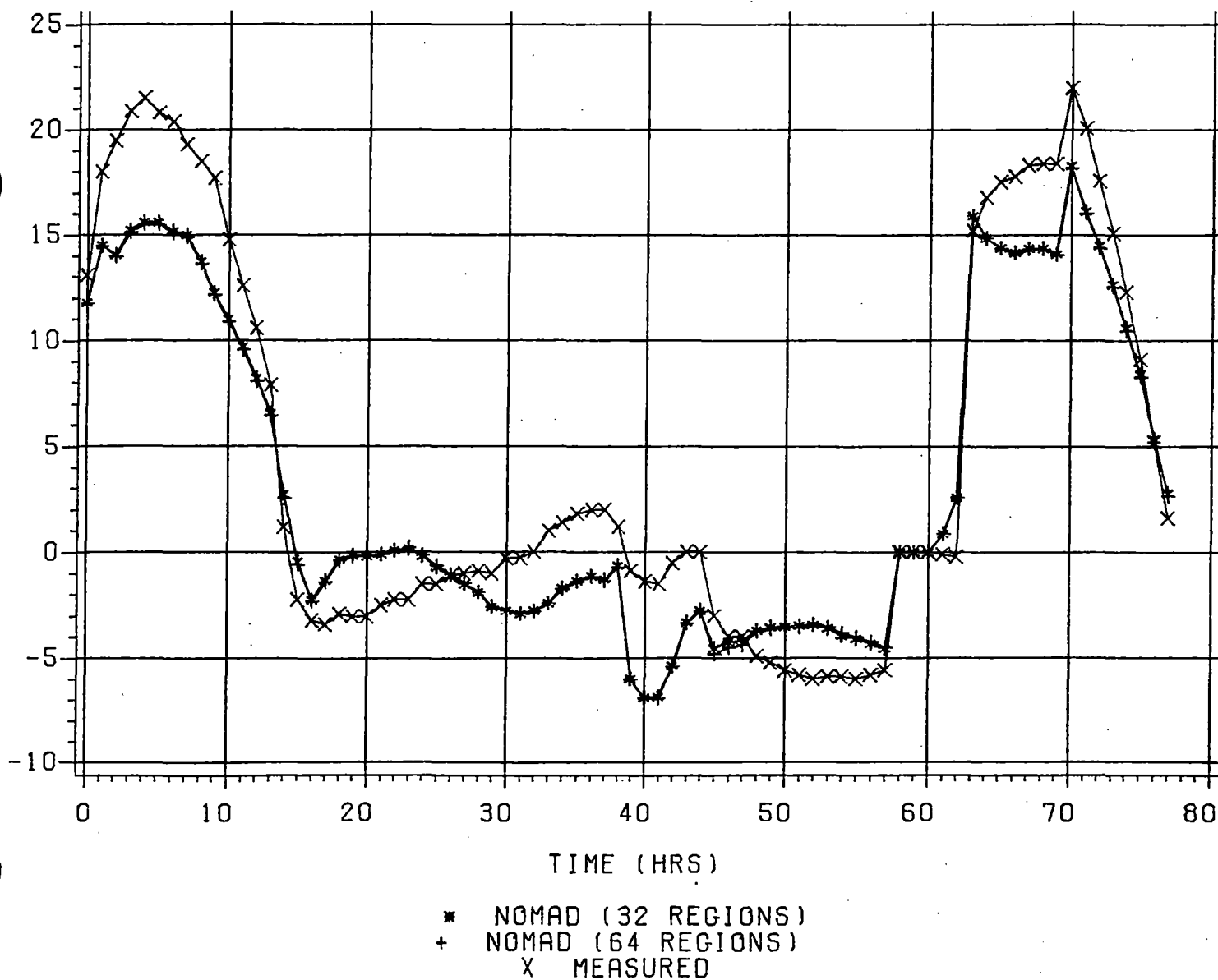


FIGURE 1.2

N1C3 SHUTDOWN/RETURN TO POWER (CASE 1) CRITICAL BORON CONCENTRATION

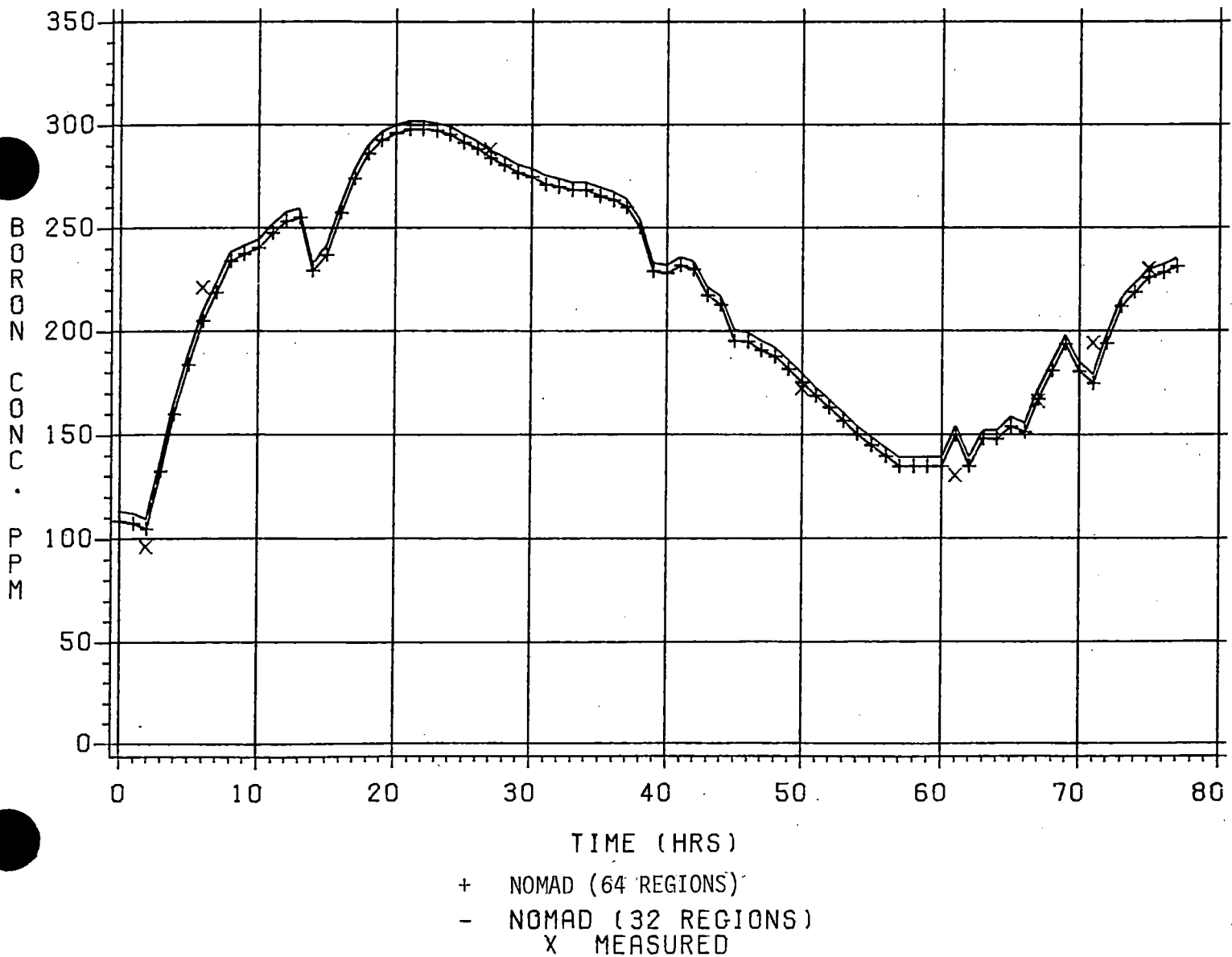


FIGURE 1.3

AXIAL POWER COMPARISON

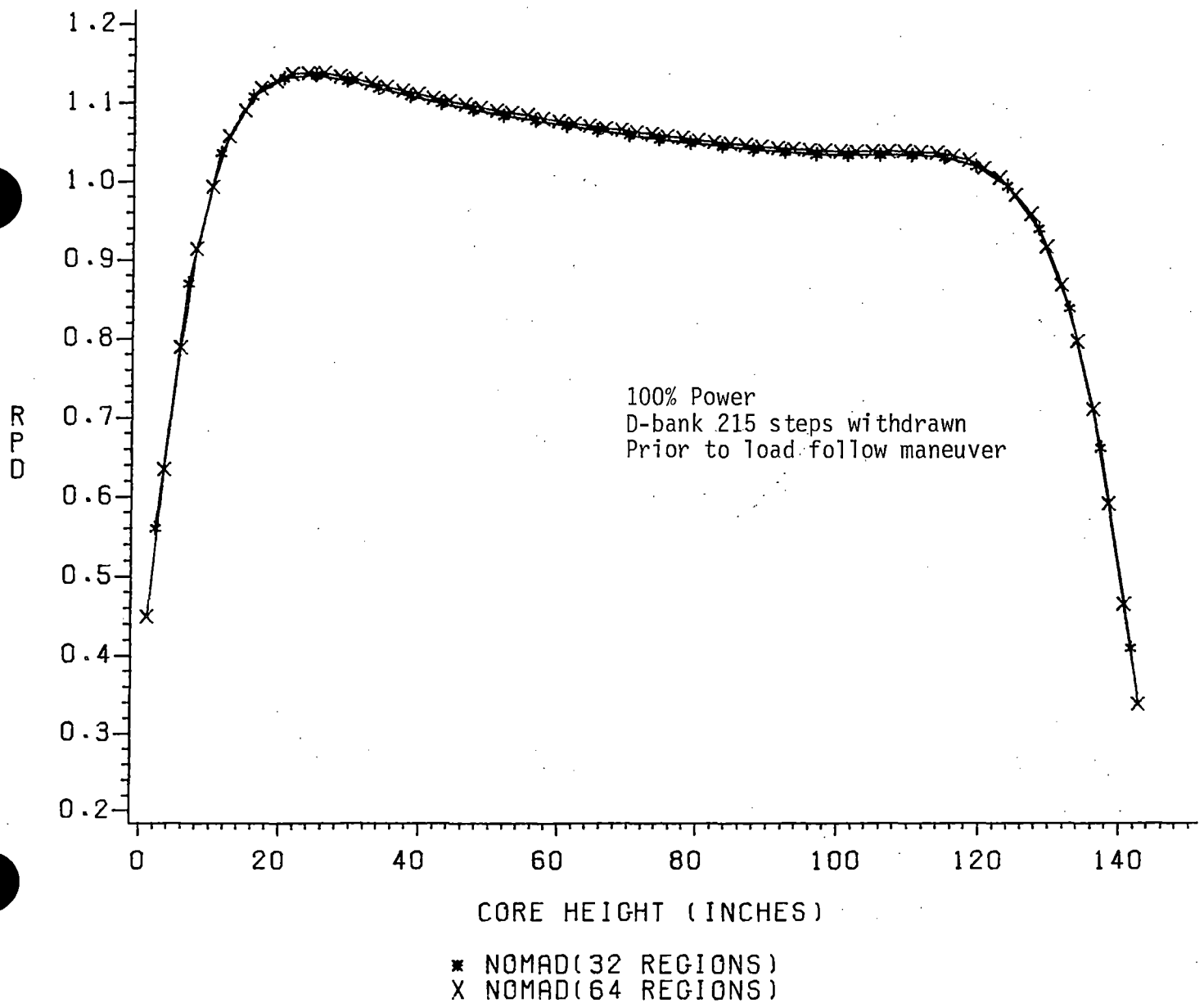


FIGURE 1.4

AXIAL POWER COMPARISON

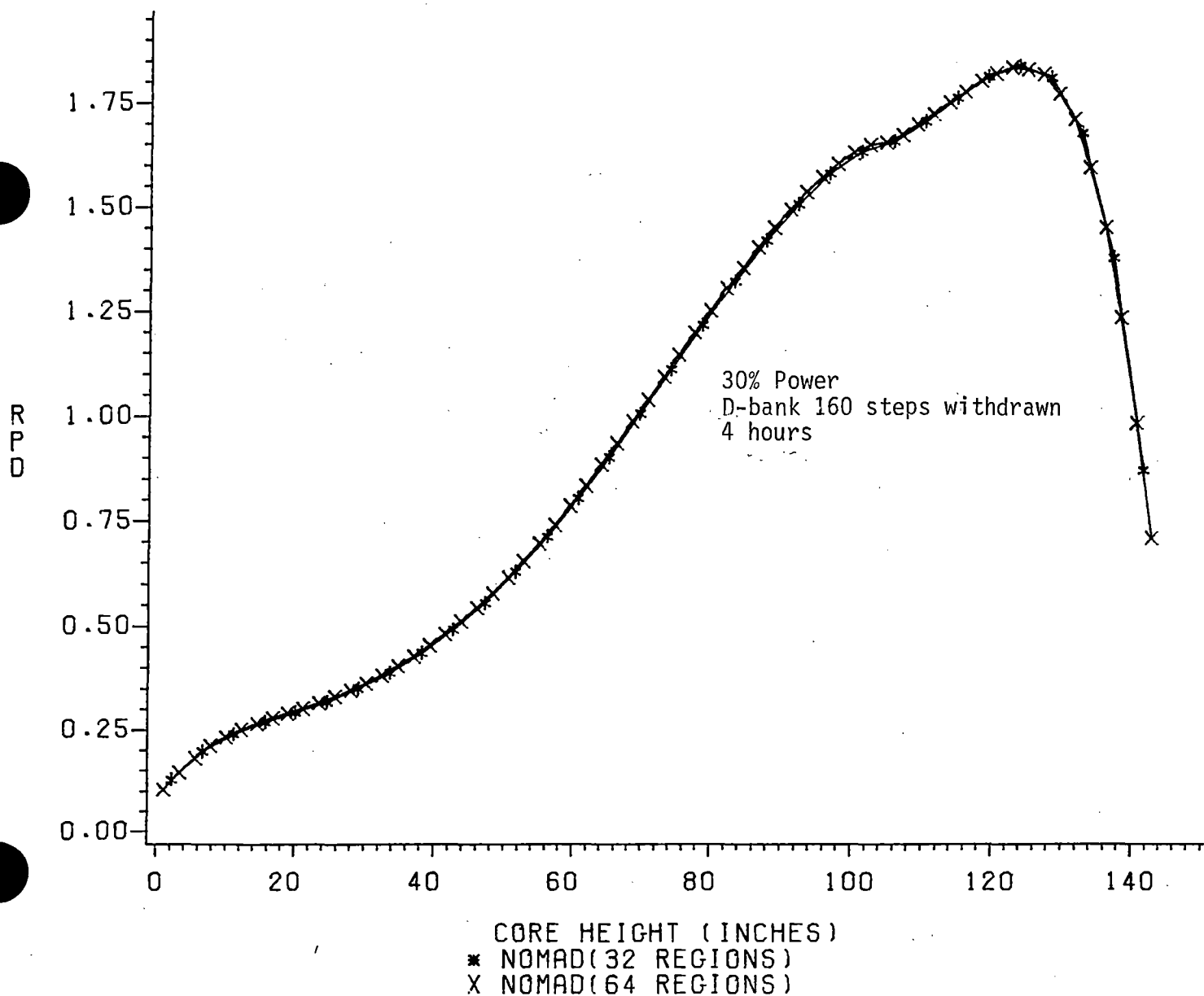


FIGURE 1.5

AXIAL POWER COMPARISON

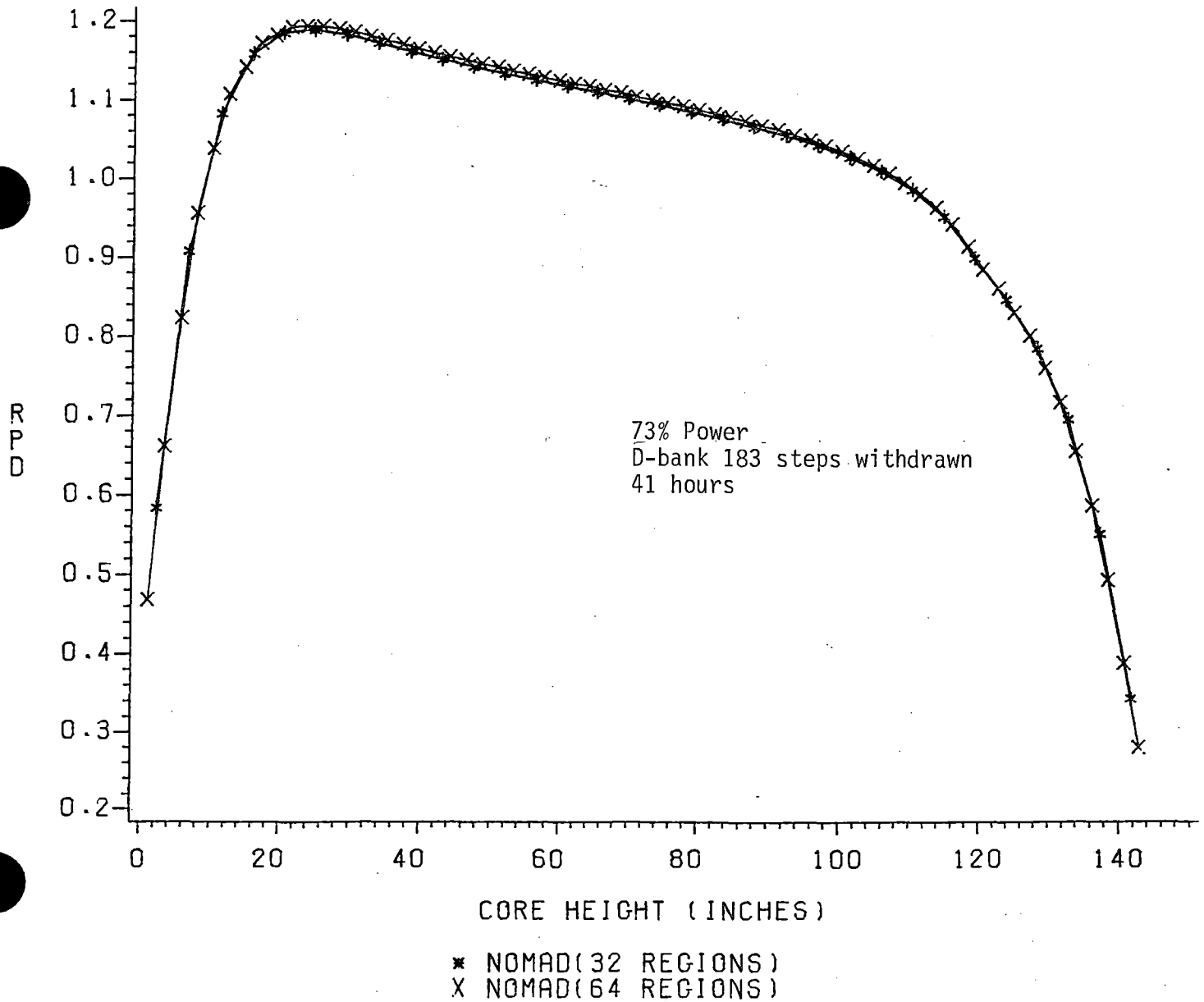
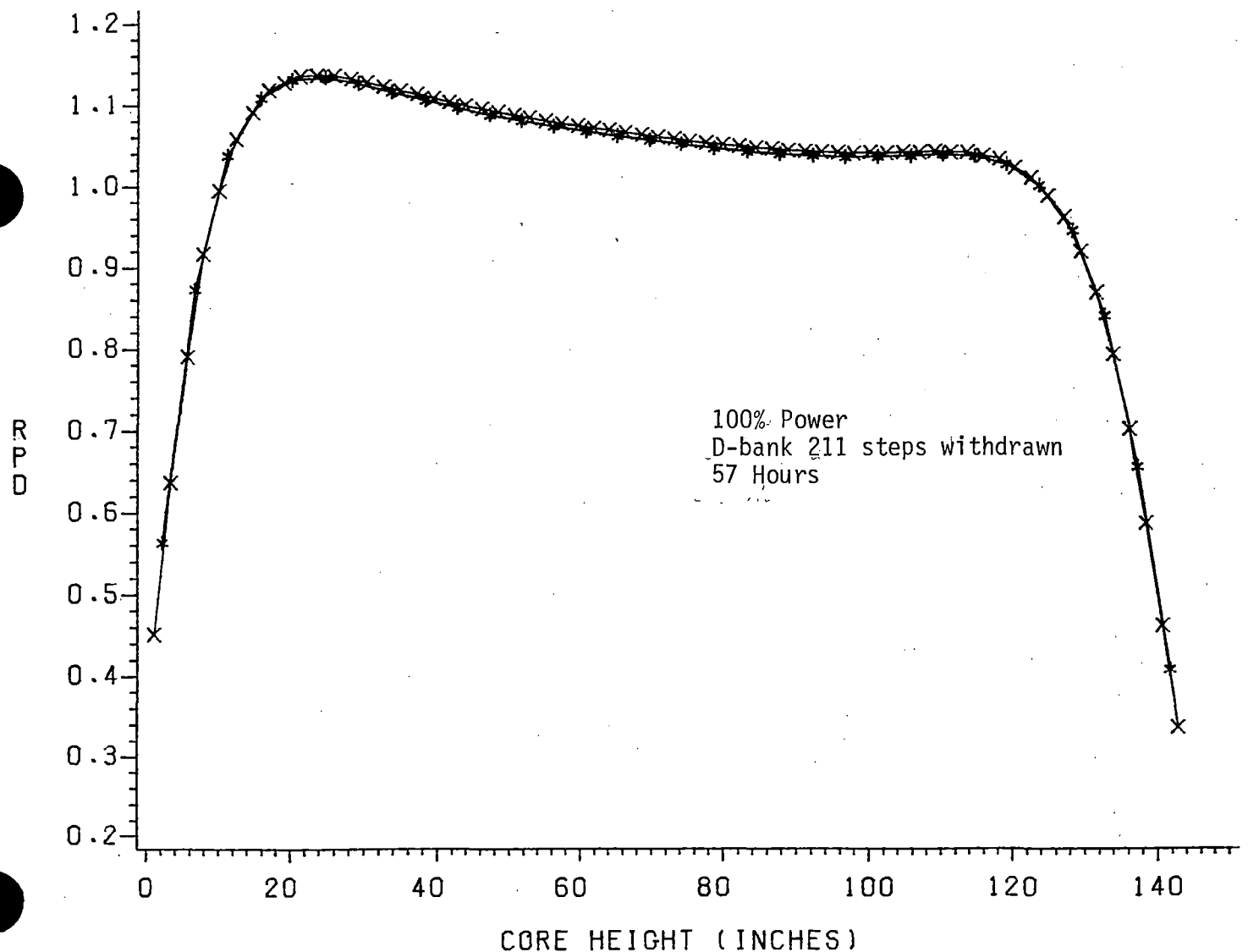


FIGURE 1.6

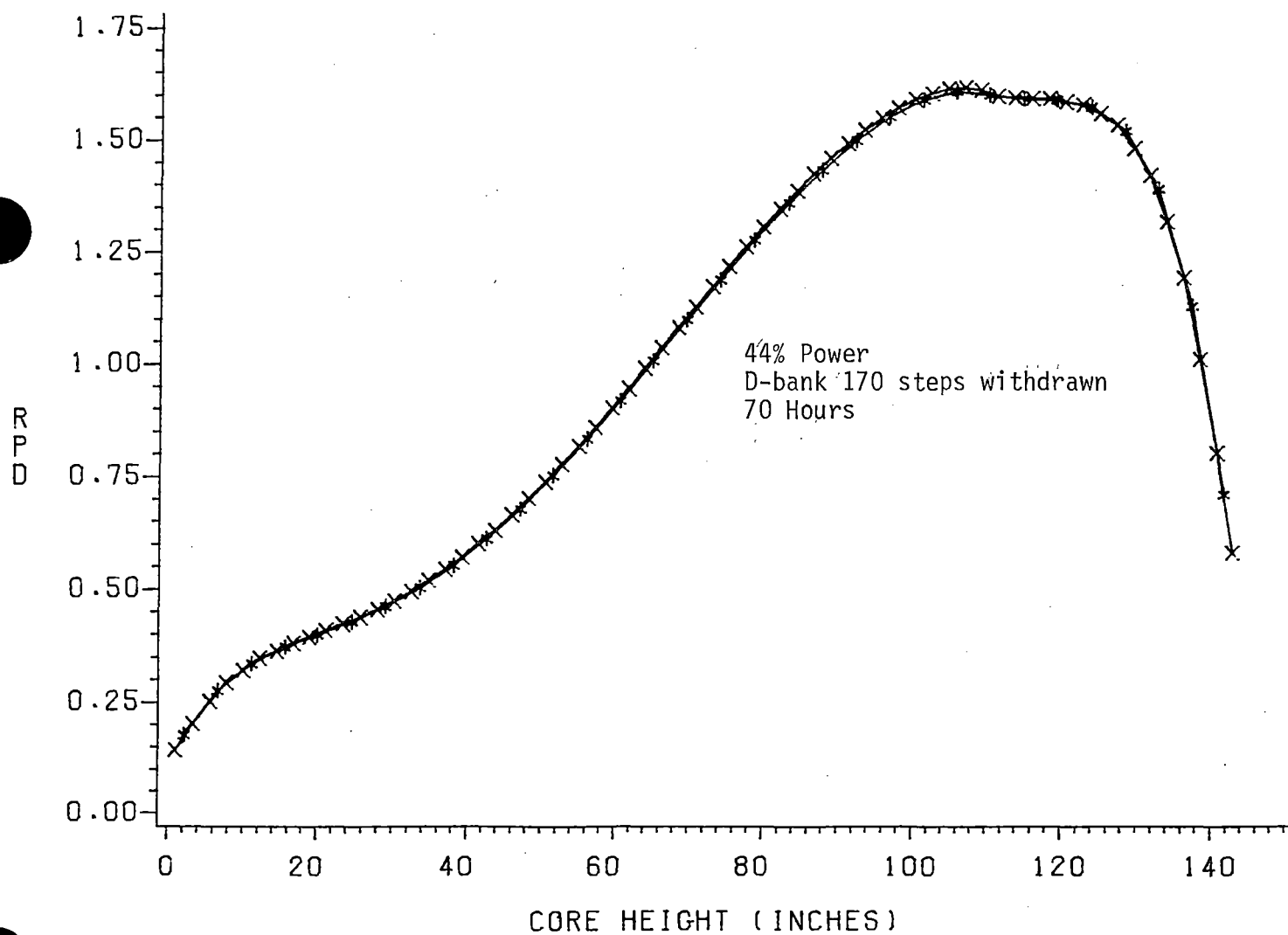
AXIAL POWER COMPARISON



* NOMAD(32 REGIONS)
X NOMAD(64 REGIONS)

FIGURE 1.7

AXIAL POWER COMPARISON



* NOMAD(32 REGIONS)
X NOMAD(64 REGIONS)

FIGURE 1.8

AXIAL POWER COMPARISON

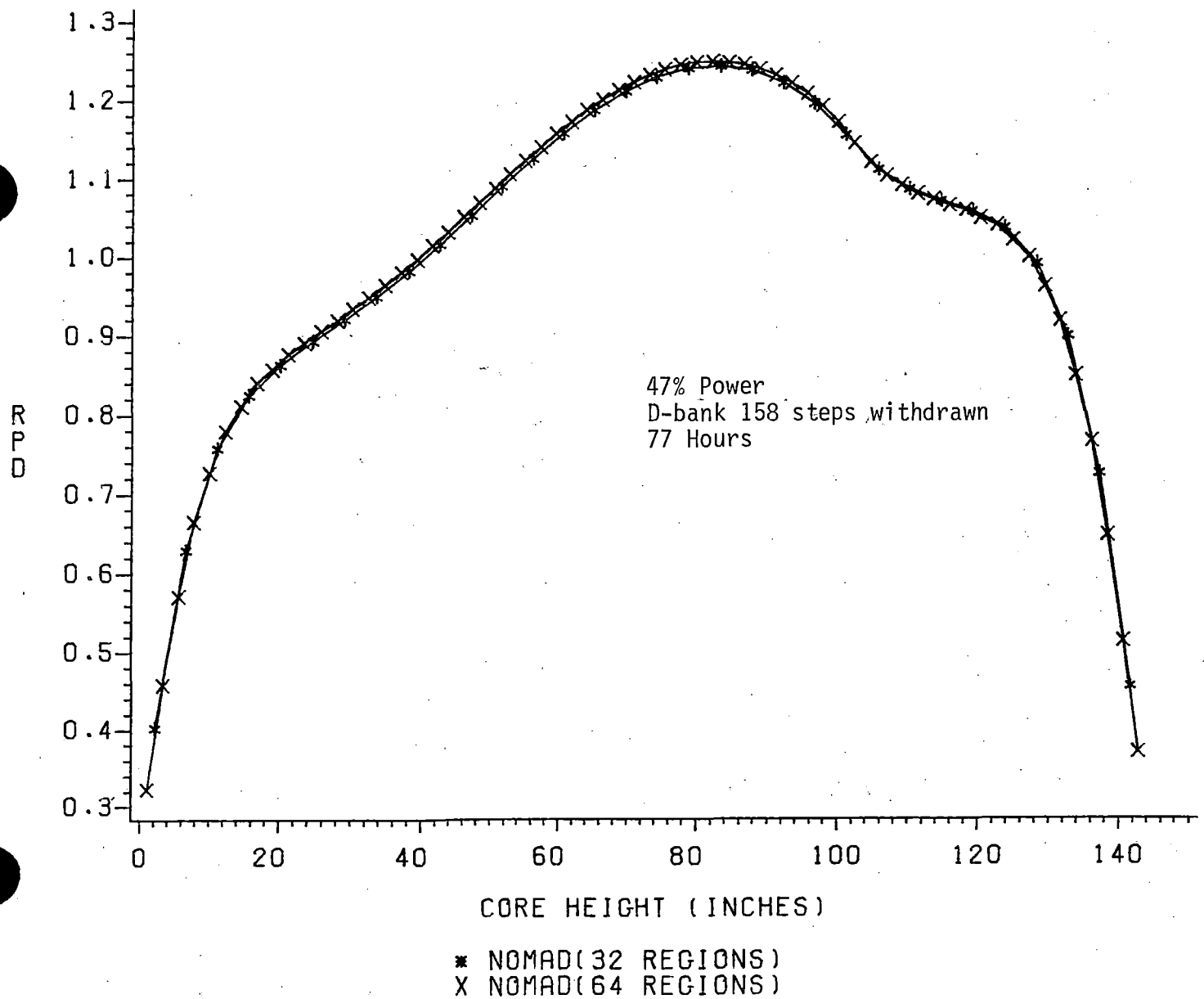


FIGURE 2.1

AXIAL POWER COMPARISON

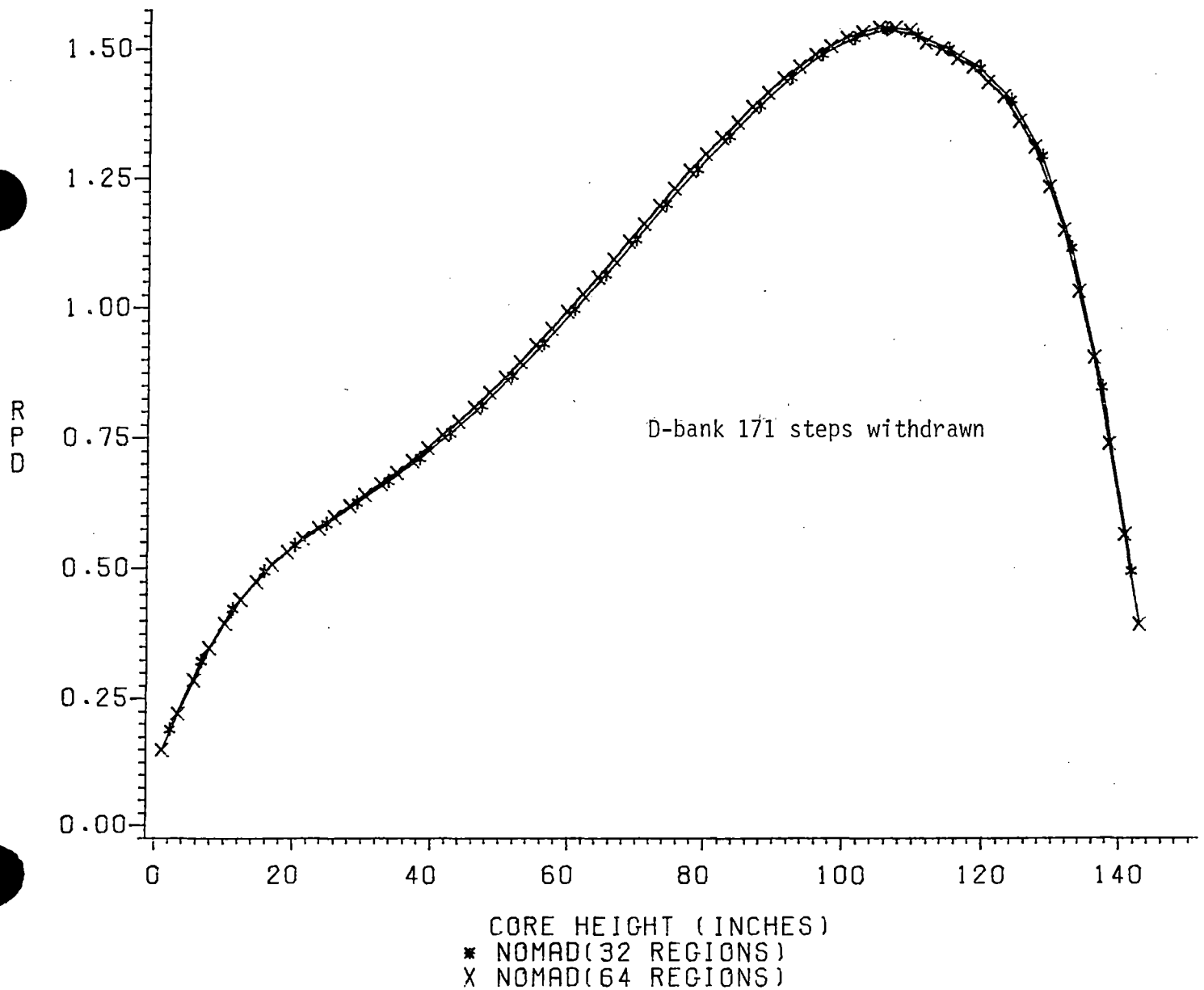


FIGURE 2.2

AXIAL POWER COMPARISON

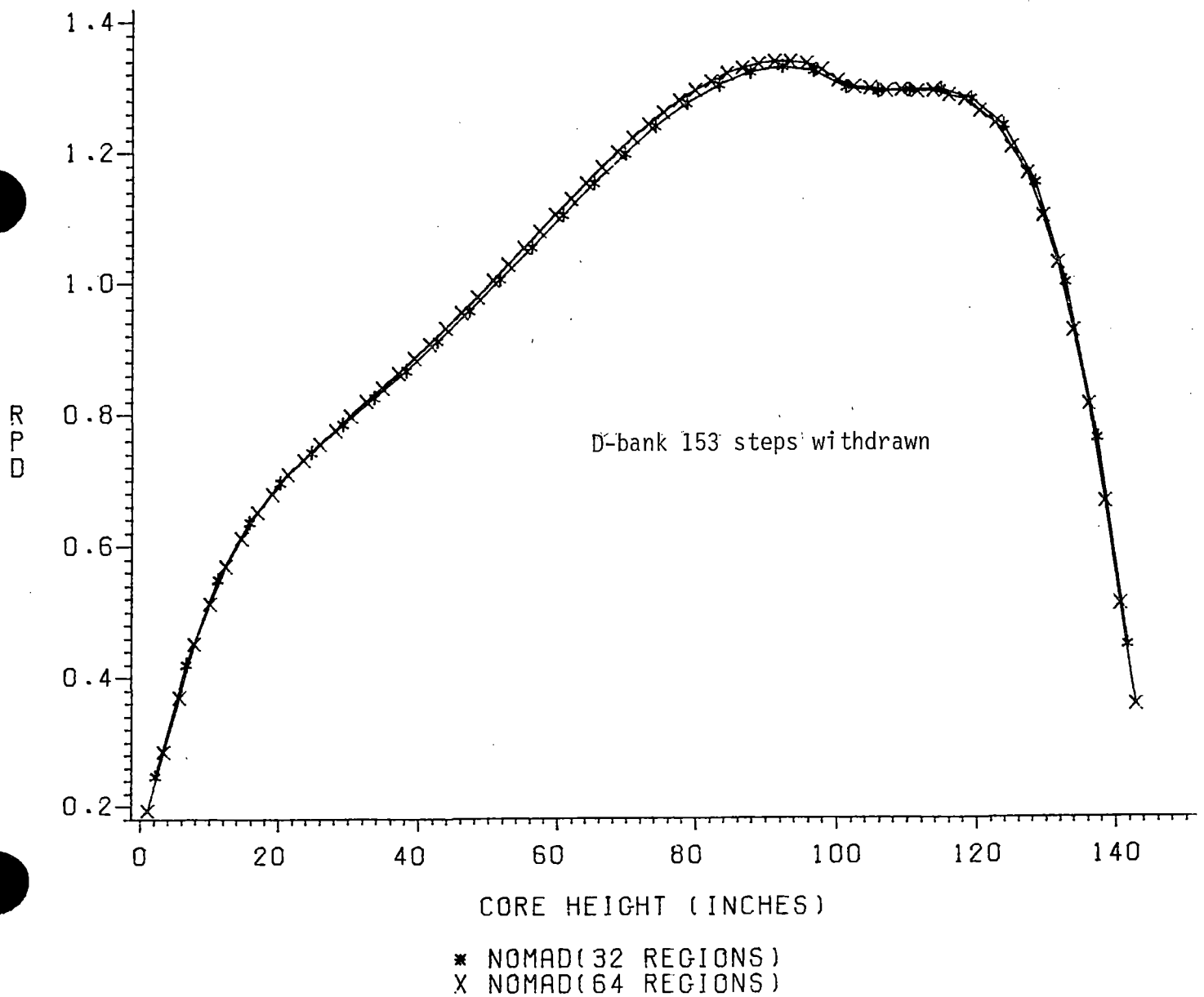


FIGURE 2.3

AXIAL POWER COMPARISON

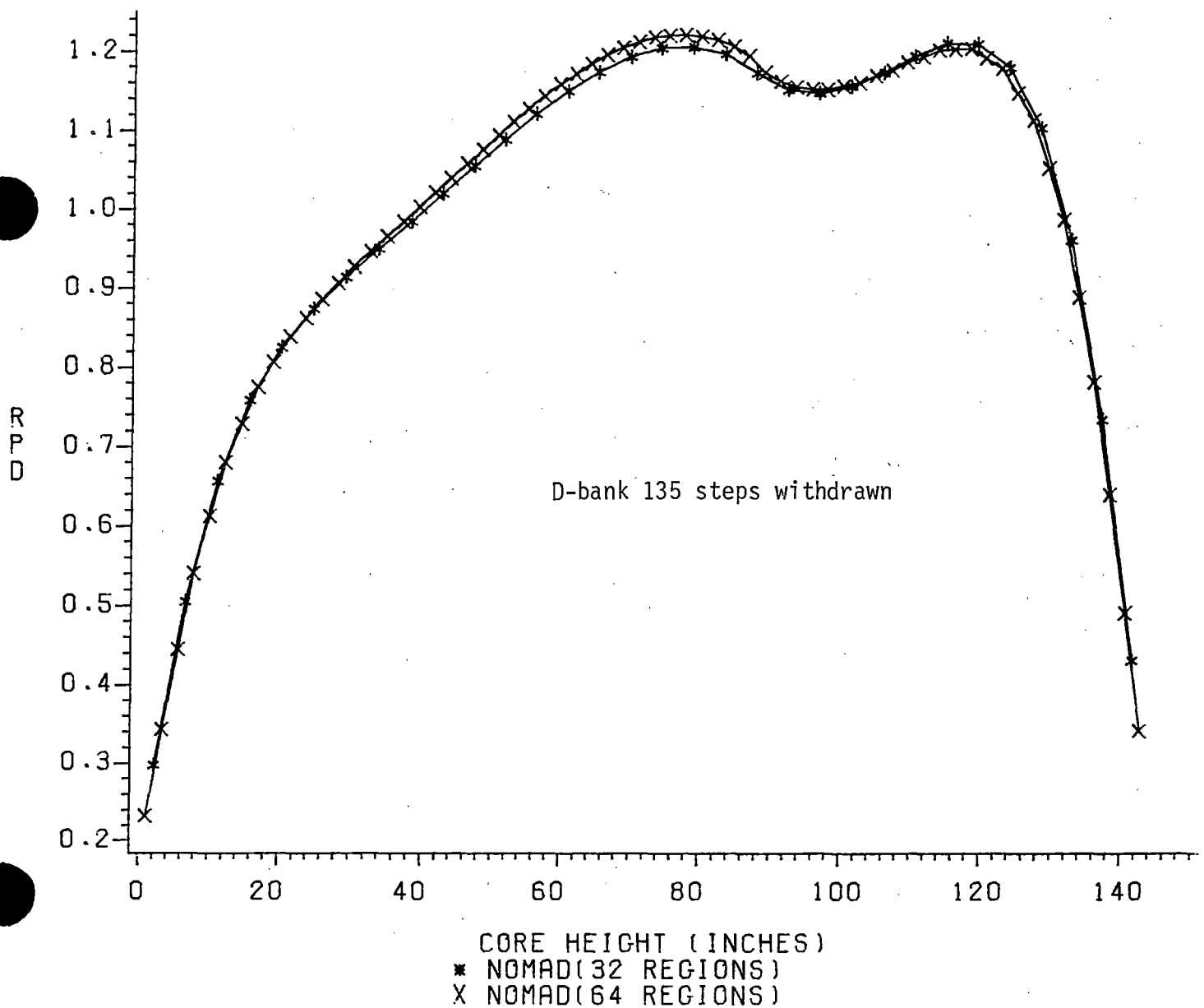


FIGURE 2.4

AXIAL POWER COMPARISON

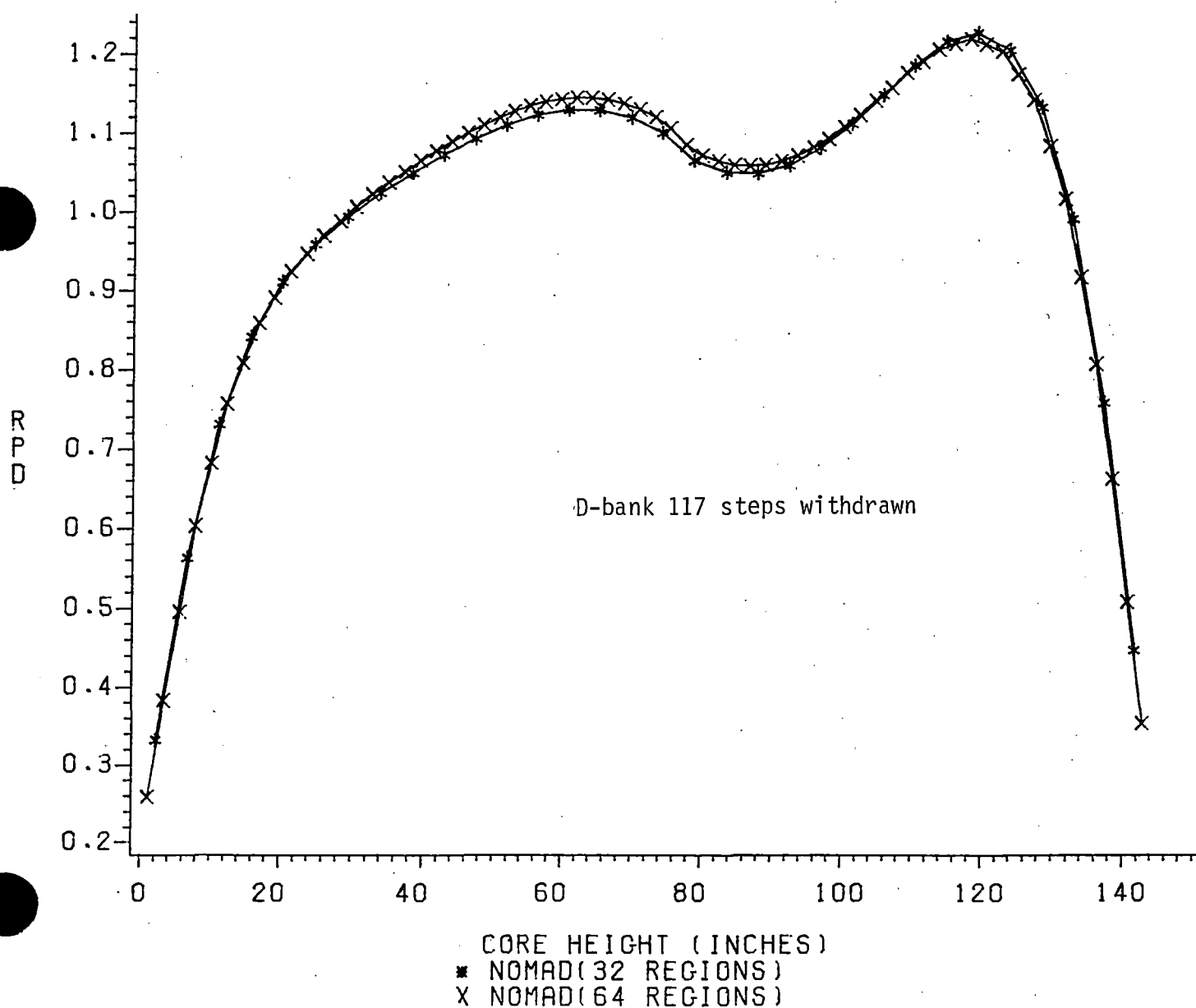
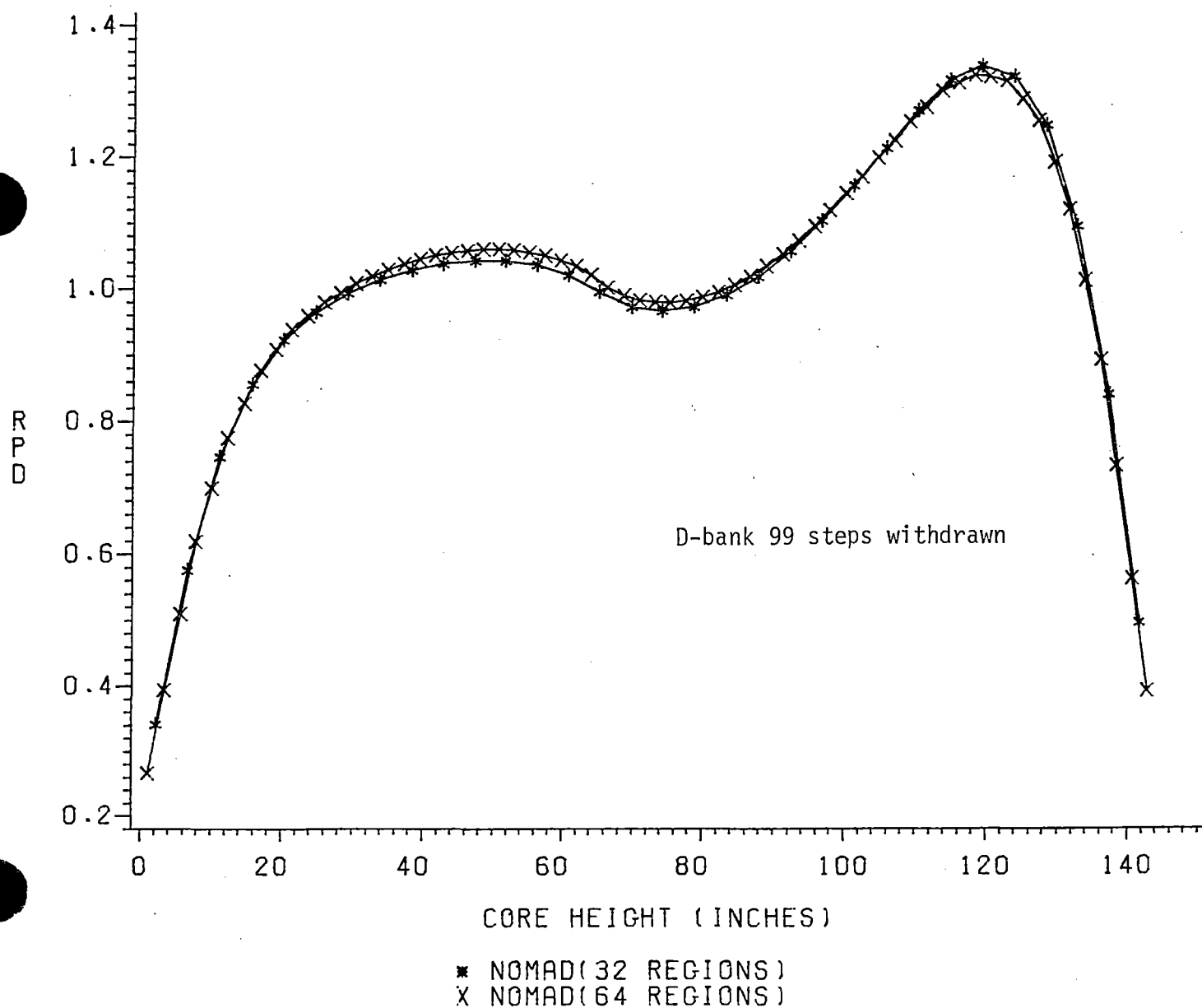


FIGURE 2.5

AXIAL POWER COMPARISON



CROSS SECTION COMPARISON

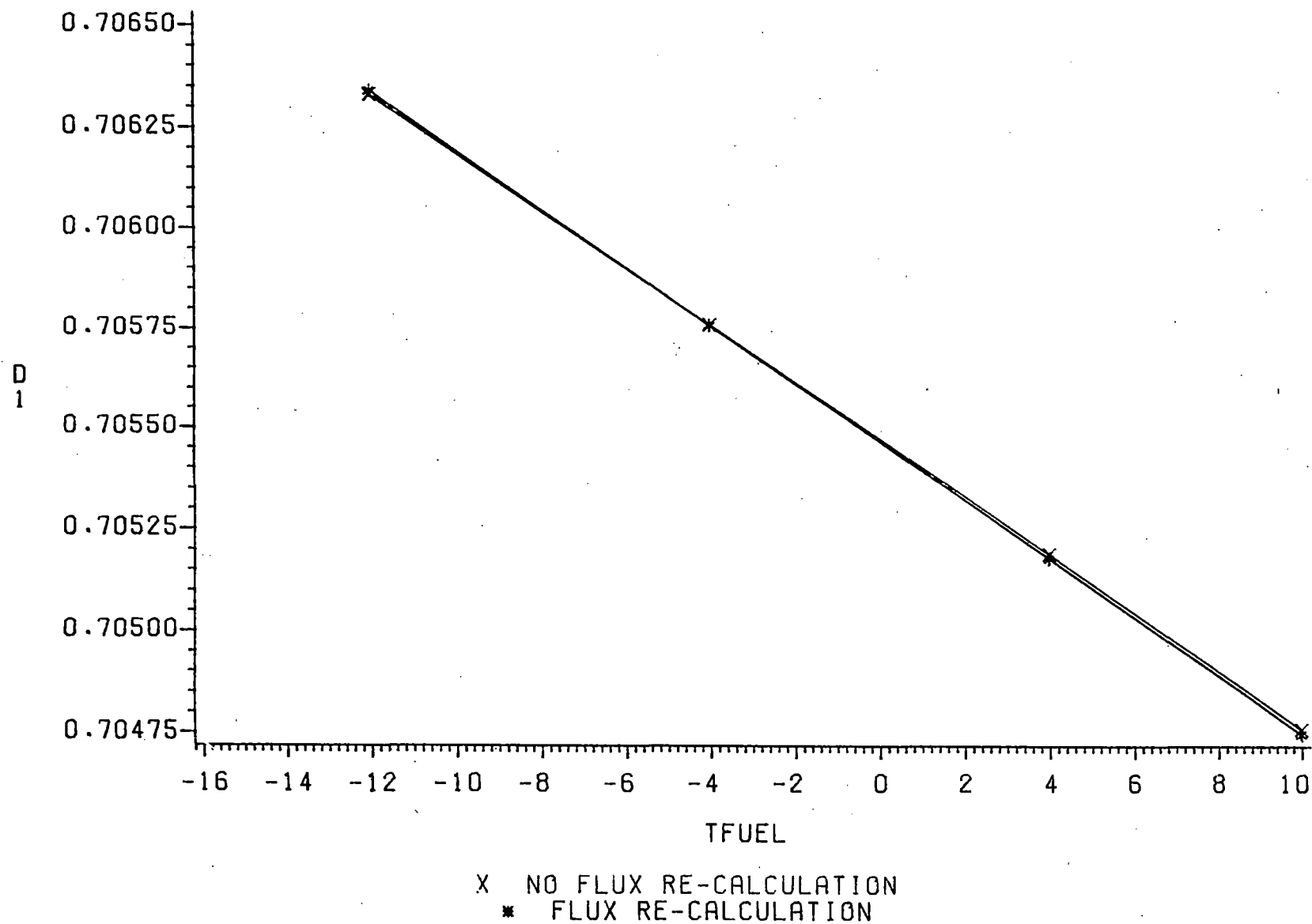
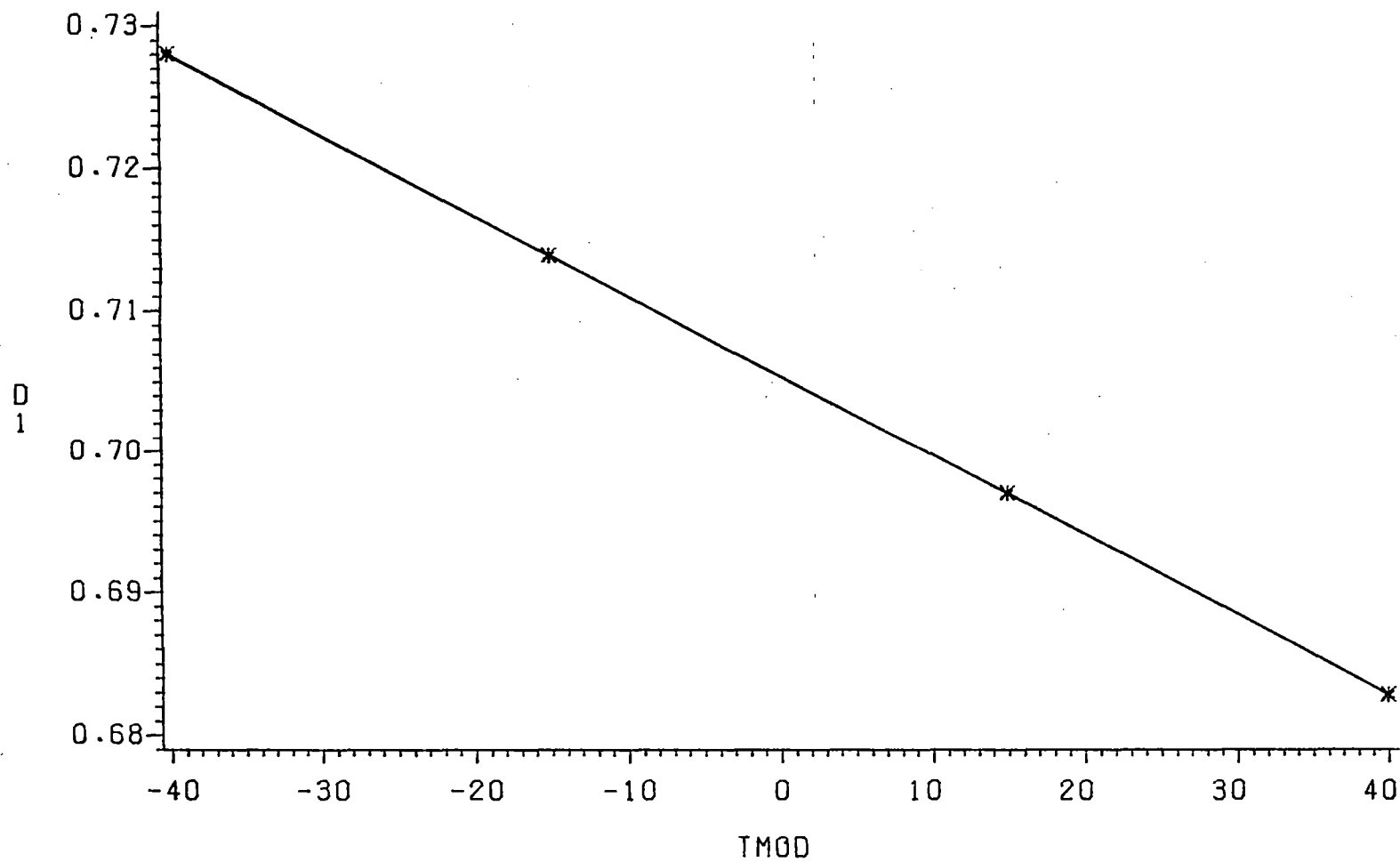


FIGURE 4.1

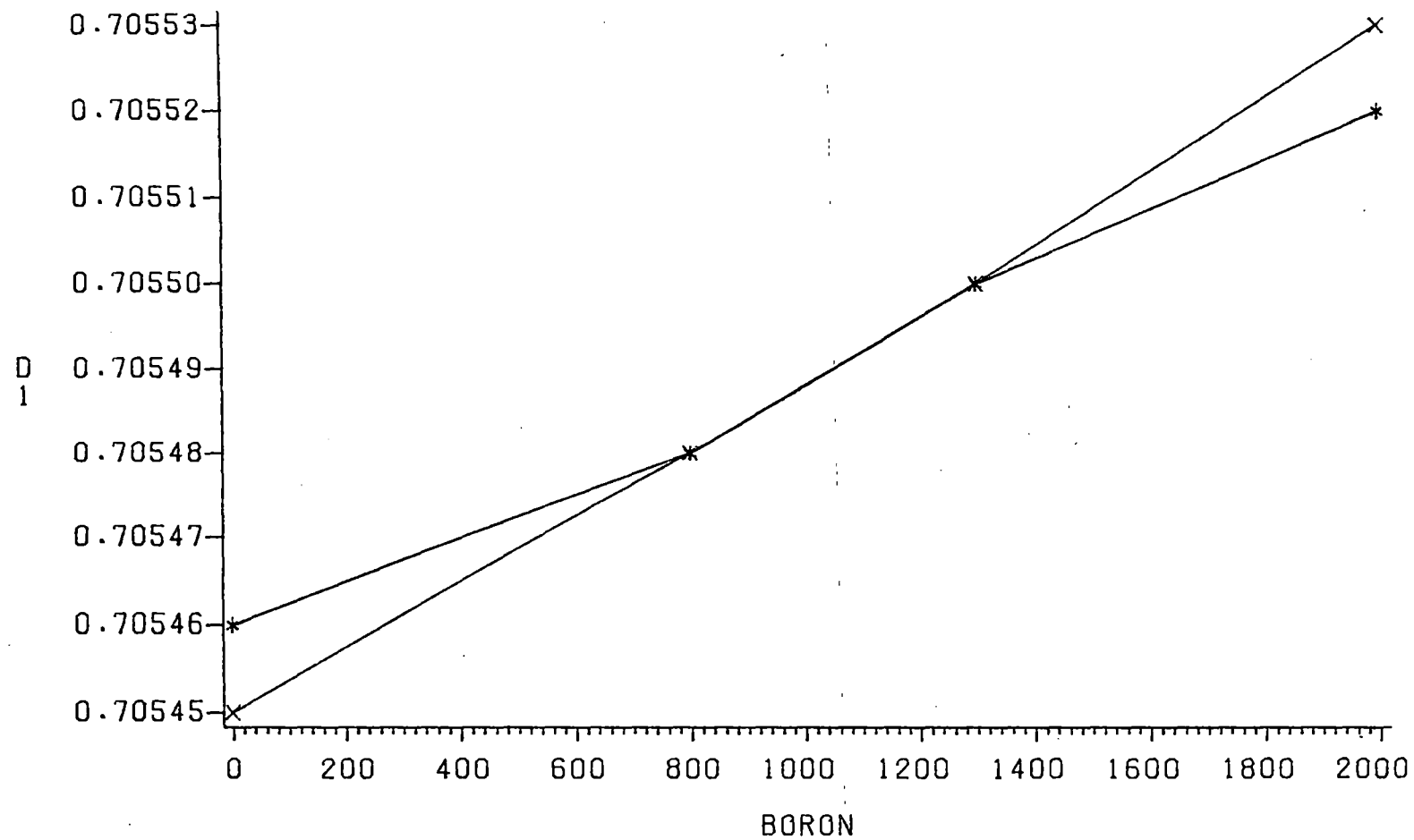
CROSS SECTION COMPARISON



X NO FLUX RE-CALCULATION
* FLUX RE-CALCULATION

FIGURE 4.2

CROSS SECTION COMPARISON



X NO FLUX RE-CALCULATION
* FLUX RE-CALCULATION

FIGURE 4.3

CROSS SECTION COMPARISON

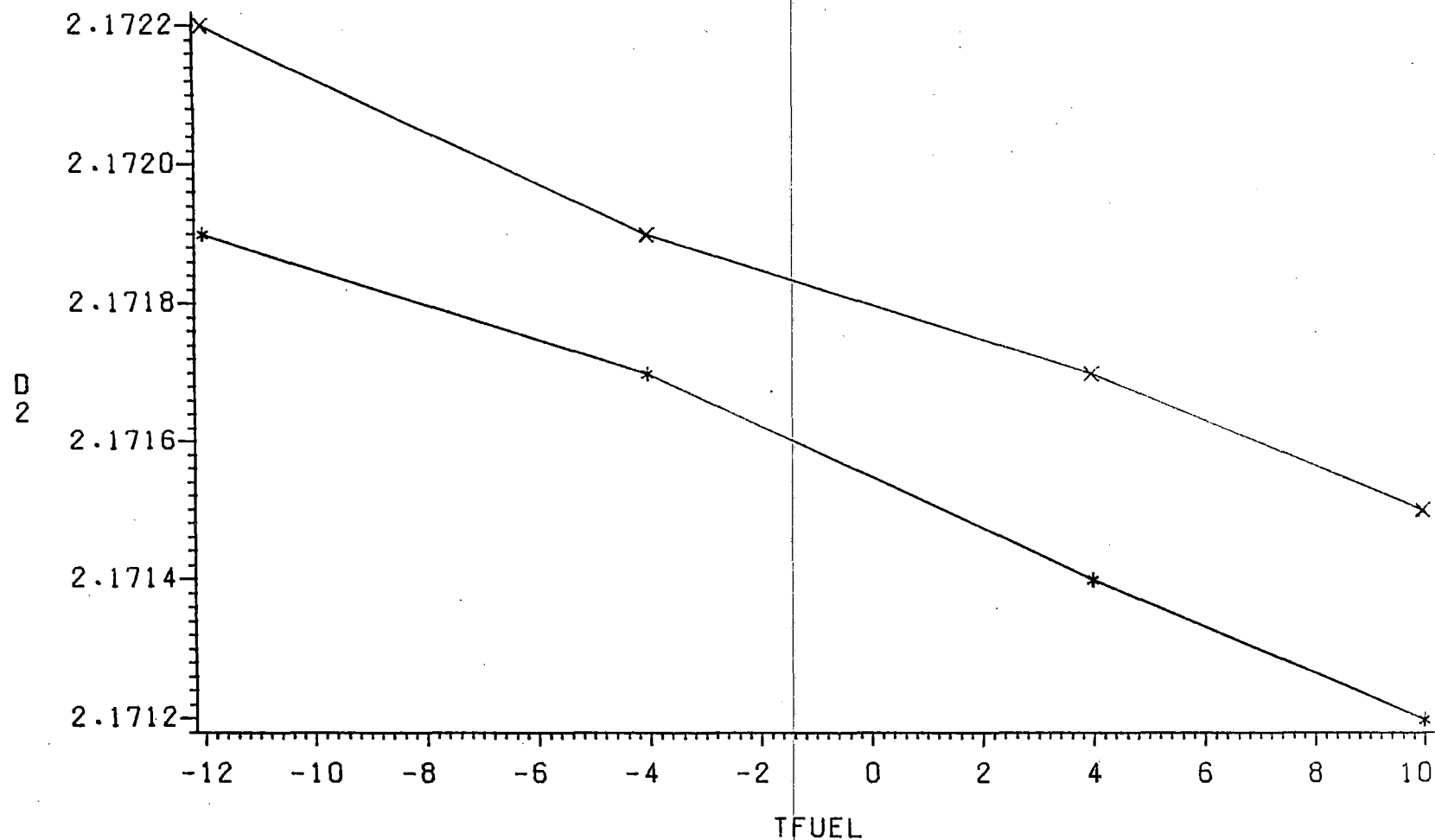


FIGURE 4.4

X NO FLUX RE-CALCULATION
* FLUX RE-CALCULATION

CROSS SECTION COMPARISON

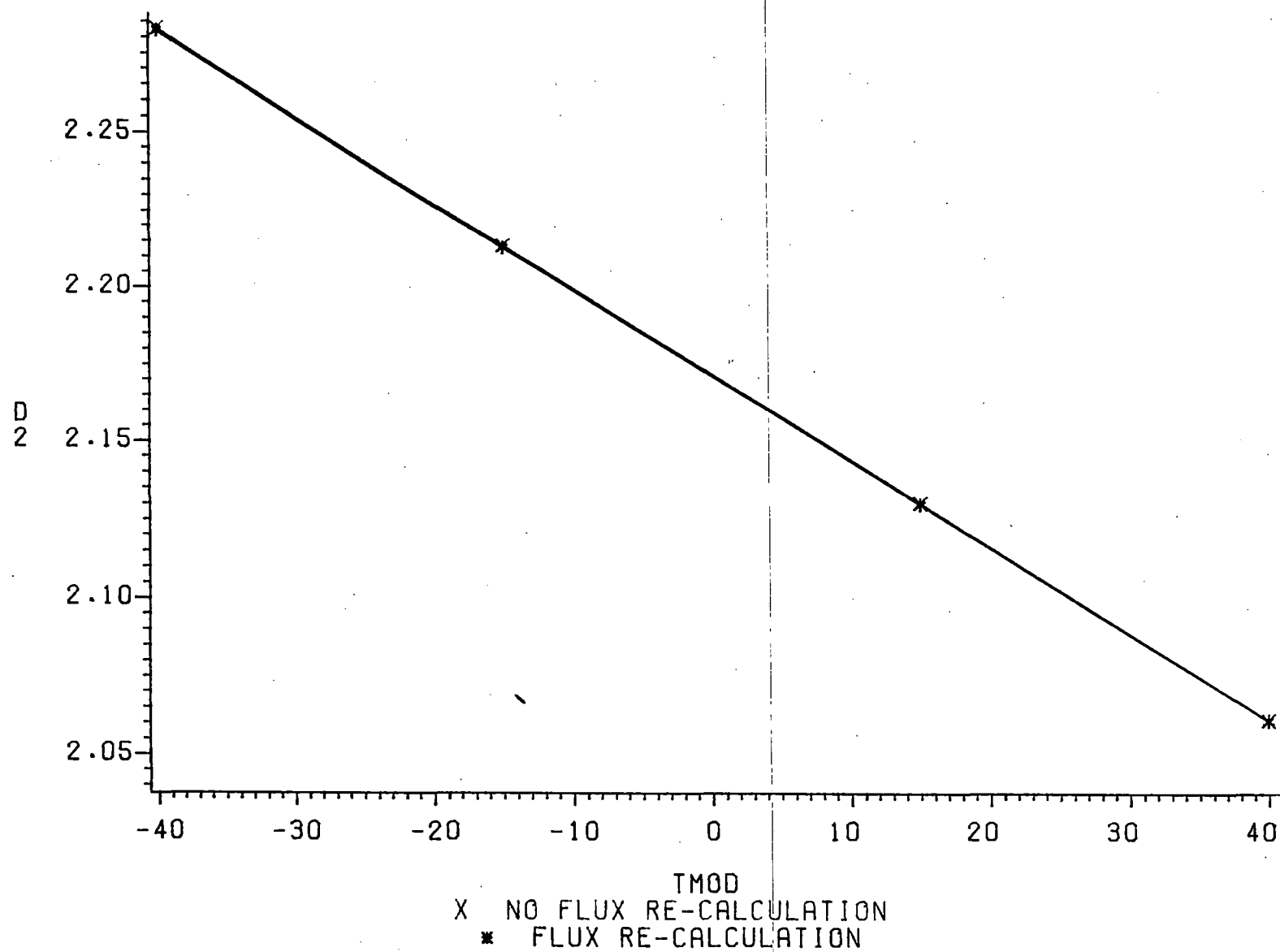


FIGURE 4.5

CROSS SECTION COMPARISON

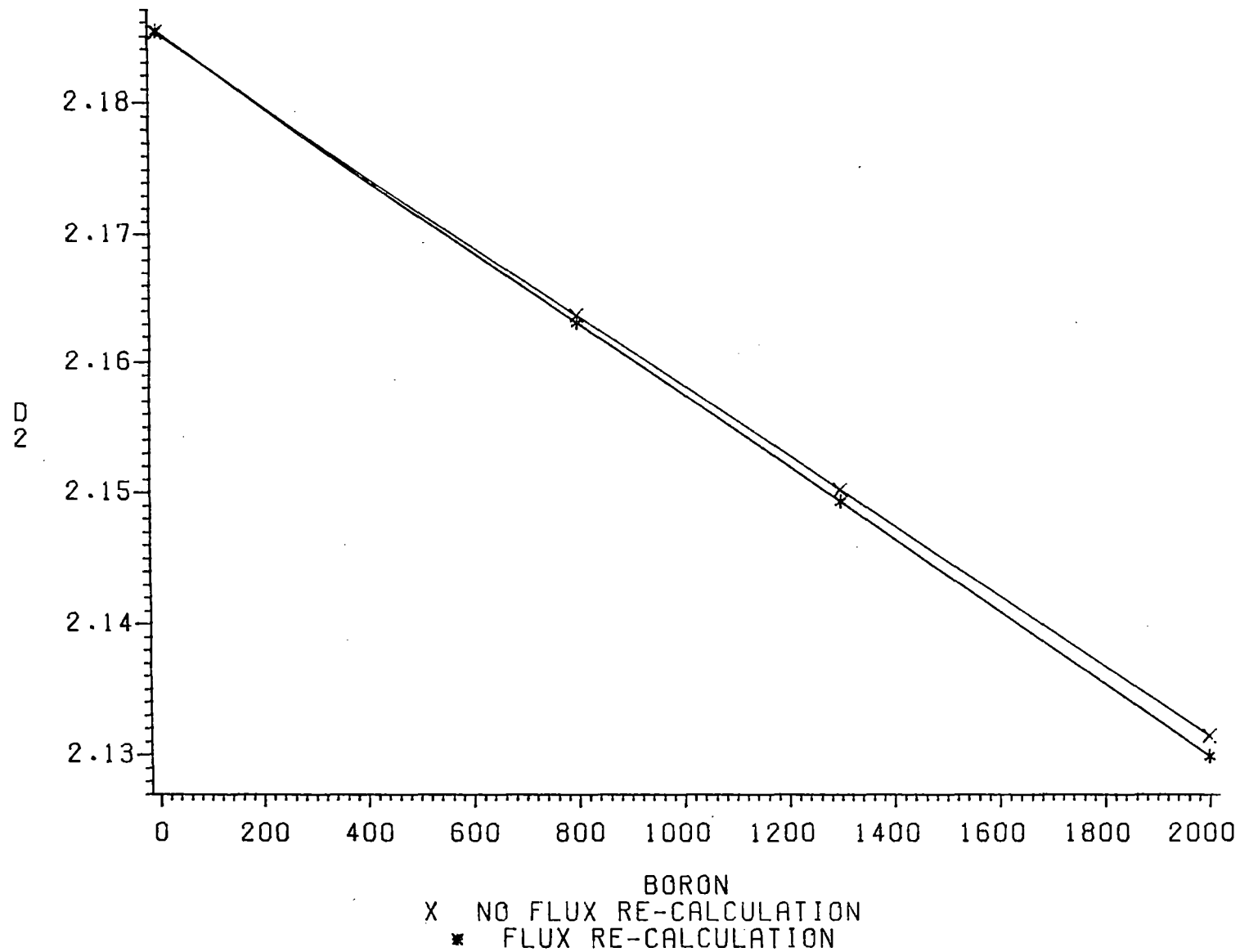


FIGURE 4.6

CROSS SECTION COMPARISON

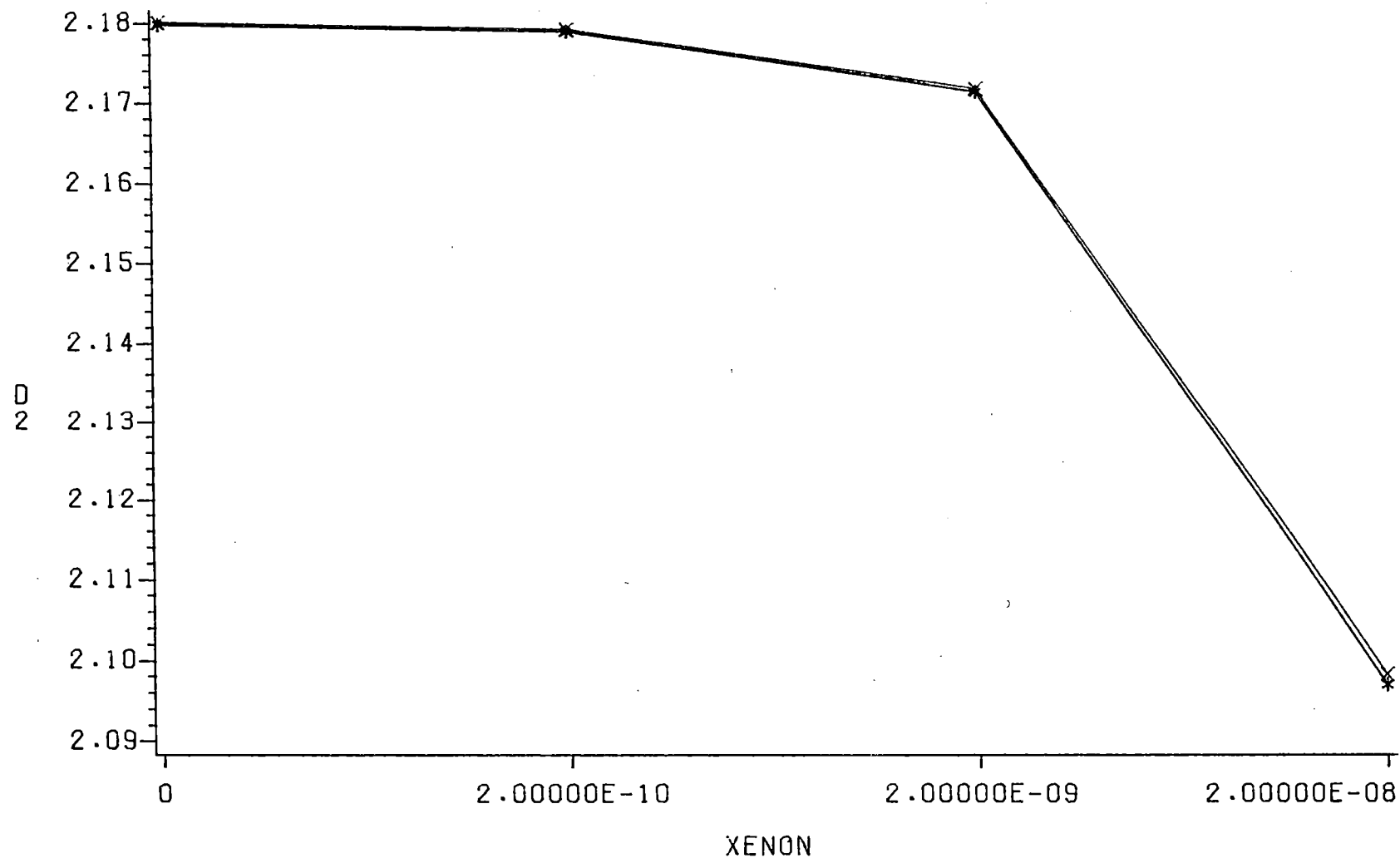


FIGURE 4.7

CROSS SECTION COMPARISON

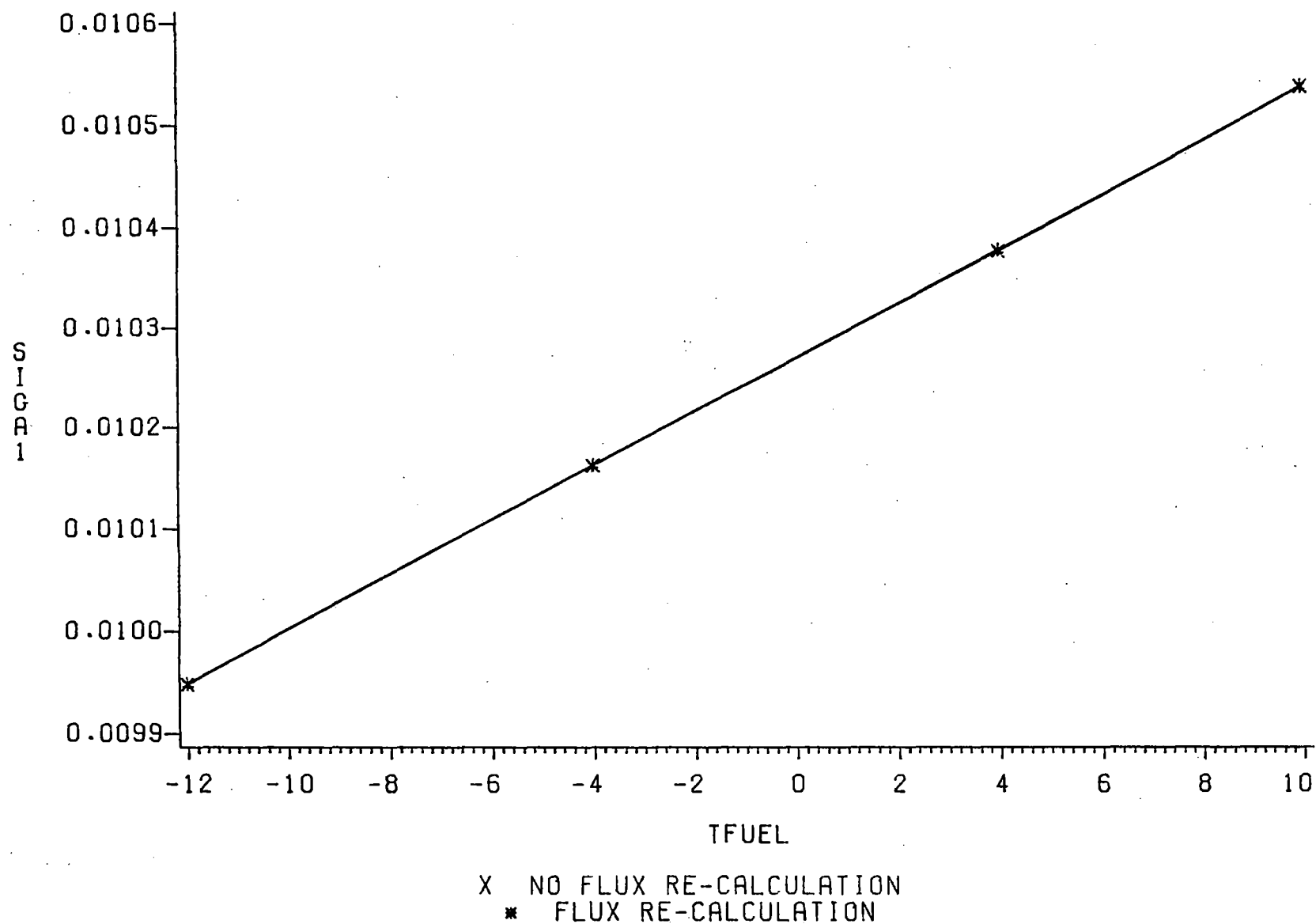


FIGURE 4.8

CROSS SECTION COMPARISON

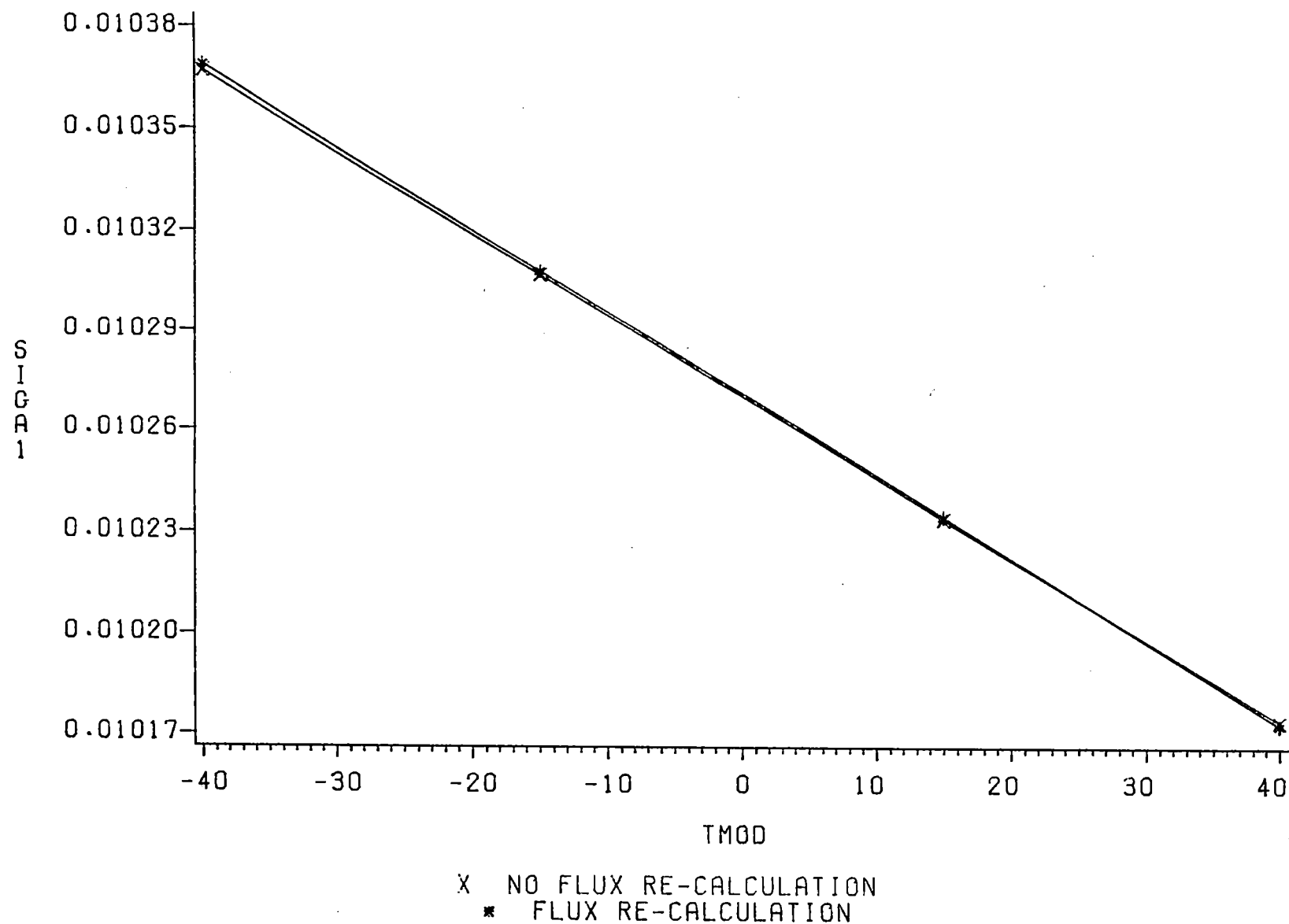


FIGURE 4.9

CROSS SECTION COMPARISON

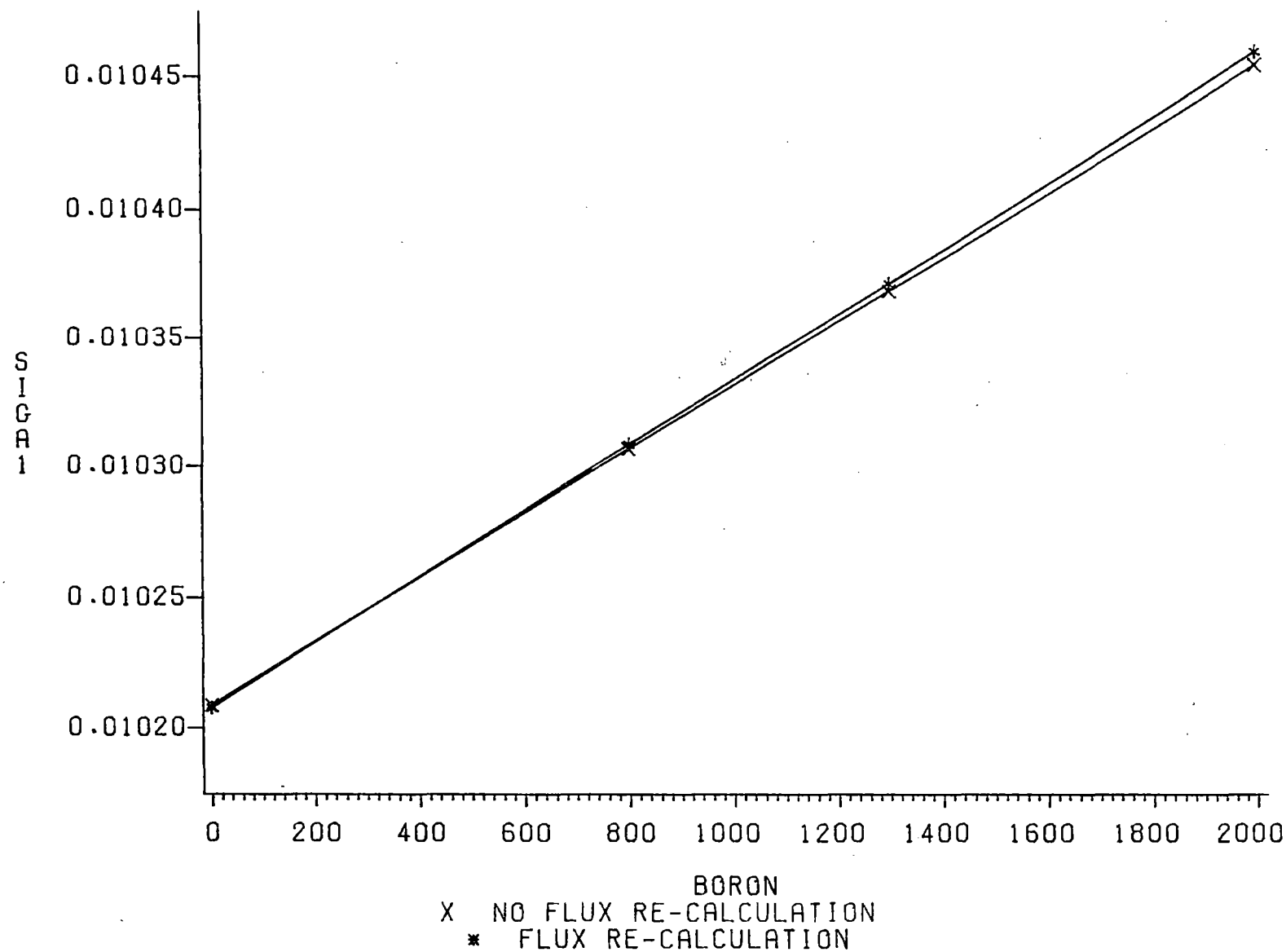


FIGURE 4.10

CROSS SECTION COMPARISON

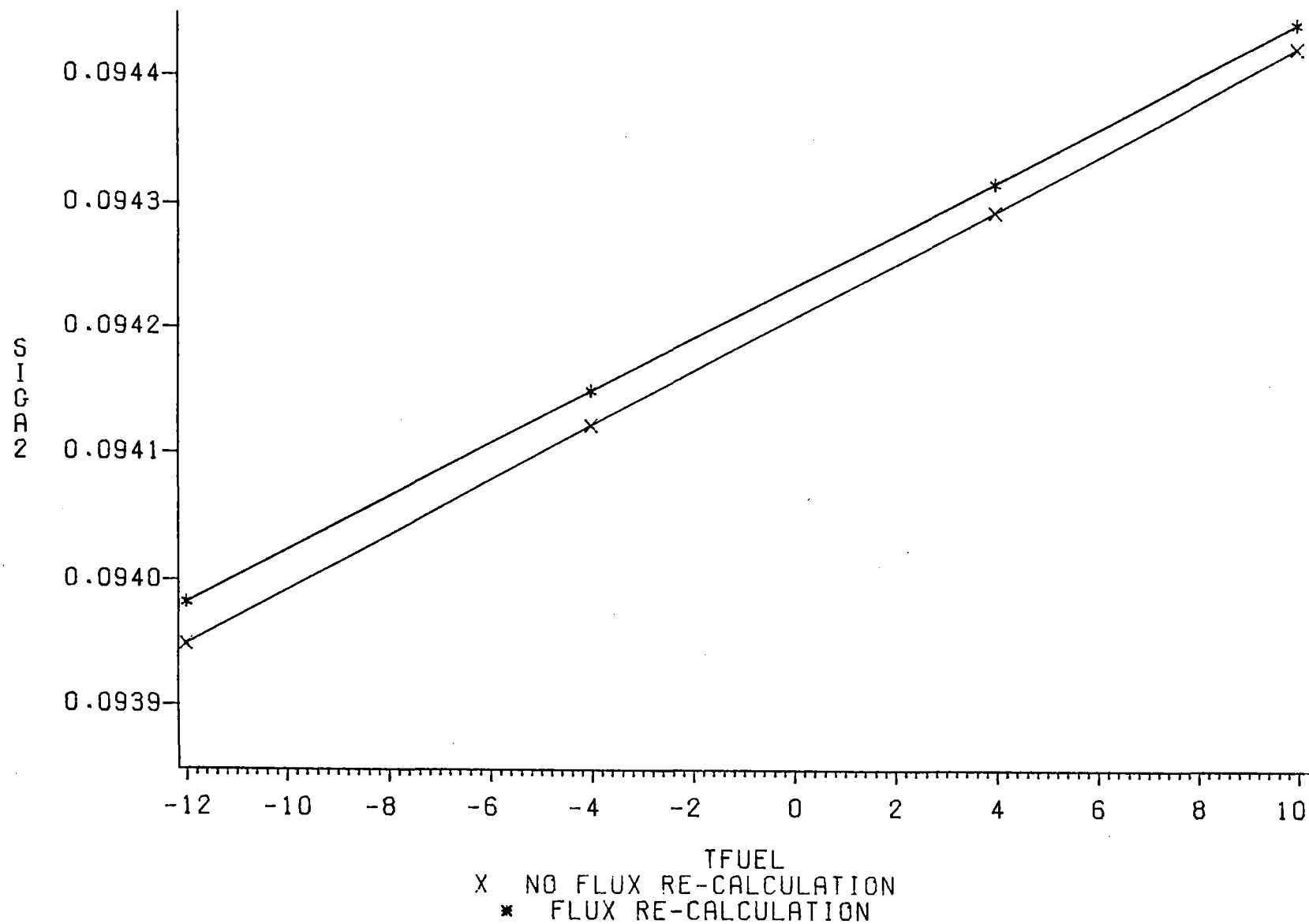


FIGURE 4.11

CROSS SECTION COMPARISON

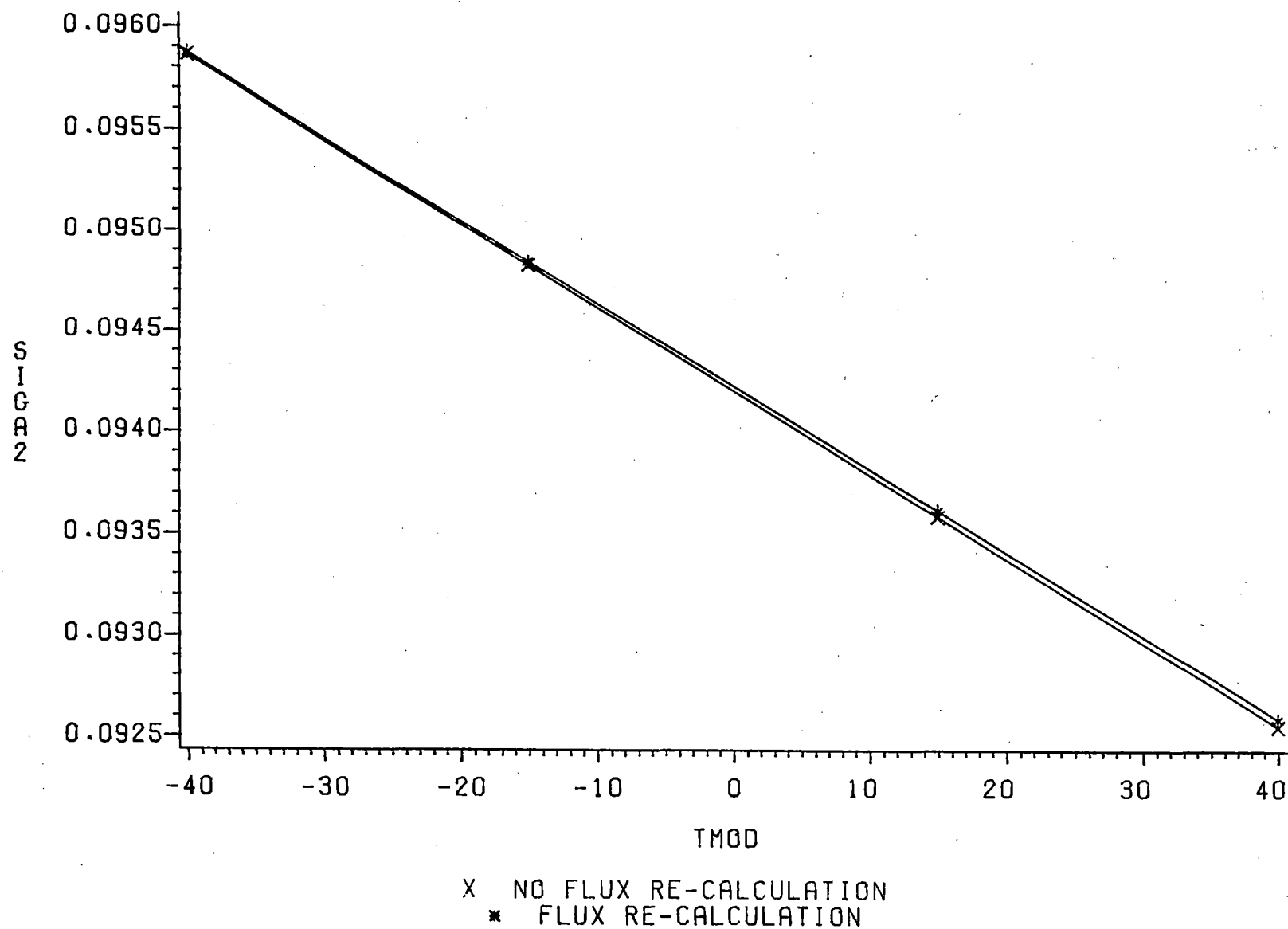


FIGURE 4.12

CROSS SECTION COMPARISON

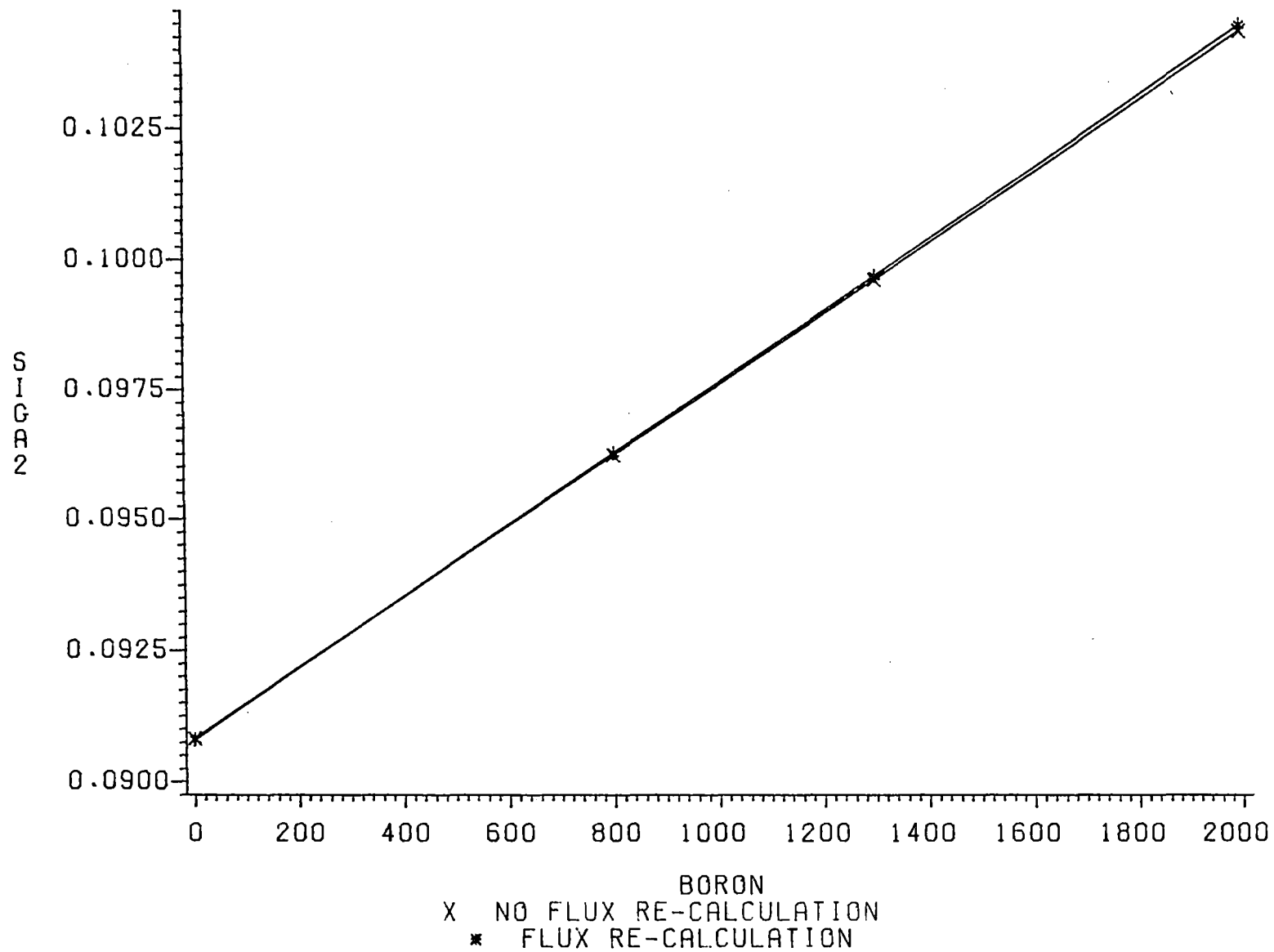


FIGURE 4.13

CROSS SECTION COMPARISON

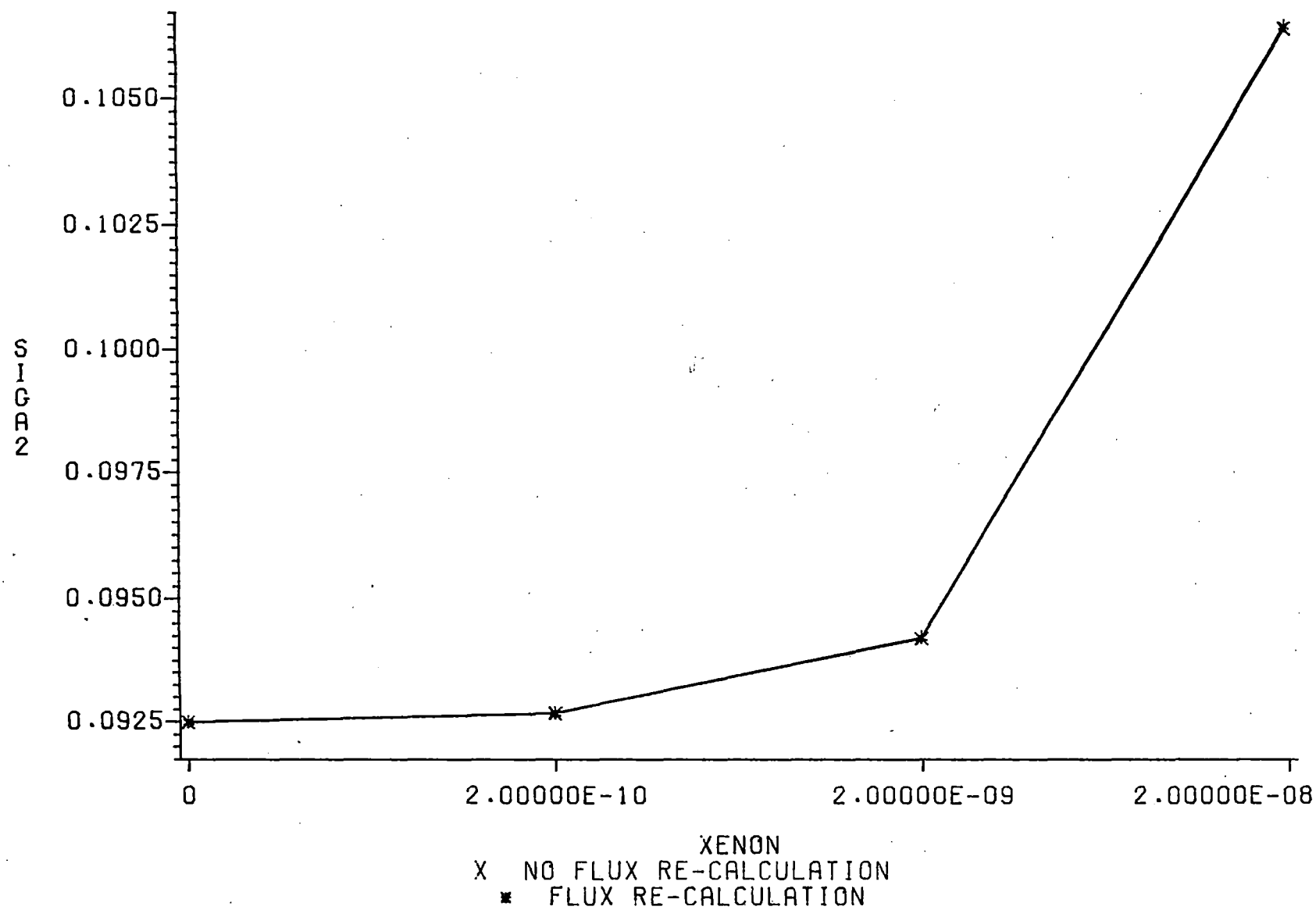


FIGURE 4.14

CROSS SECTION COMPARISON

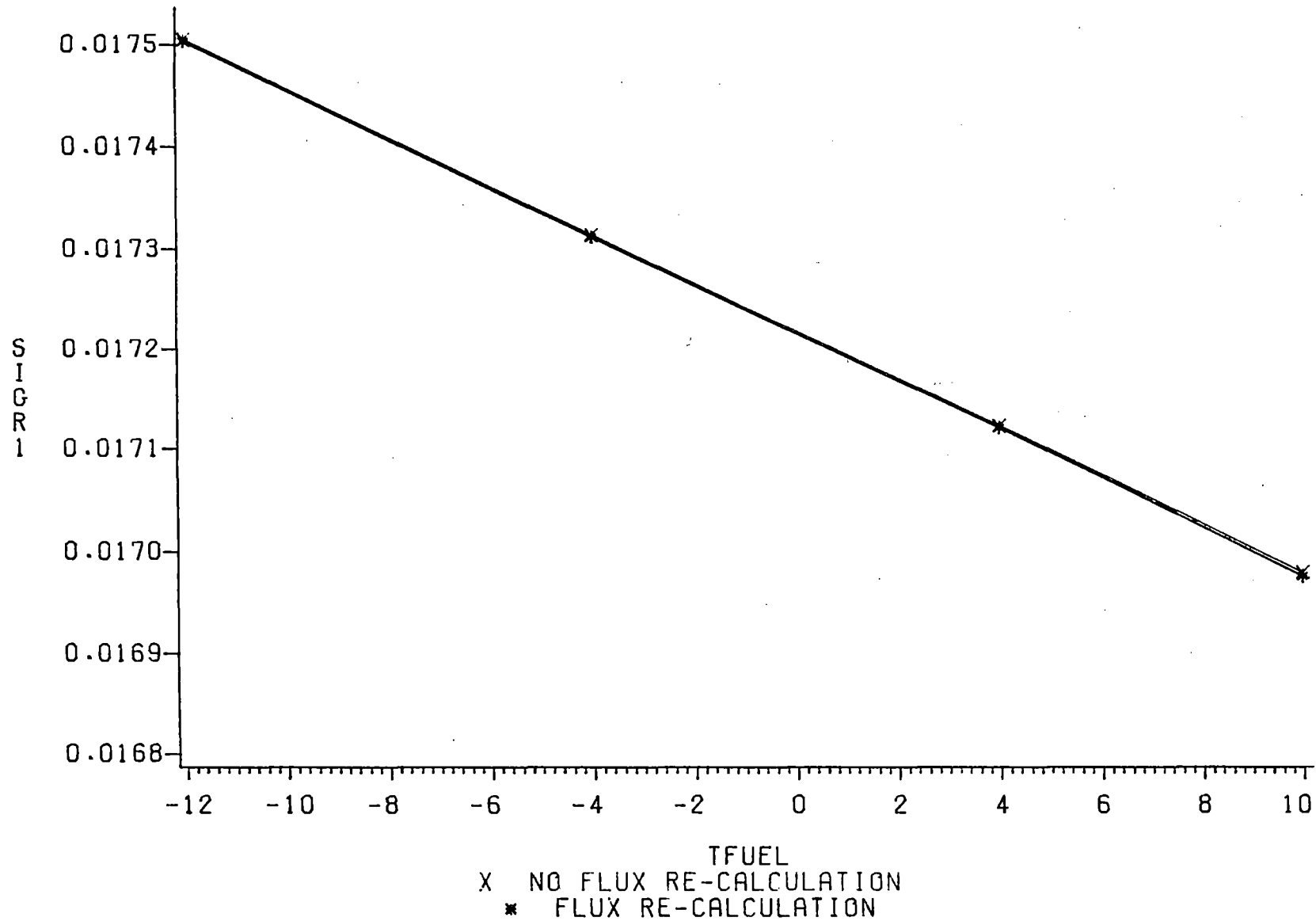


FIGURE 4.15

CROSS SECTION COMPARISON

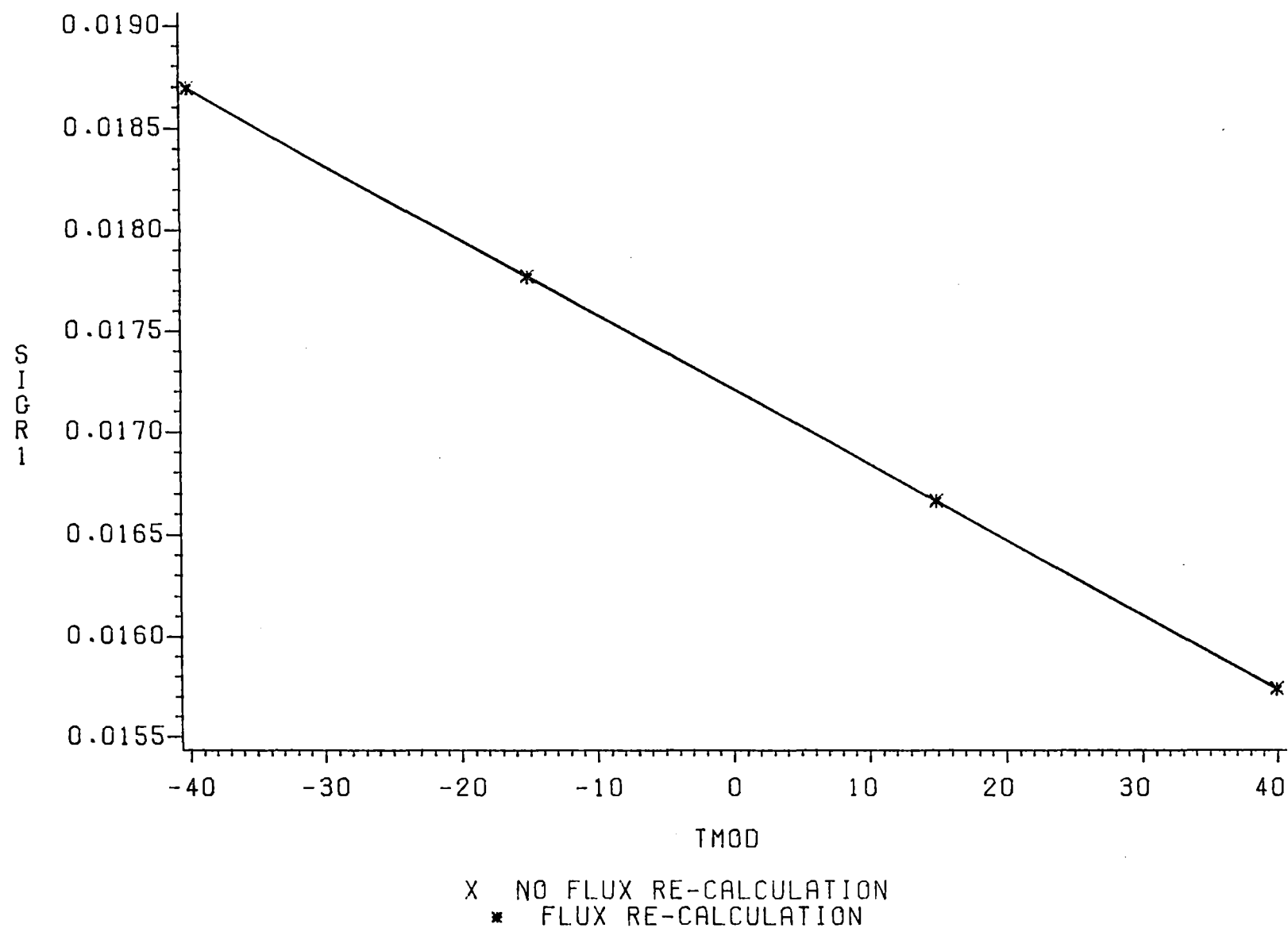


FIGURE 4.16

CROSS SECTION COMPARISON

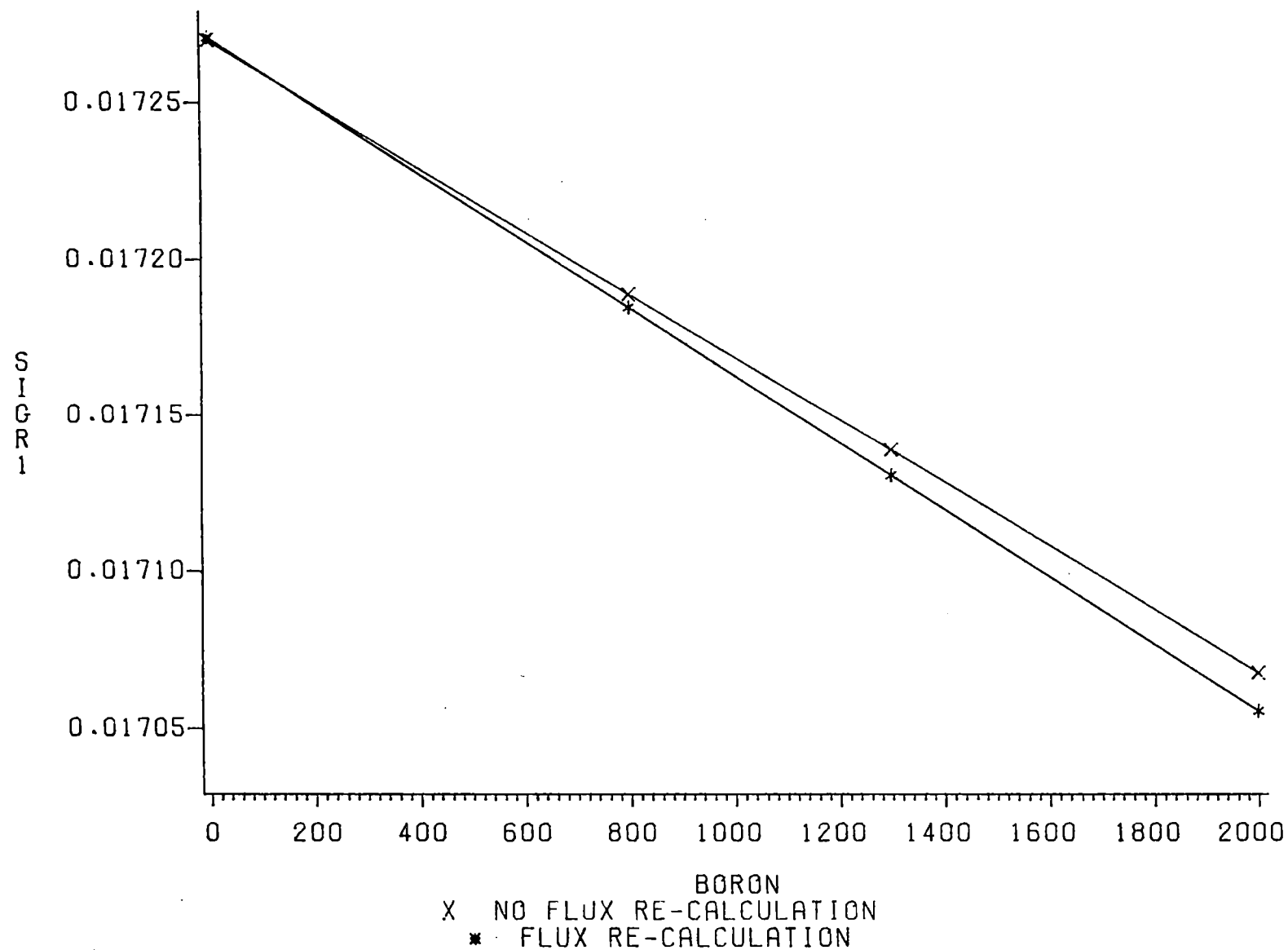


FIGURE 4.17

CROSS SECTION COMPARISON

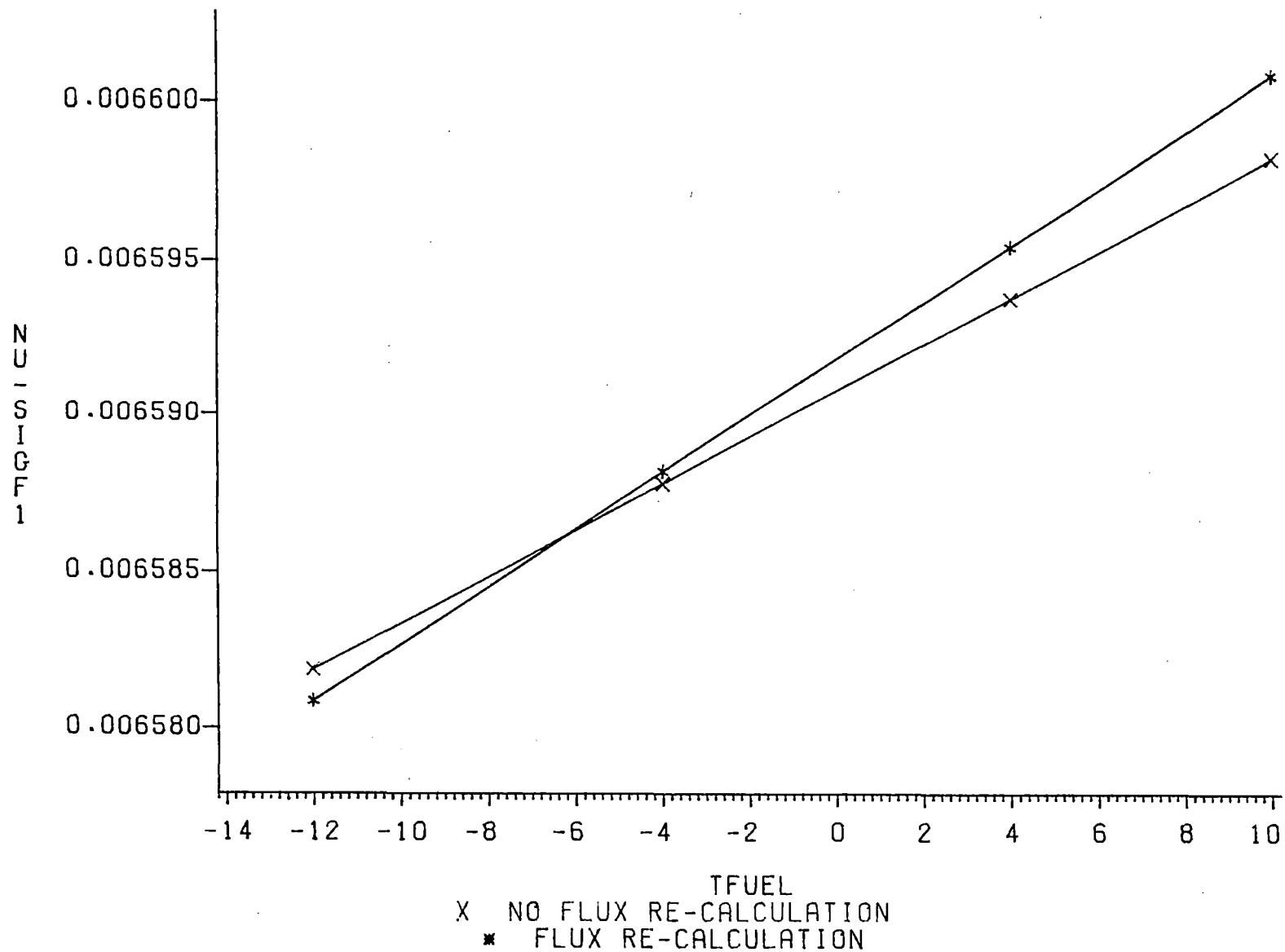
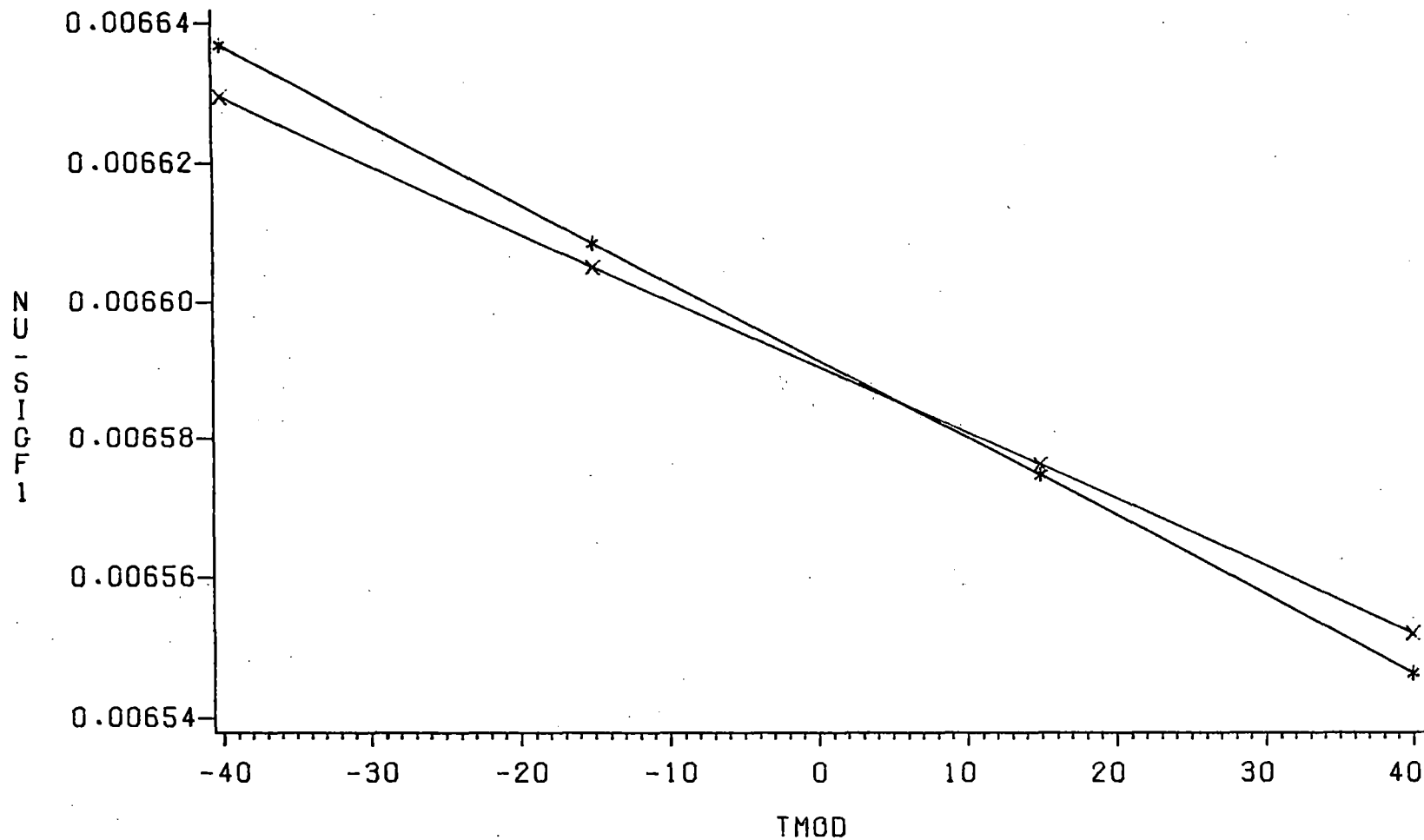


FIGURE 4.18

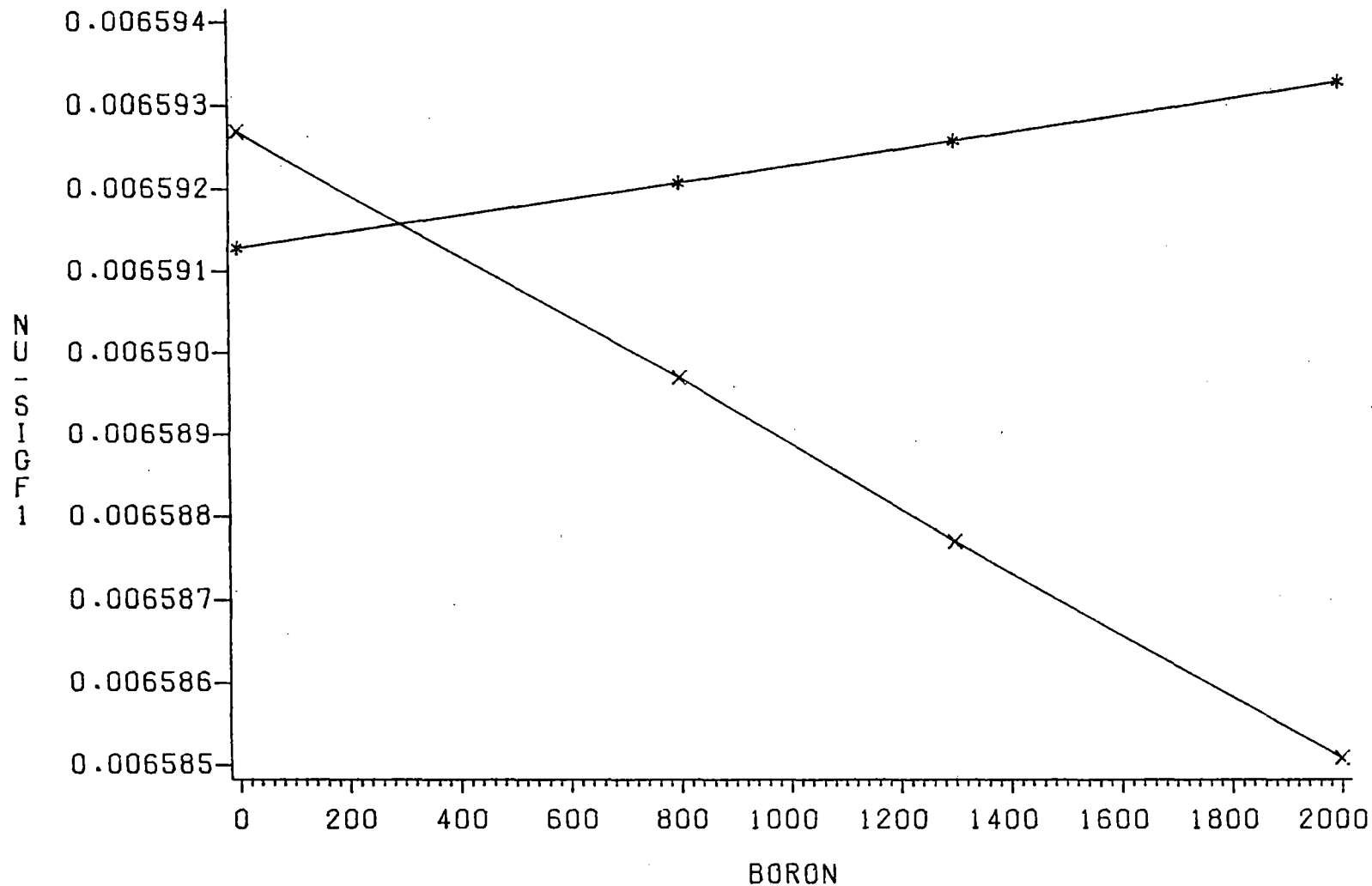
CROSS SECTION COMPARISON



x NO FLUX RE-CALCULATION
* FLUX RE-CALCULATION

FIGURE 4.19

CROSS SECTION COMPARISON



X NO FLUX RE-CALCULATION
* FLUX RE-CALCULATION

FIGURE 4.20

CROSS SECTION COMPARISON

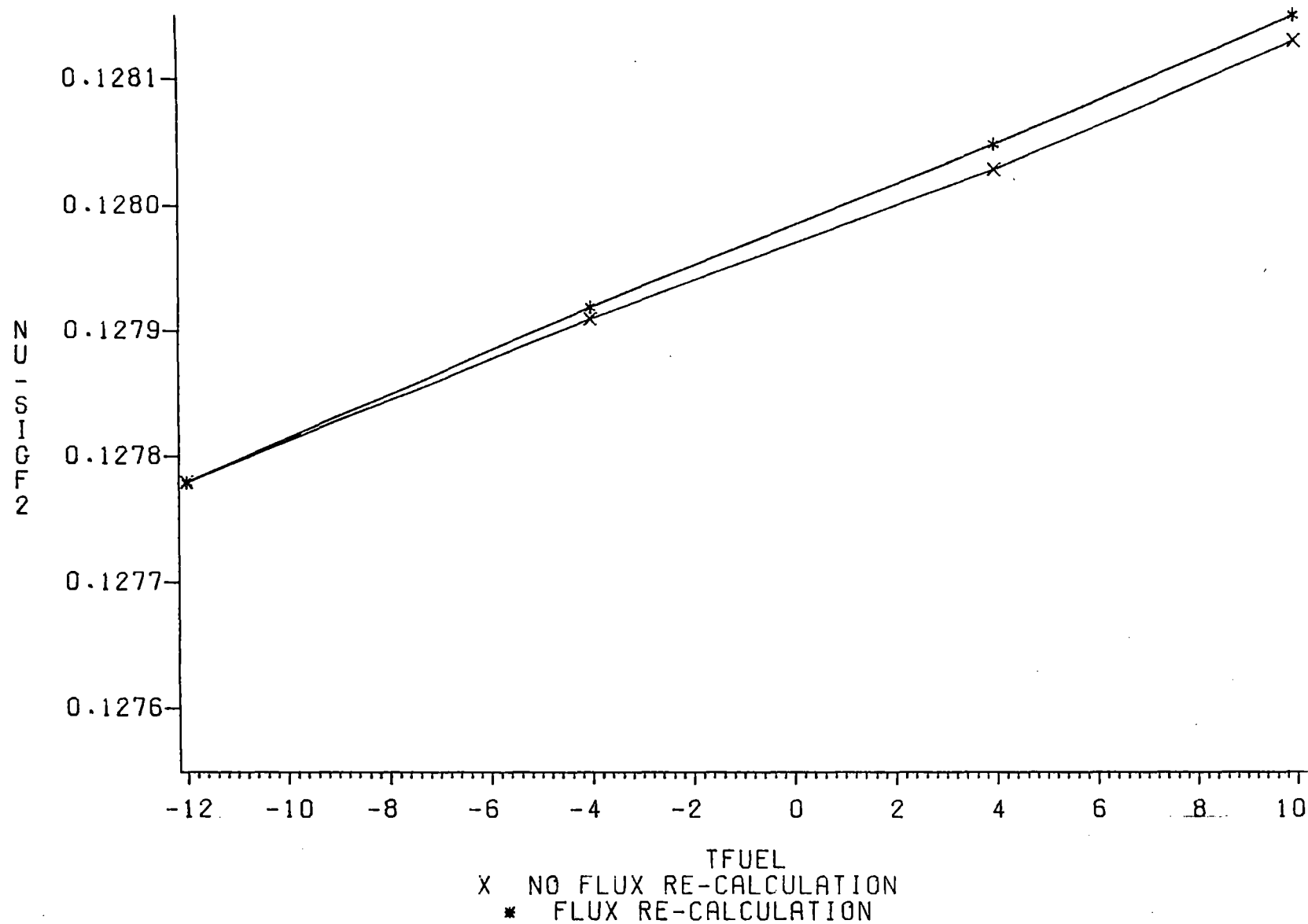


FIGURE 4.21

CROSS SECTION COMPARISON

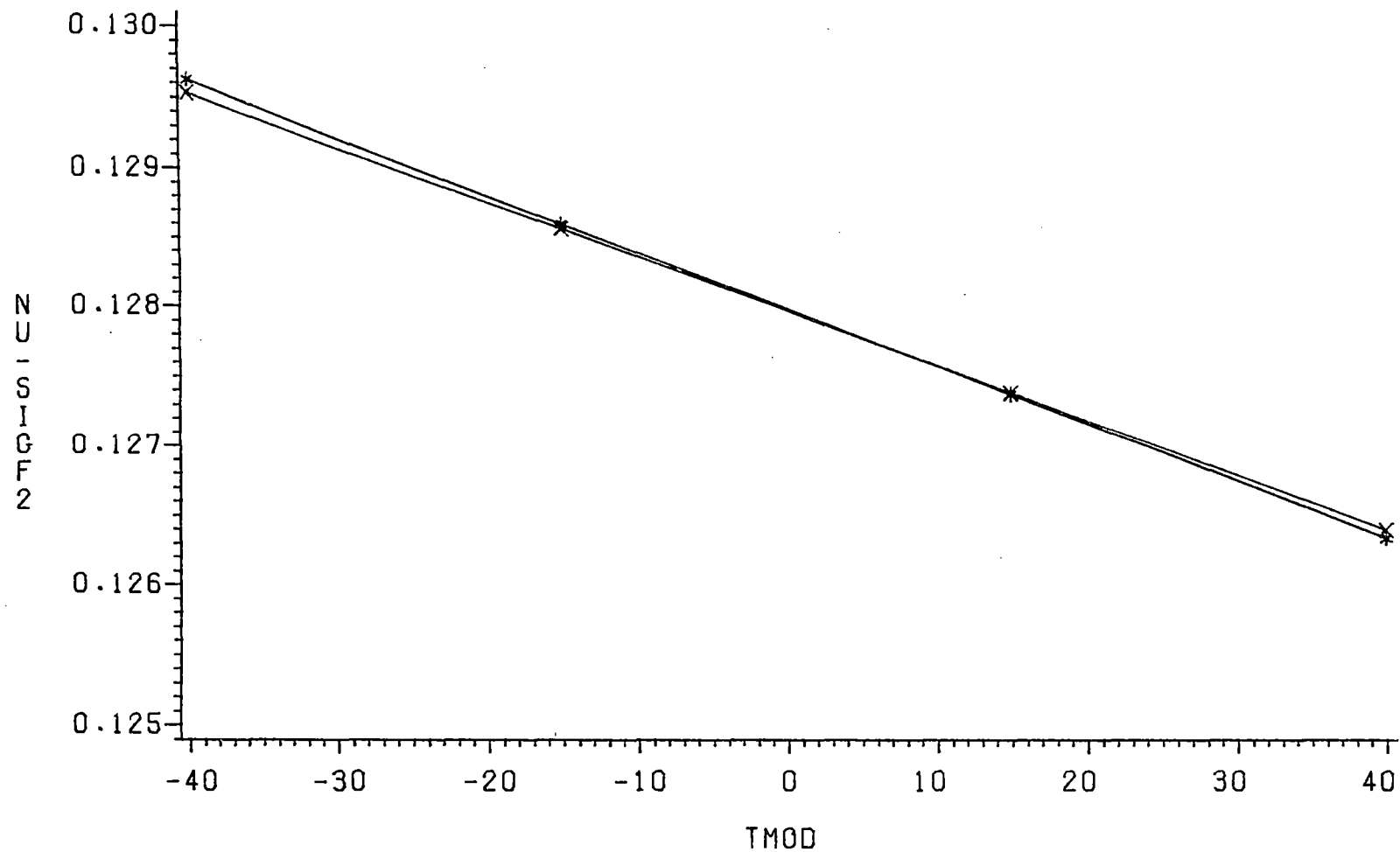


FIGURE 4.22

X NO FLUX RE-CALCULATION
* FLUX RE-CALCULATION

CROSS SECTION COMPARISON

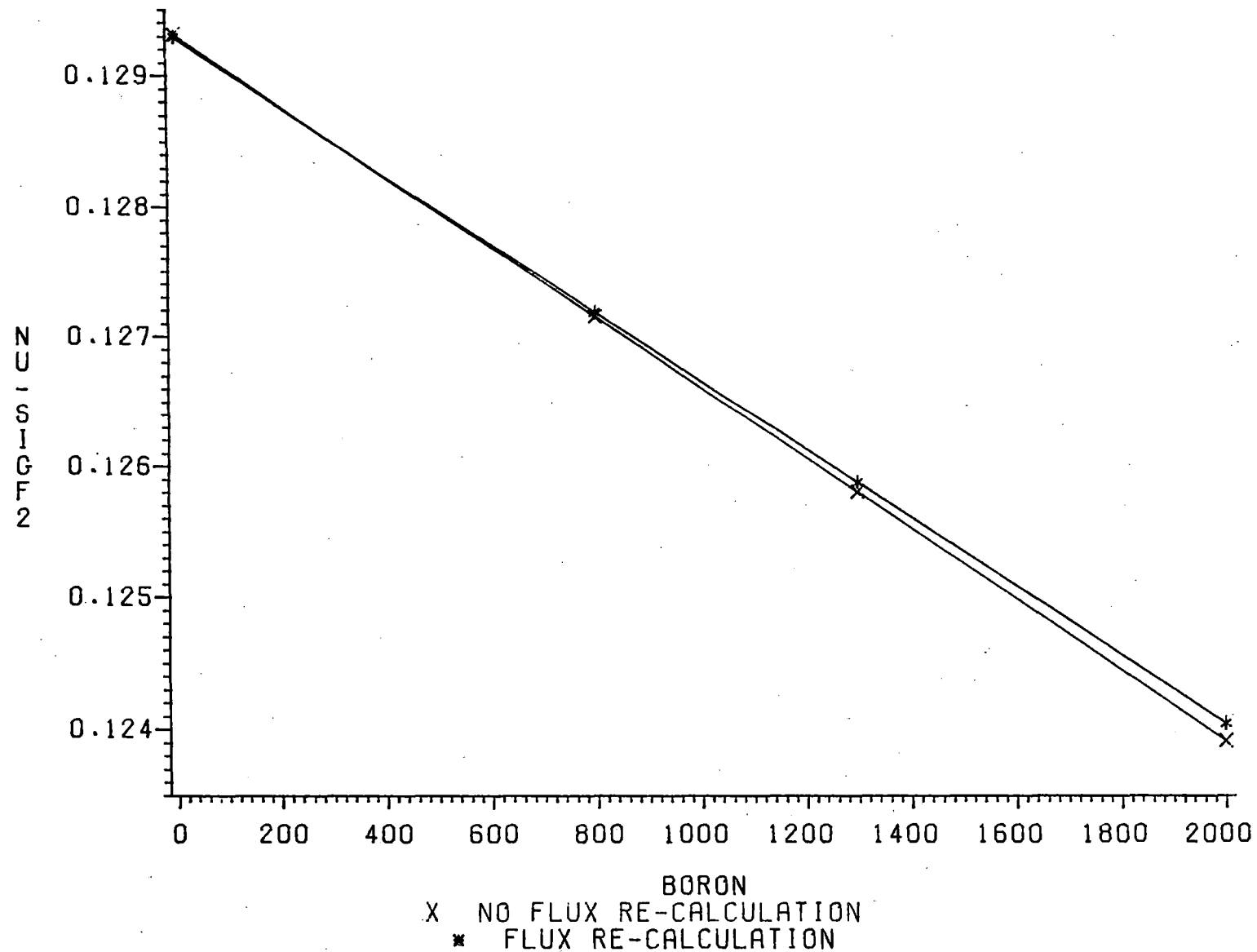


FIGURE 4.23

CROSS SECTION COMPARISON

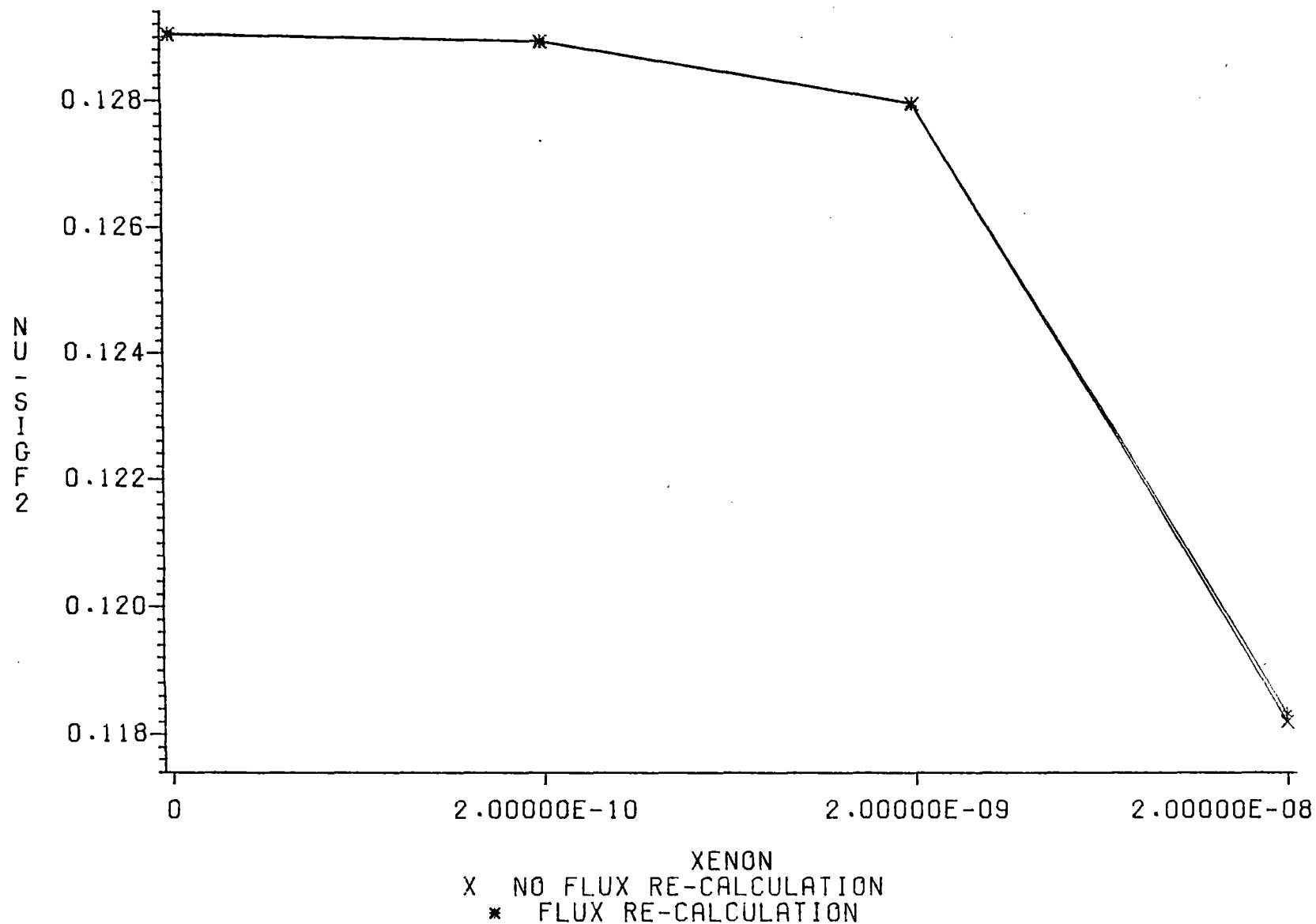
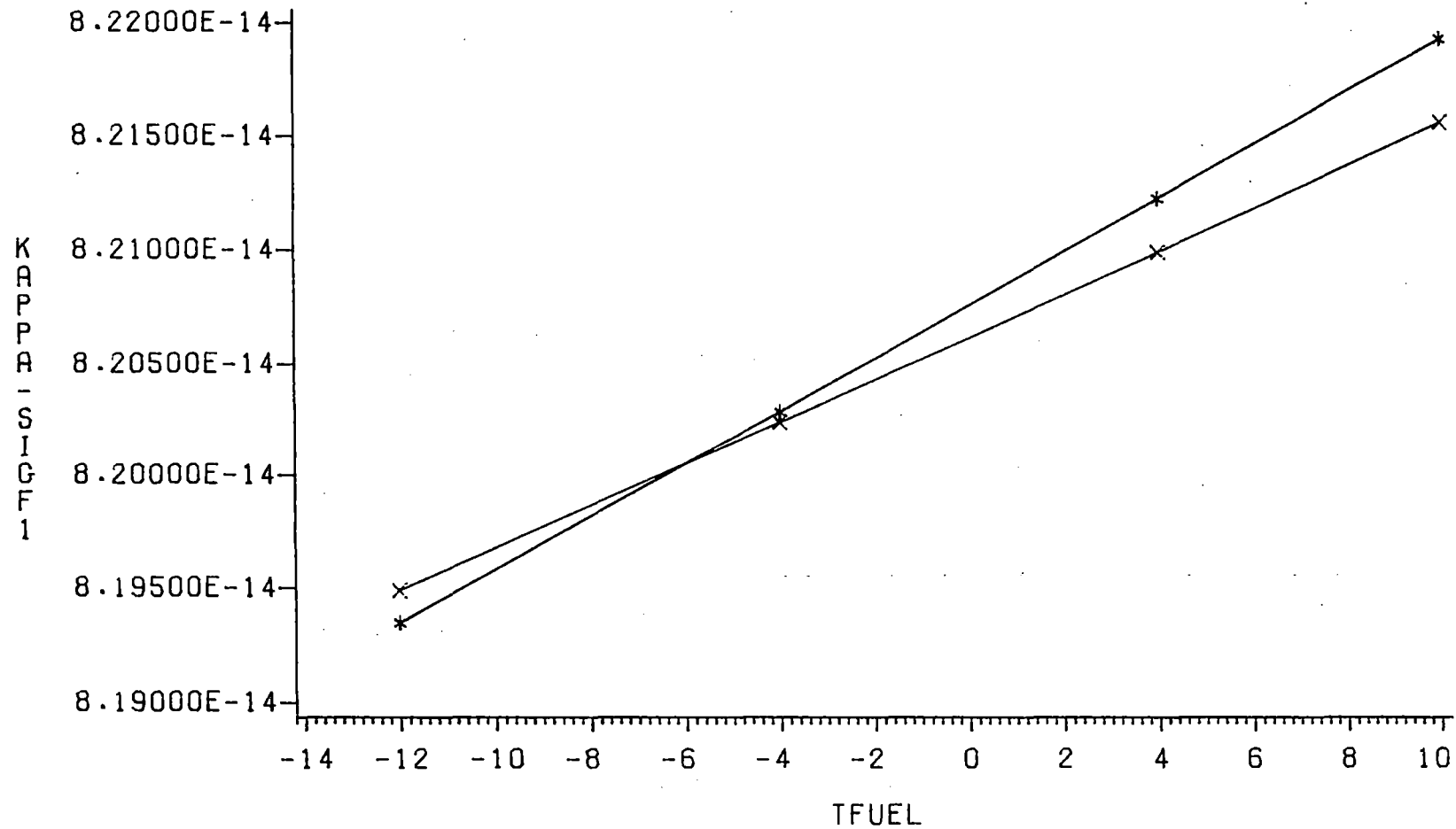


FIGURE 4.24

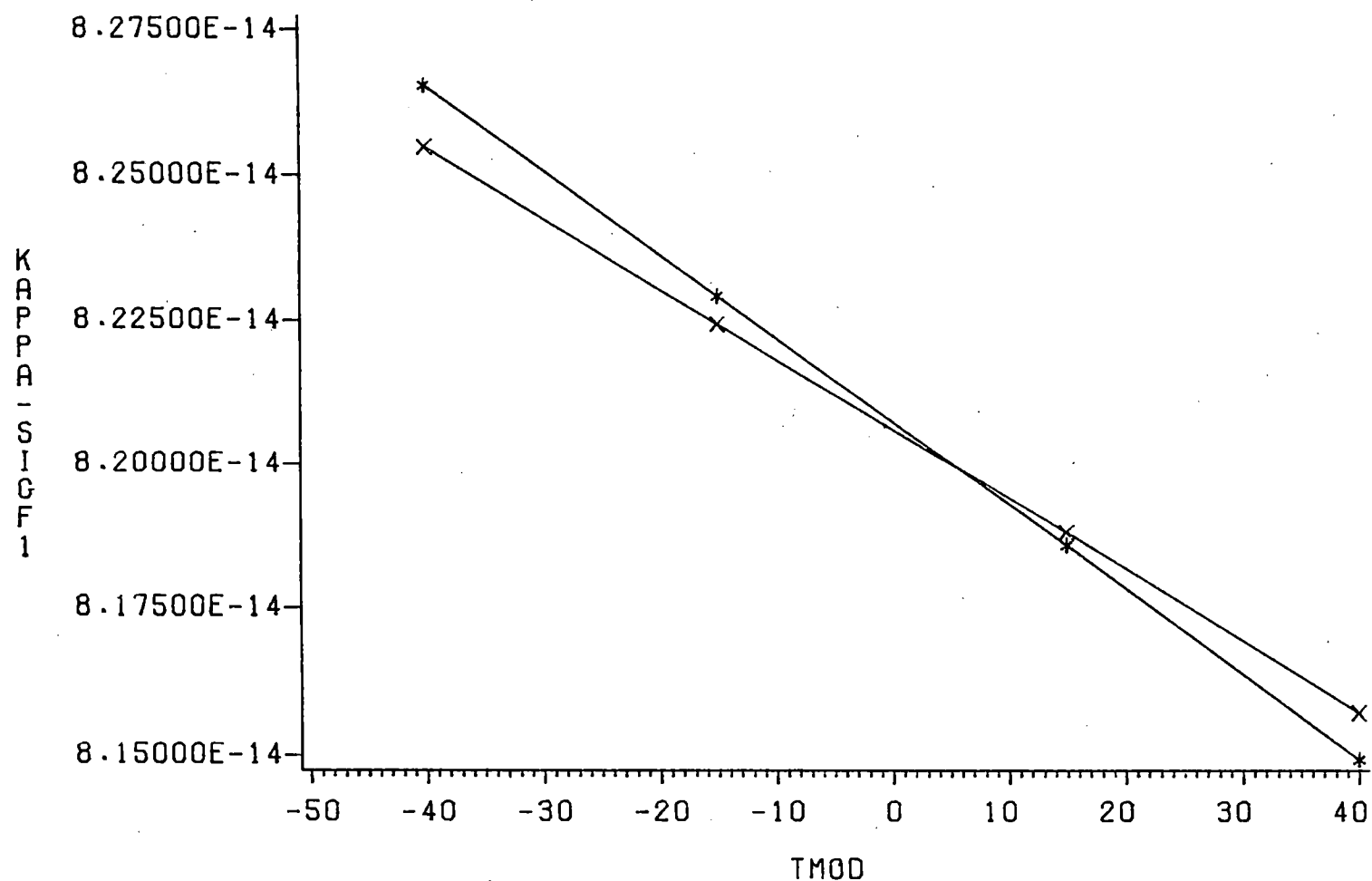
CROSS SECTION COMPARISON



X NO FLUX RE-CALCULATION
* FLUX RE-CALCULATION

FIGURE 4.25

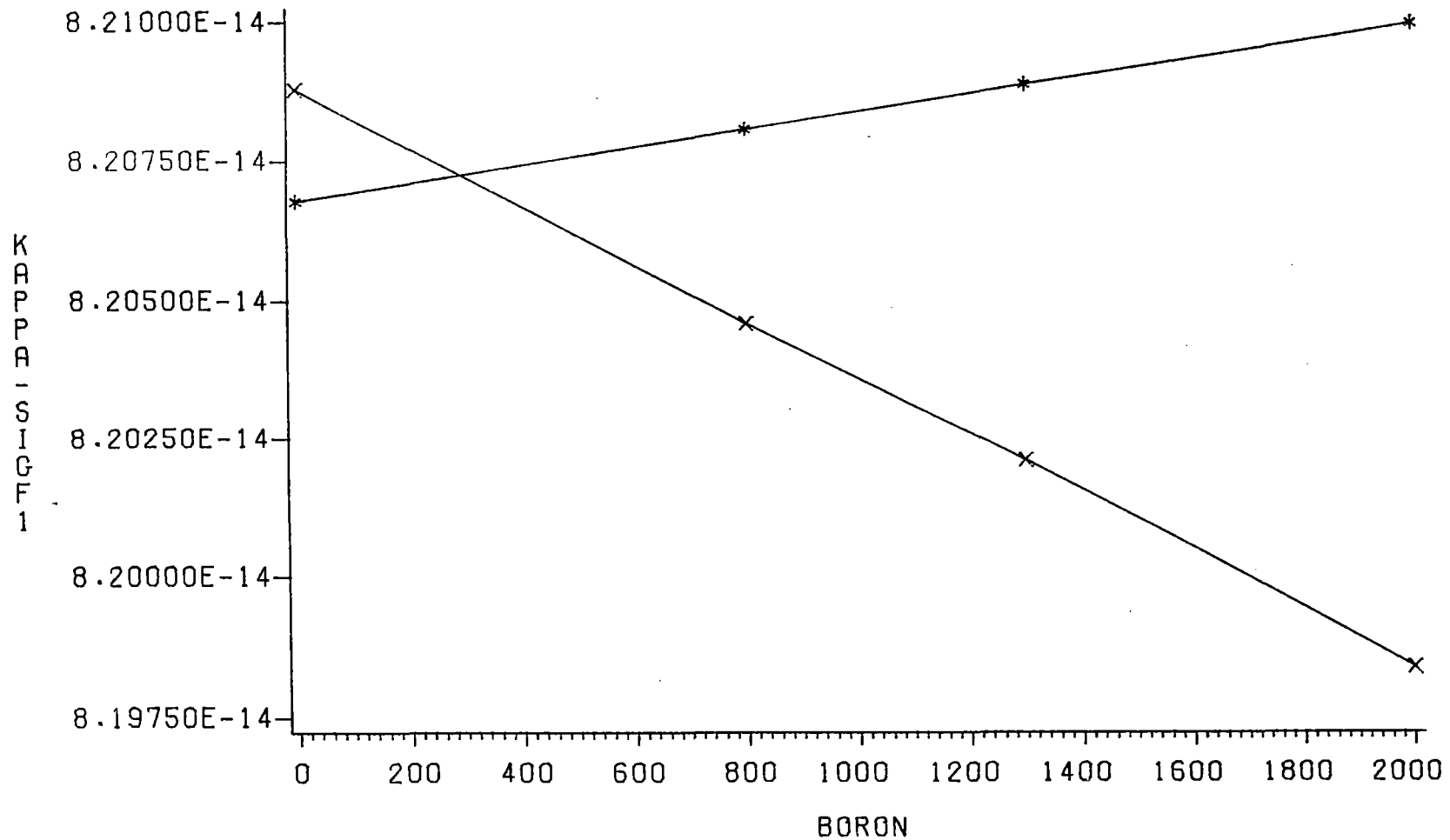
CROSS SECTION COMPARISON



X NO FLUX RE-CALCULATION
* FLUX RE-CALCULATION

FIGURE 4.26

CROSS SECTION COMPARISON



X NO FLUX RE-CALCULATION
* FLUX RE-CALCULATION

FIGURE 4.27

CROSS SECTION COMPARISON

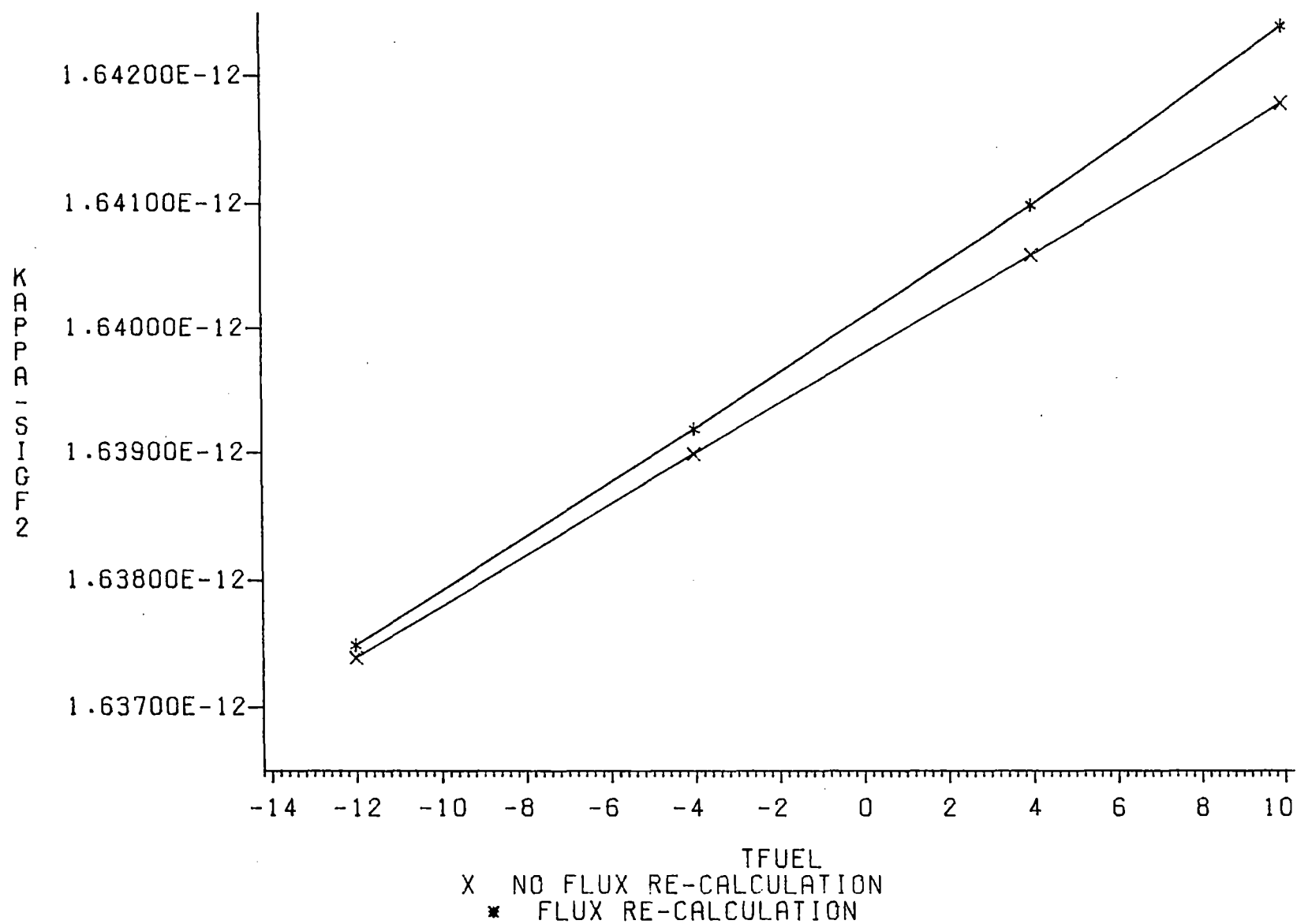


FIGURE 4.28

CROSS SECTION COMPARISON

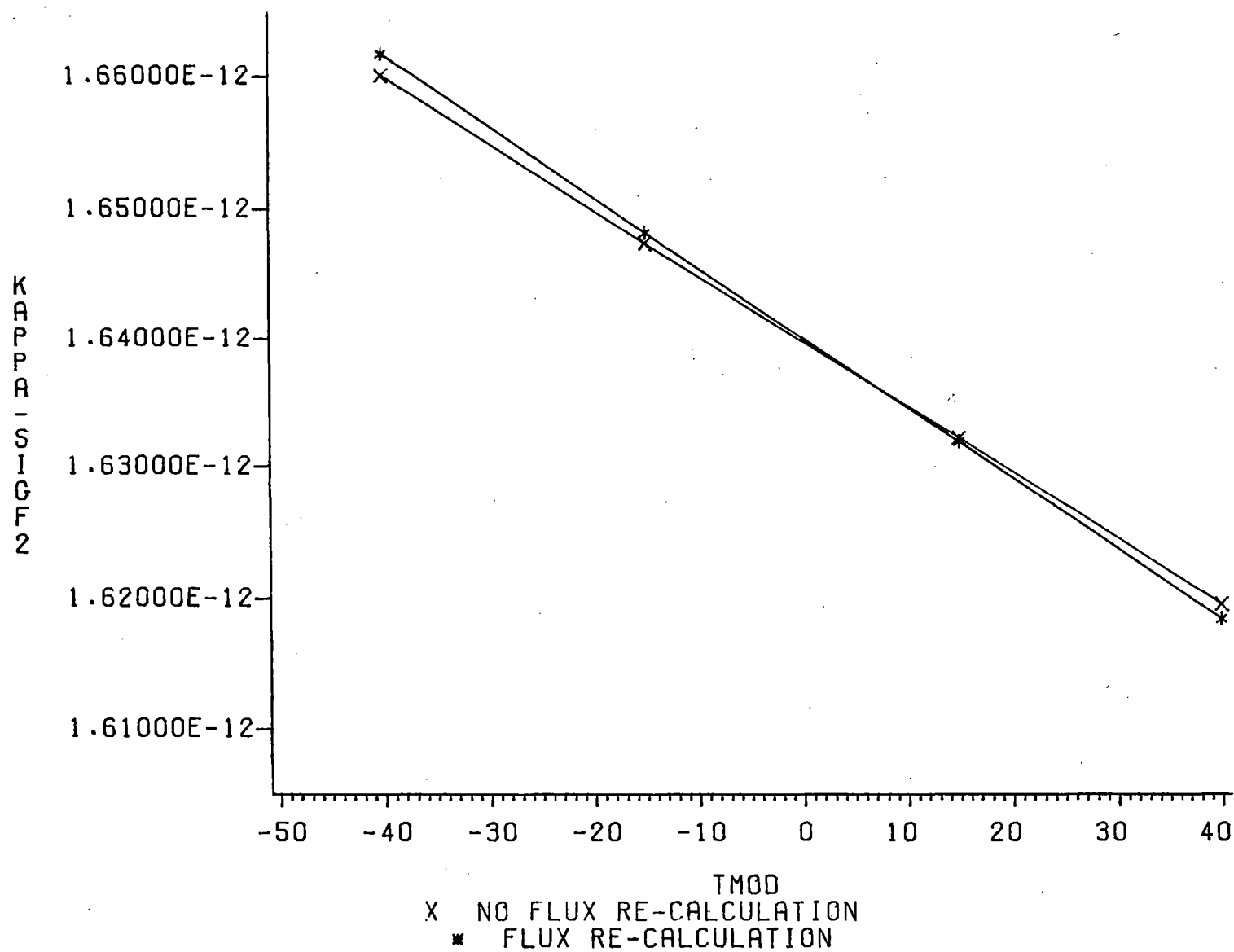


FIGURE 4.29

CROSS SECTION COMPARISON

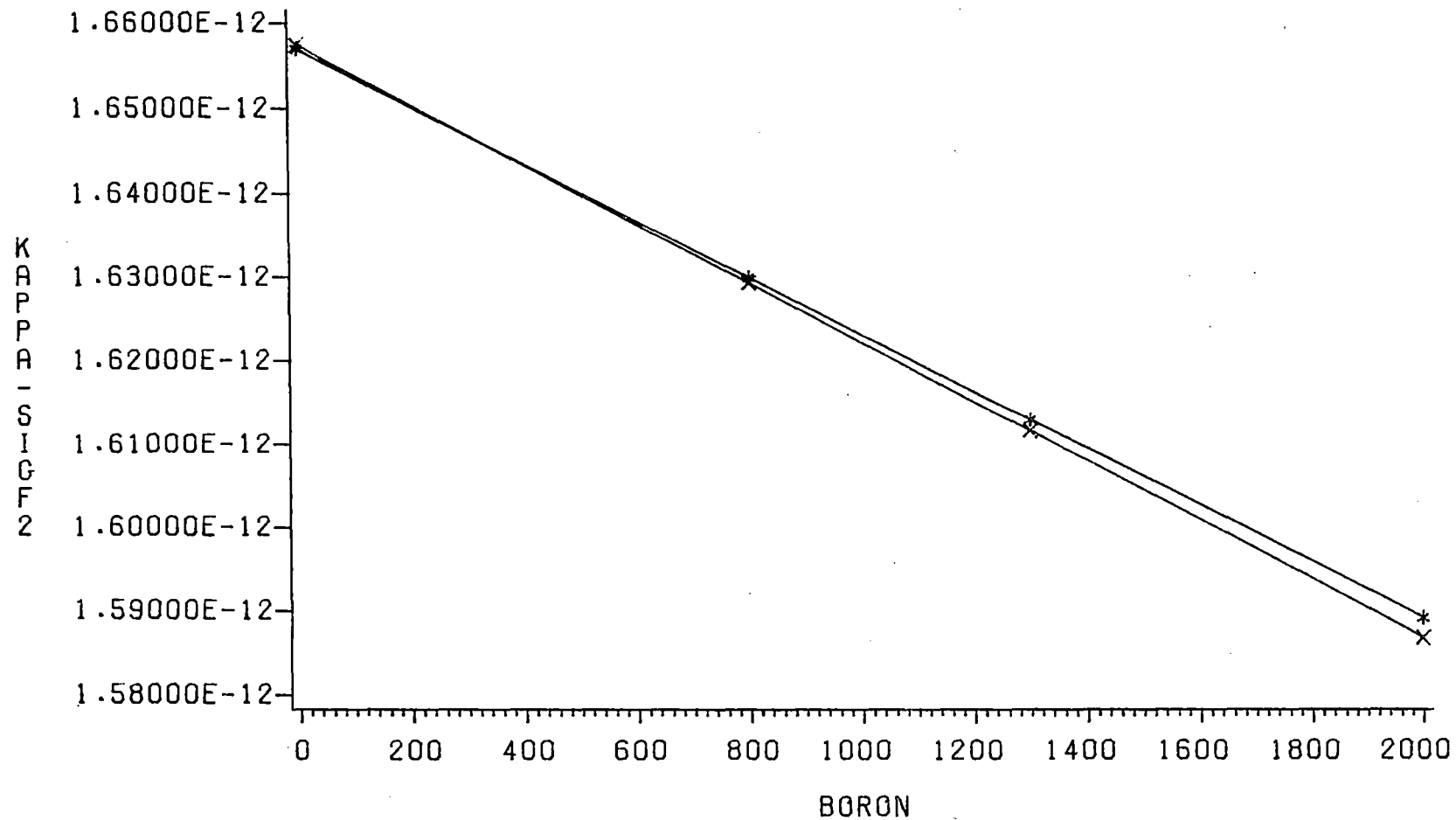


FIGURE 4.30

X NO FLUX RE-CALCULATION
* FLUX RE-CALCULATION

CROSS SECTION COMPARISON

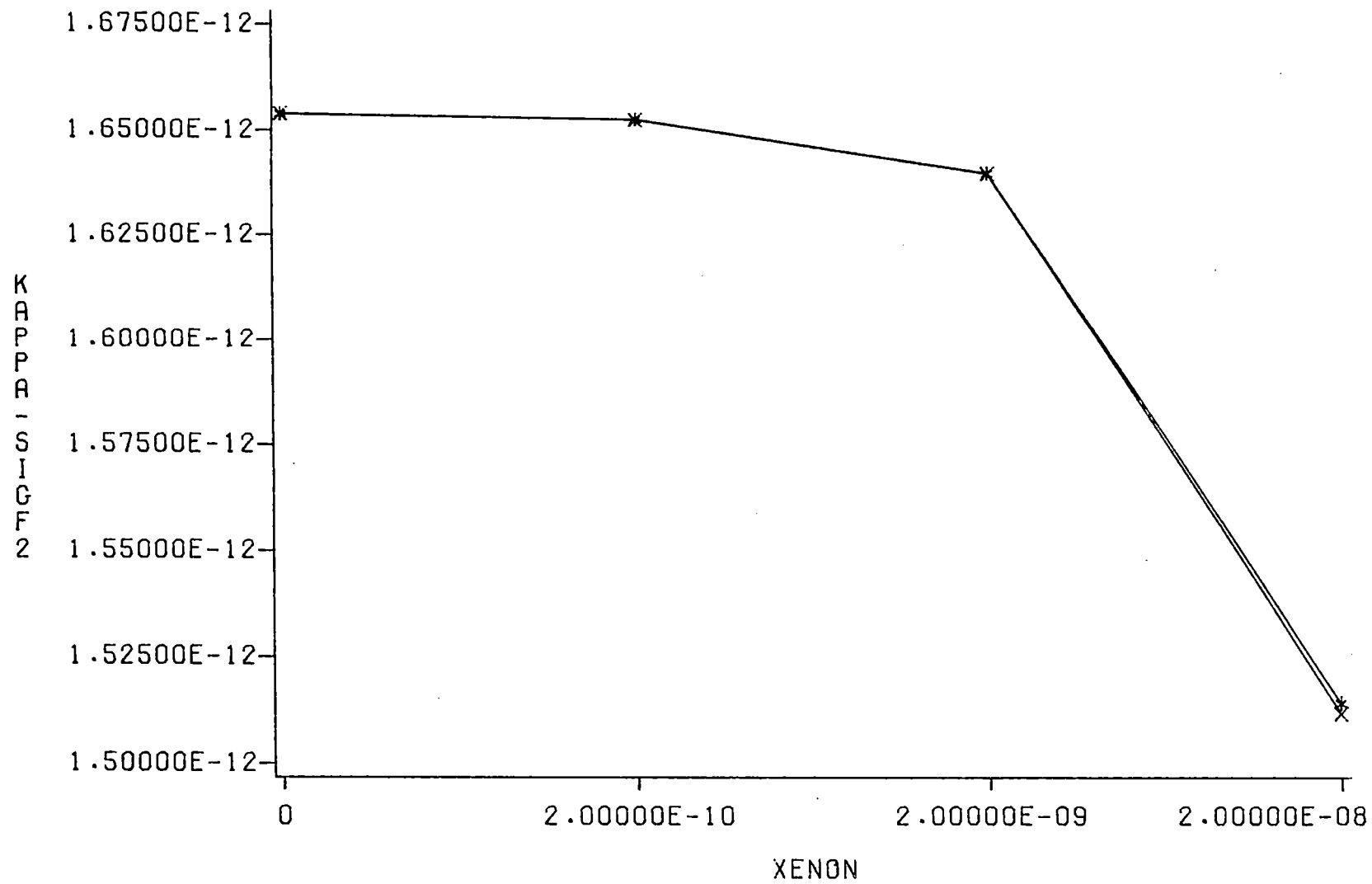


FIGURE 4.31

X NO FLUX RE-CALCULATION
* FLUX RE-CALCULATION

FIGURE 5.1

1-D TO 3-D AXIAL POWER COMPARISON 0 MWD/MTU

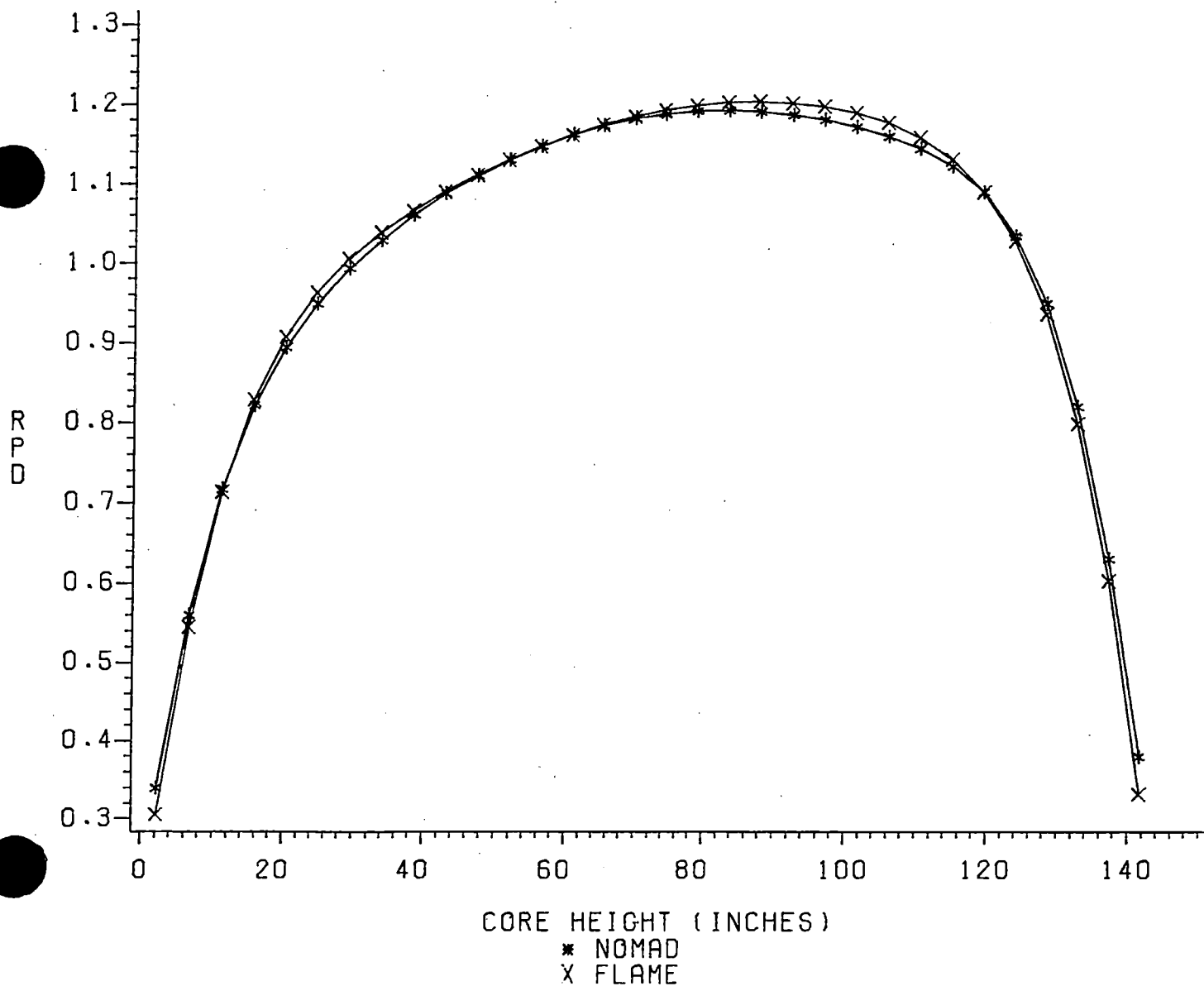


FIGURE 5.2

1-D TO 3-D AXIAL POWER COMPARISON 150 MWD/MTU

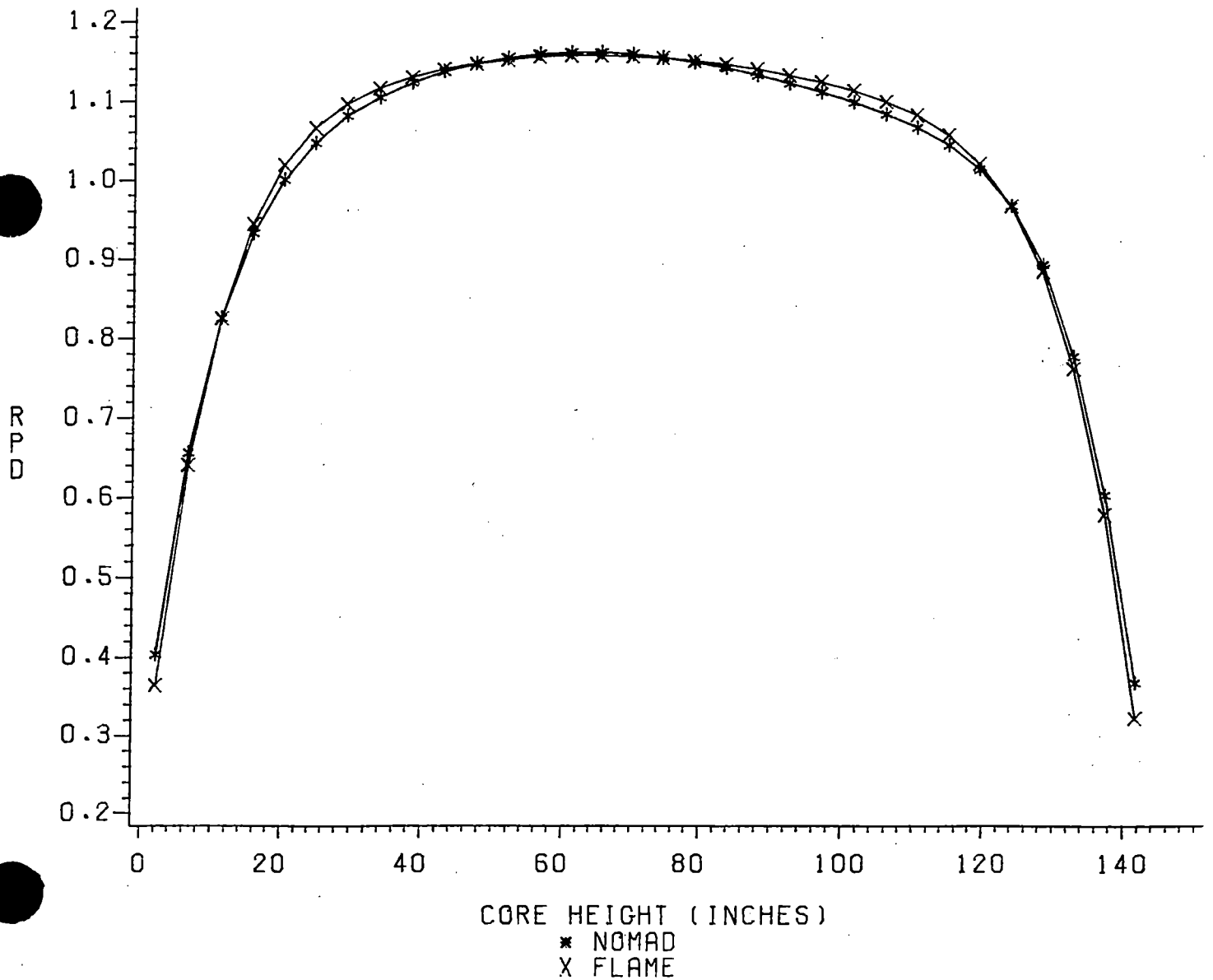


FIGURE 5.3

1-D TO 3-D AXIAL POWER COMPARISON 1000 MWD/MTU

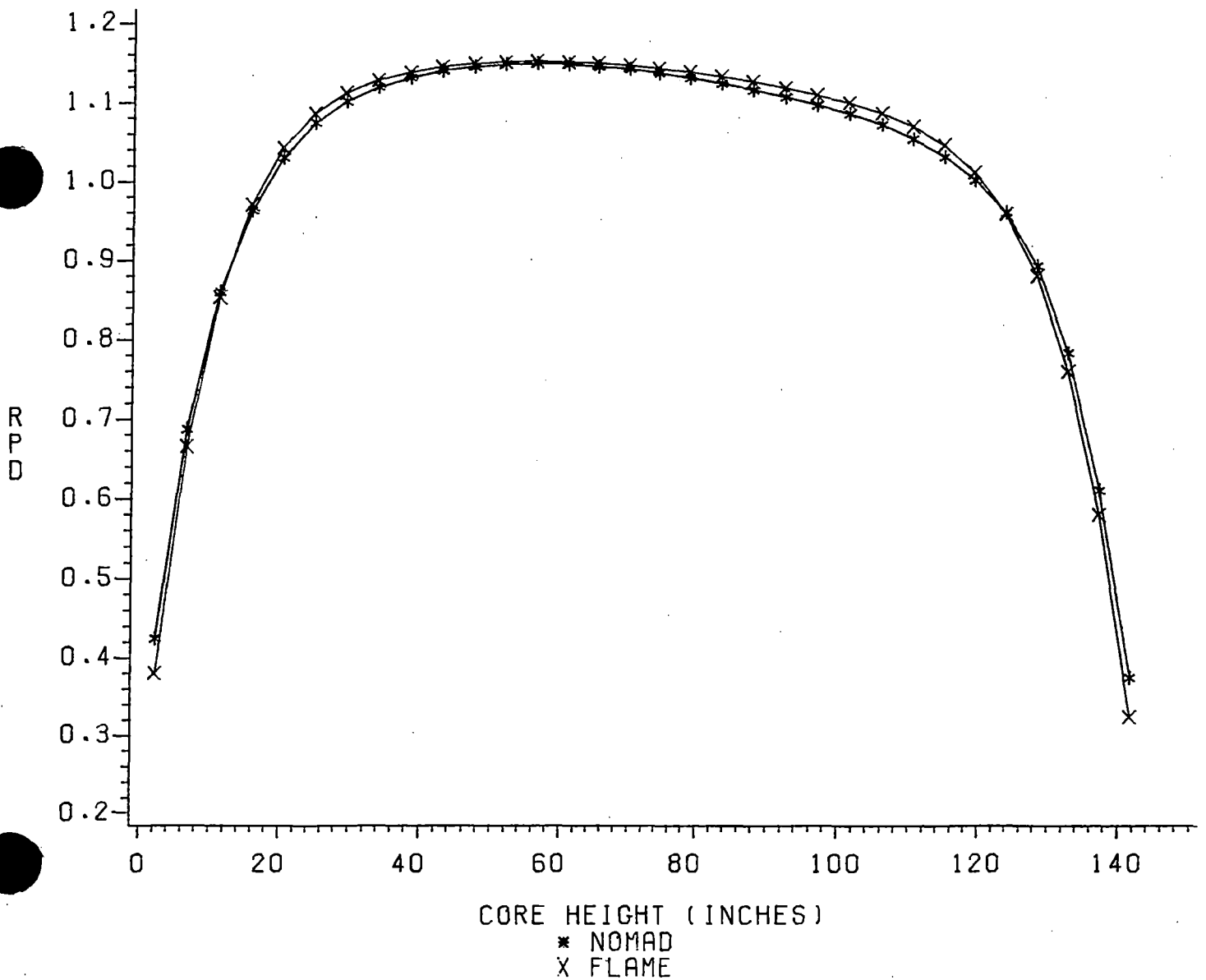


FIGURE 5.4

1-D TO 3-D AXIAL POWER COMPARISON 3000 MWD/MTU

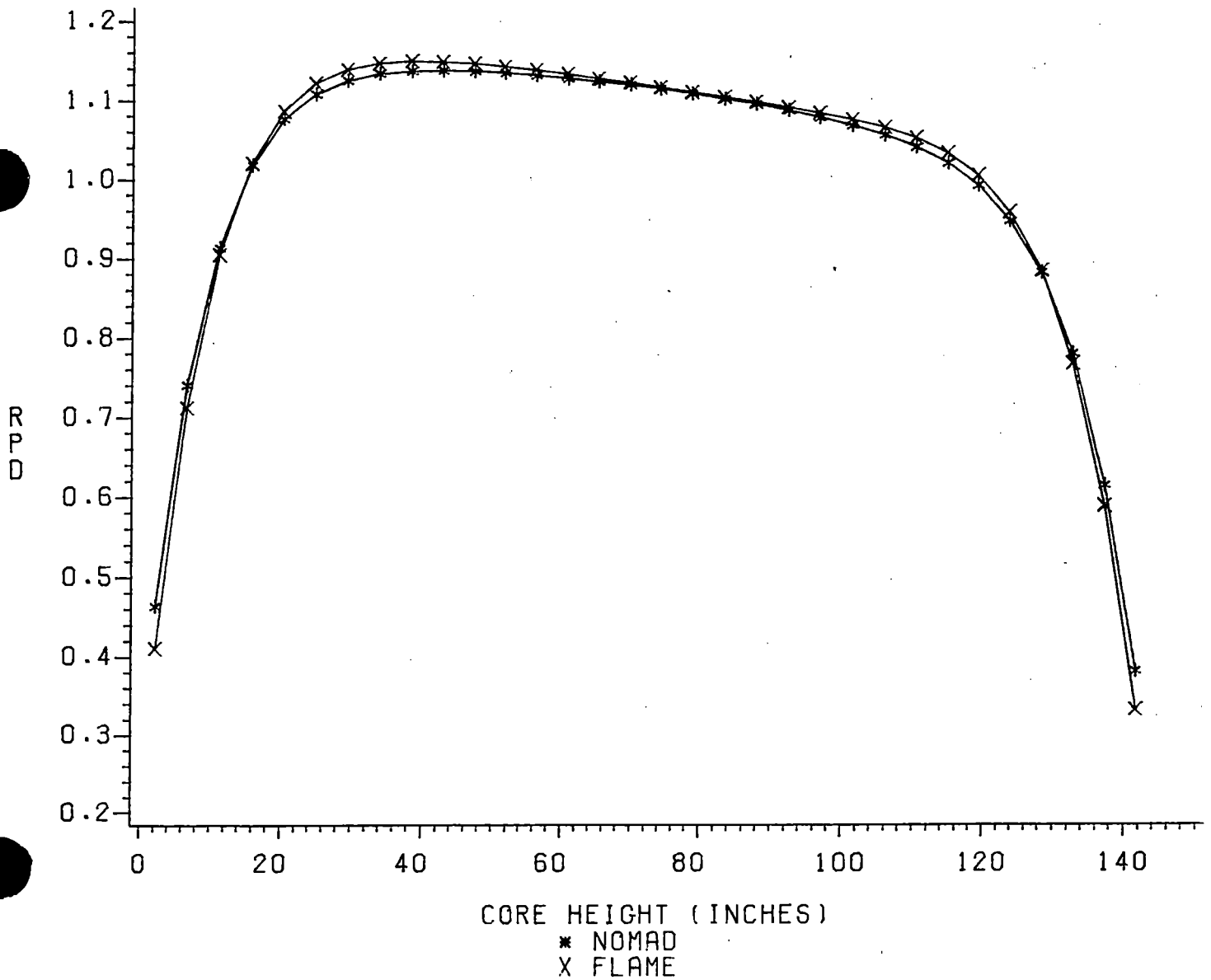


FIGURE 5.5

1-D TO 3-D AXIAL POWER COMPARISON 5000 MWD/MTU

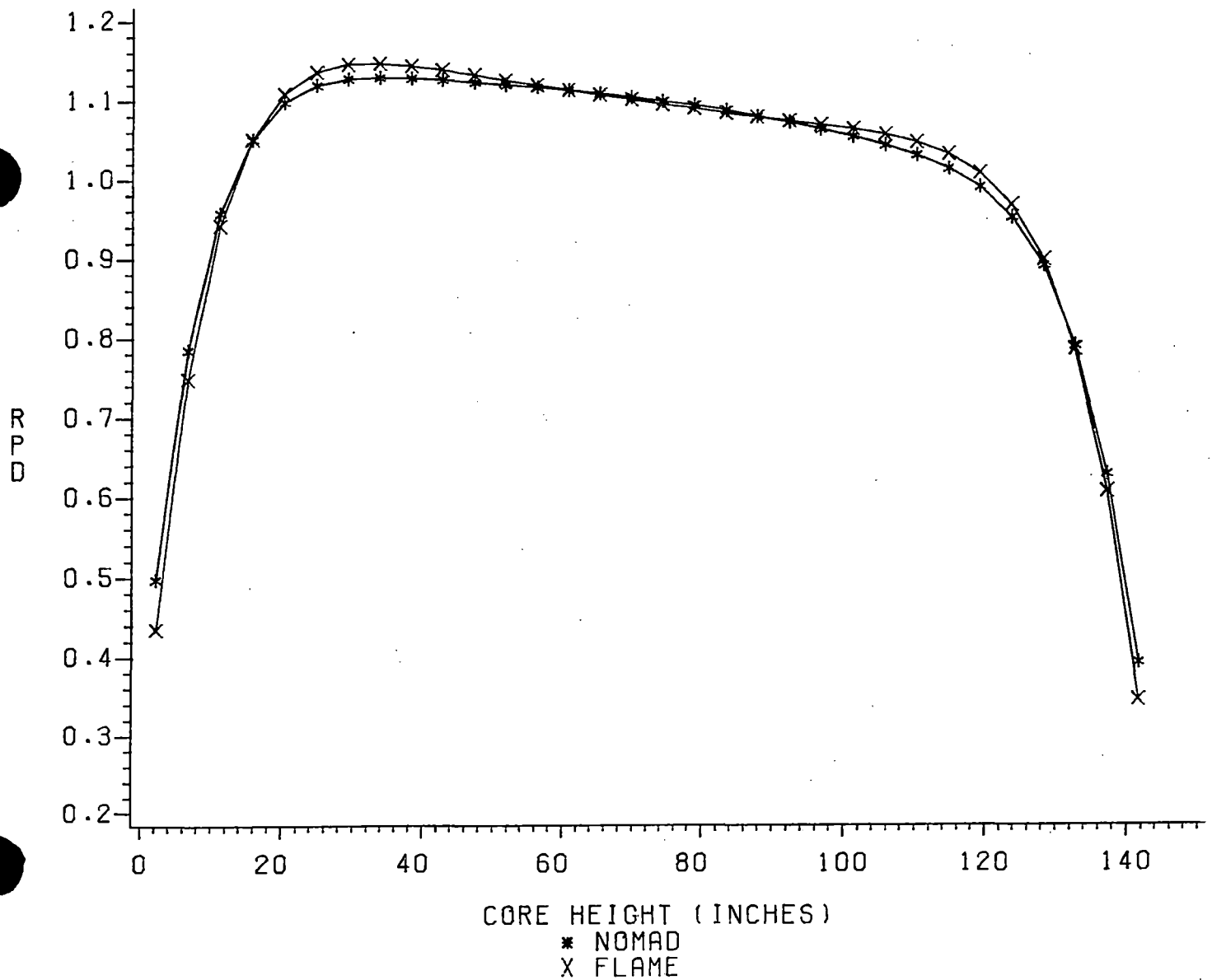


FIGURE 5.6

1-D TO 3-D AXIAL POWER COMPARISON 6000 MWD/MTU

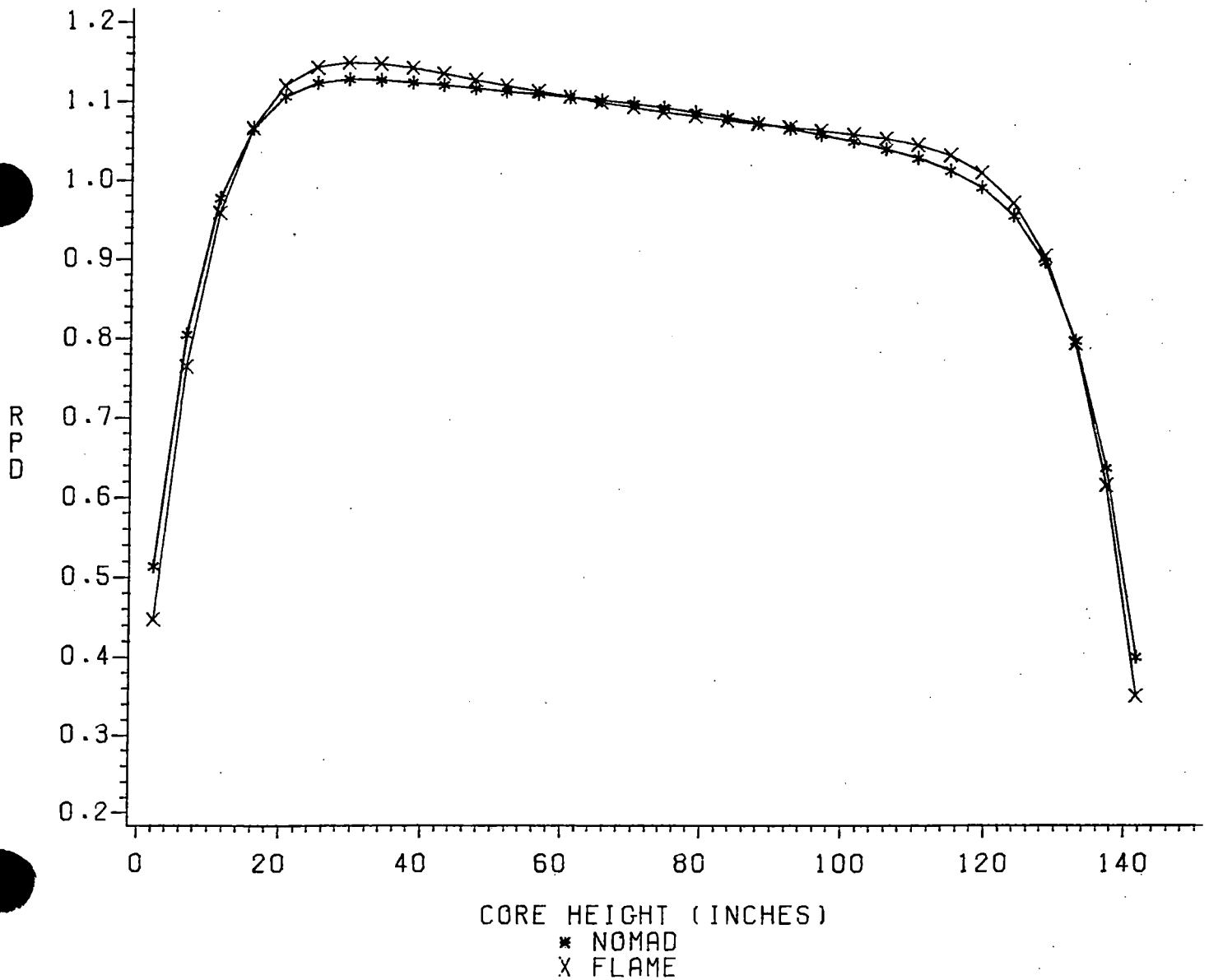


FIGURE 5.7

1-D TO 3-D AXIAL POWER COMPARISON 7000 MWD/MTU

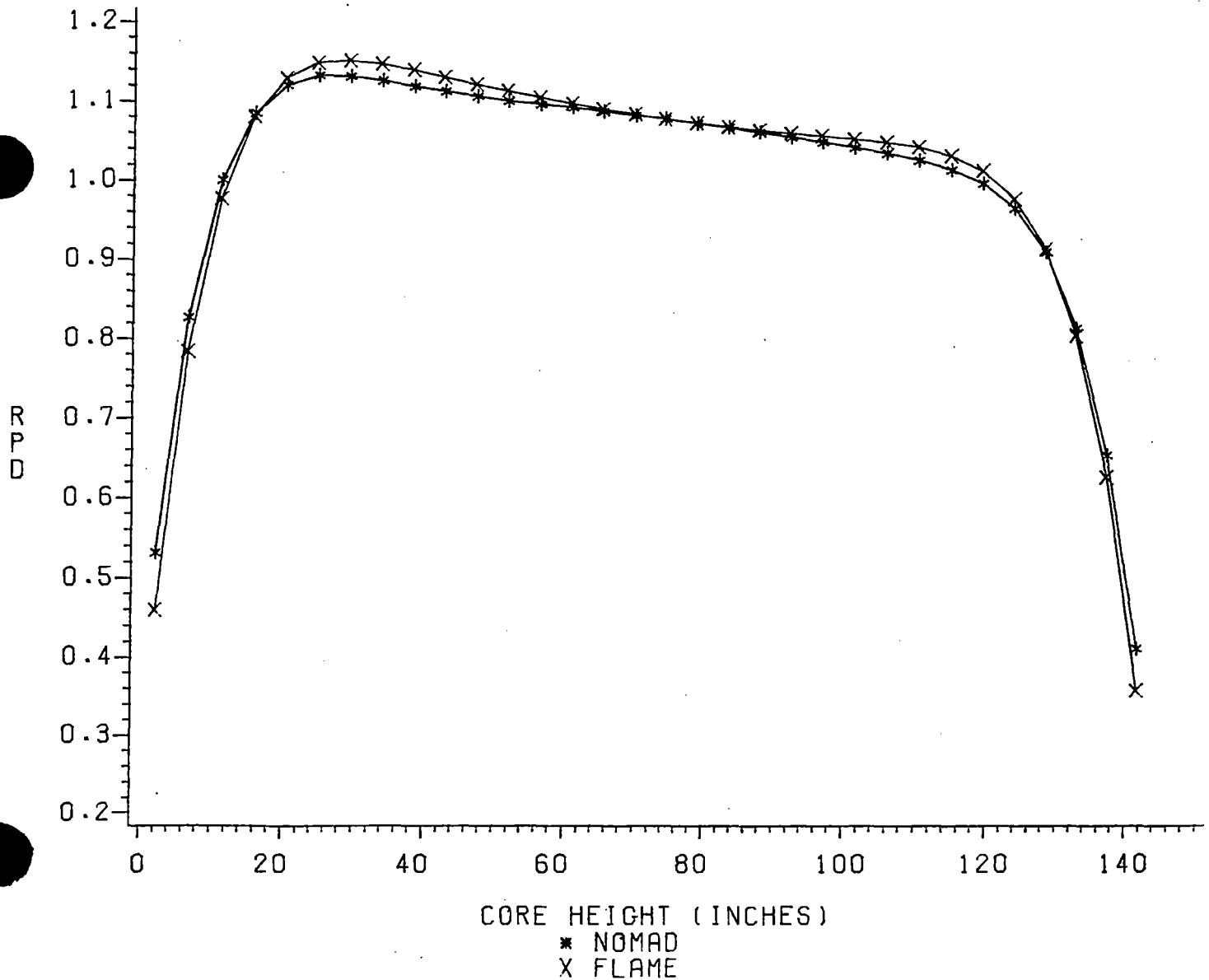


FIGURE 5.8

1-D TO 3-D AXIAL POWER COMPARISON 9000 MWD/MTU

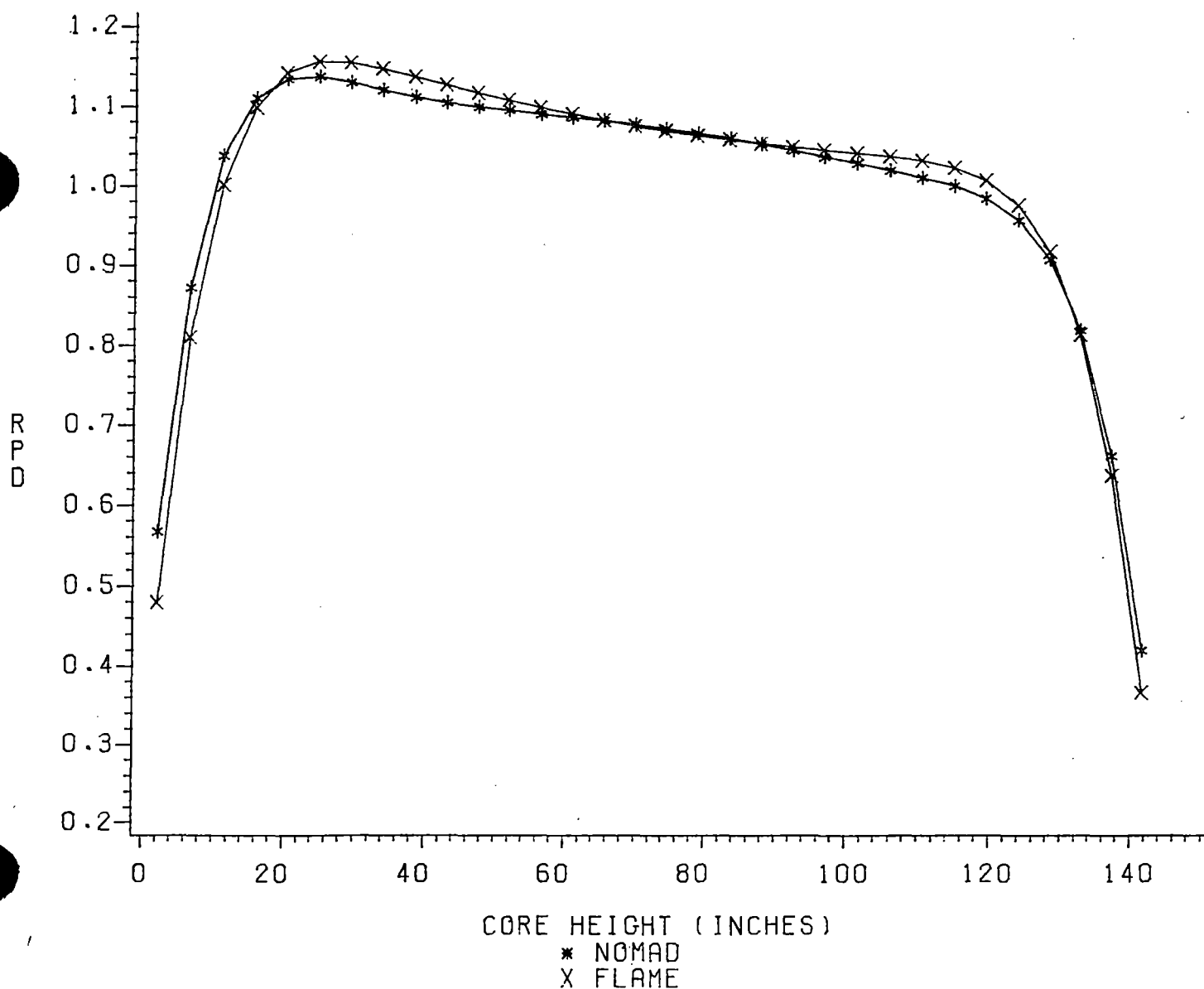


FIGURE 5.9

1-D TO 3-D AXIAL POWER COMPARISON 11000 MWD/MTU

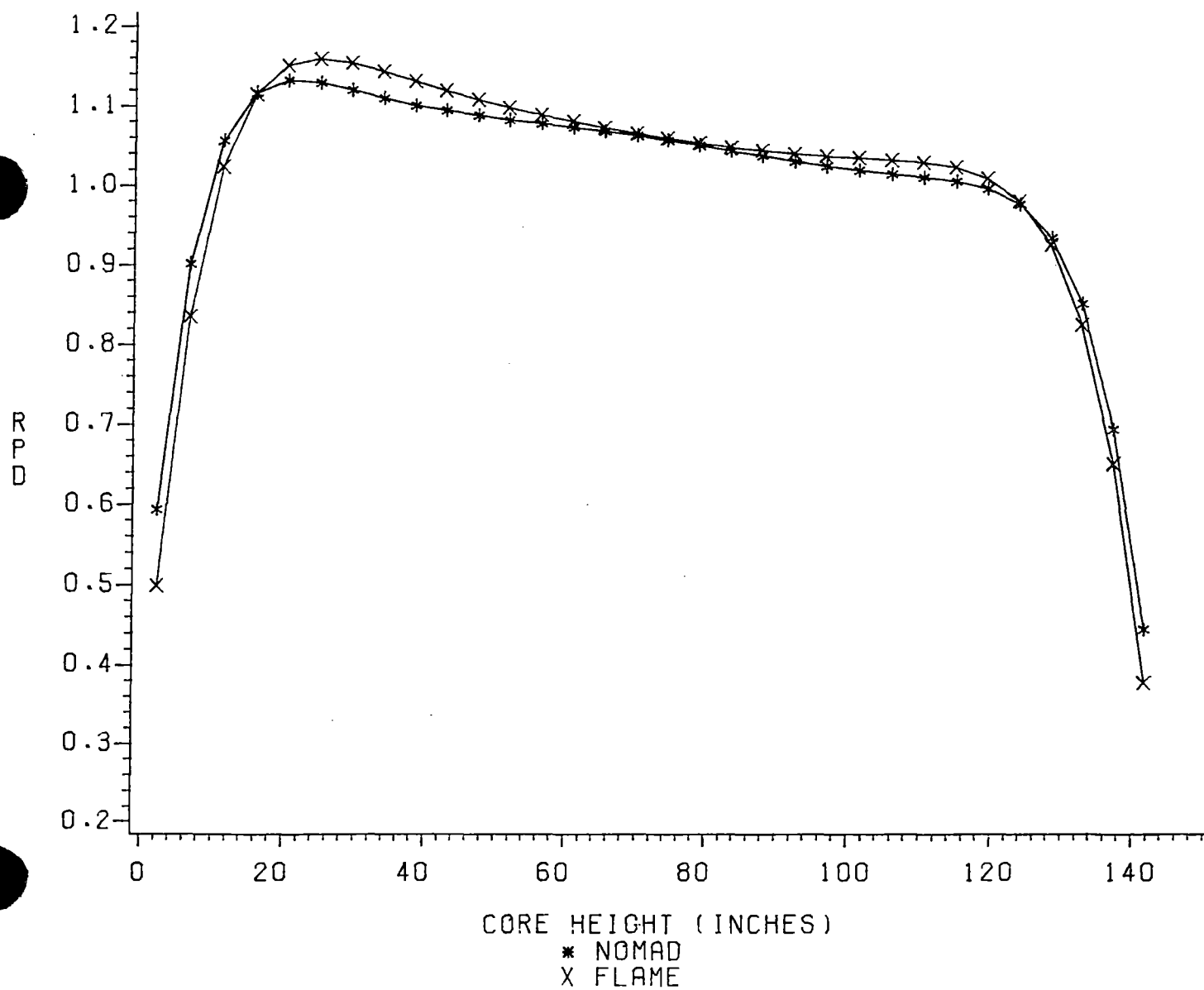


FIGURE 5.10

1-D TO 3-D AXIAL POWER COMPARISON 12000 MWD/MTU

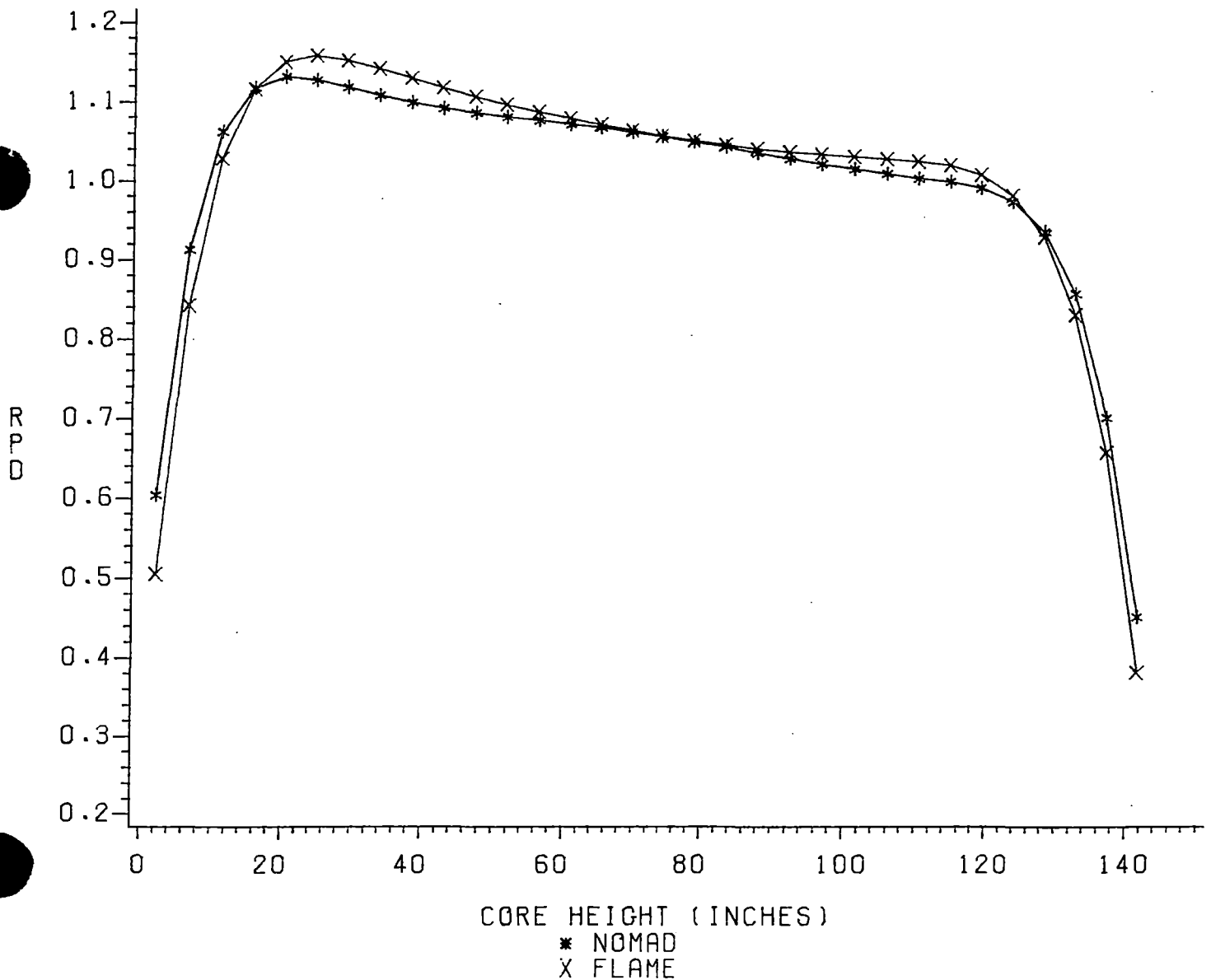
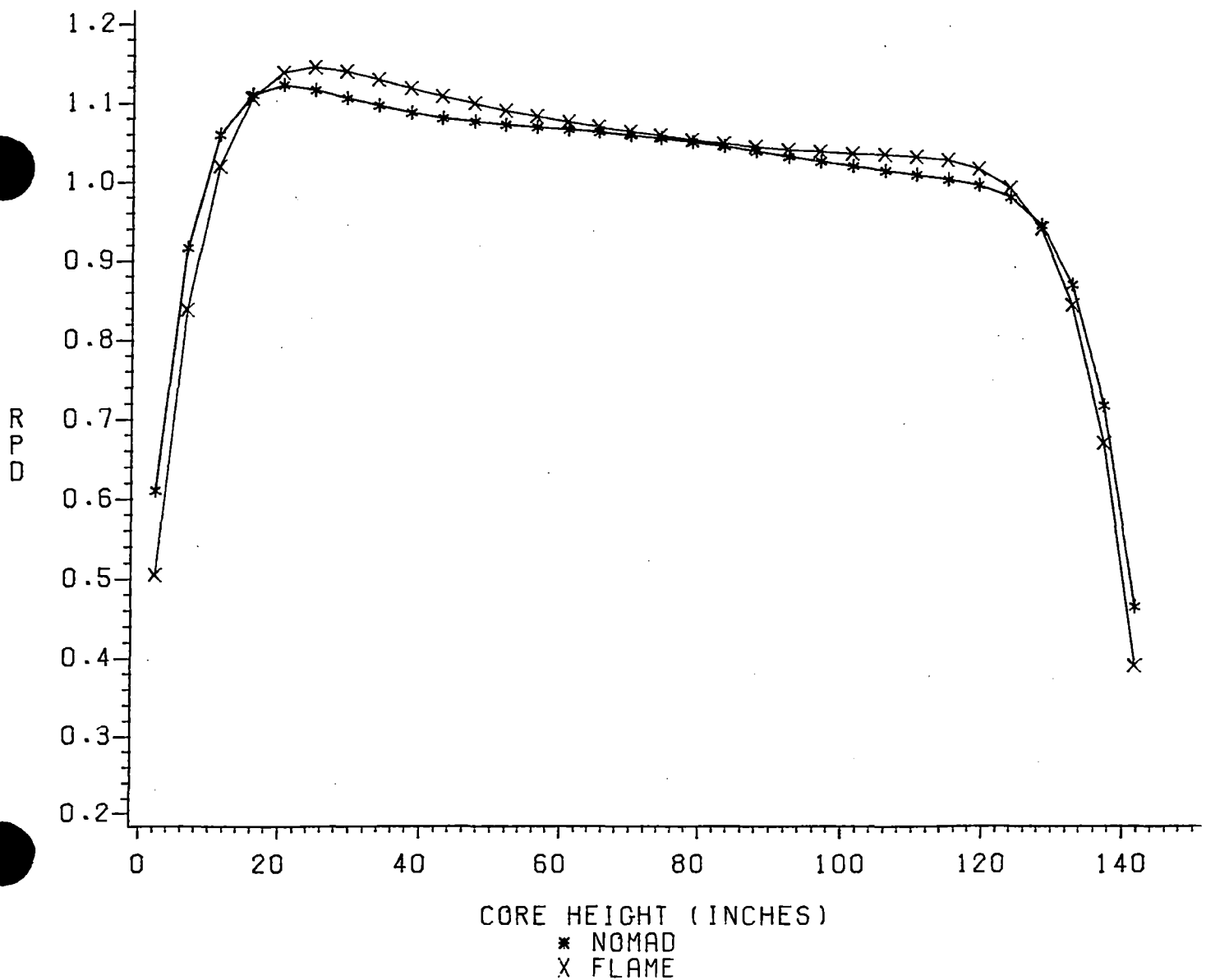


FIGURE 5.11

1-D TO 3-D AXIAL POWER COMPARISON 13000 MWD/MTU



PLOT OF FLAM3*NOMADFIX SYMBOL IS VALUE OF FLAG

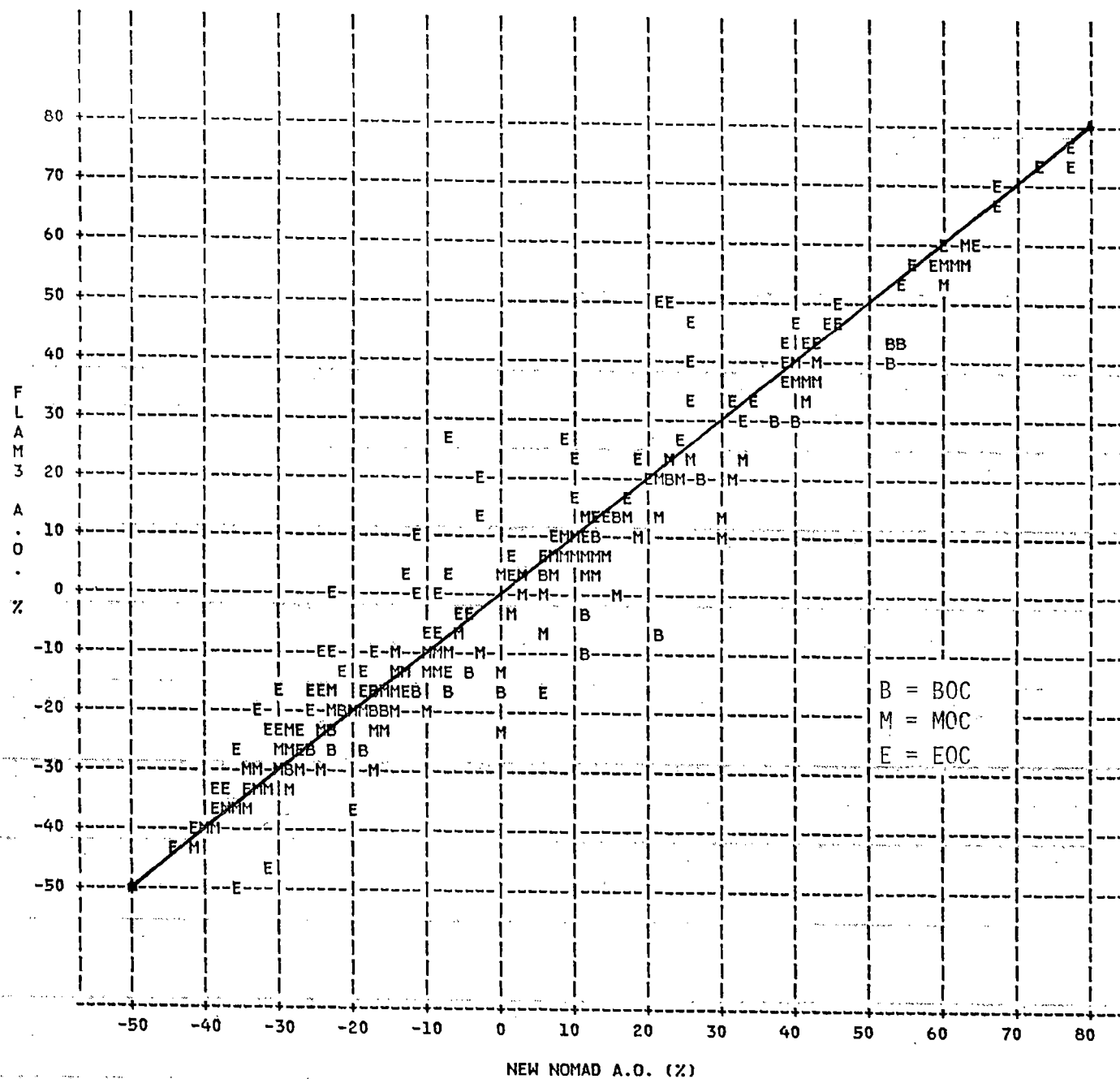


FIGURE 6.1

NOTE: 79 OBS HIDDEN

N1C2 70 LOAD REDUCTION TEST AXIAL FLUX DIFFERENCE

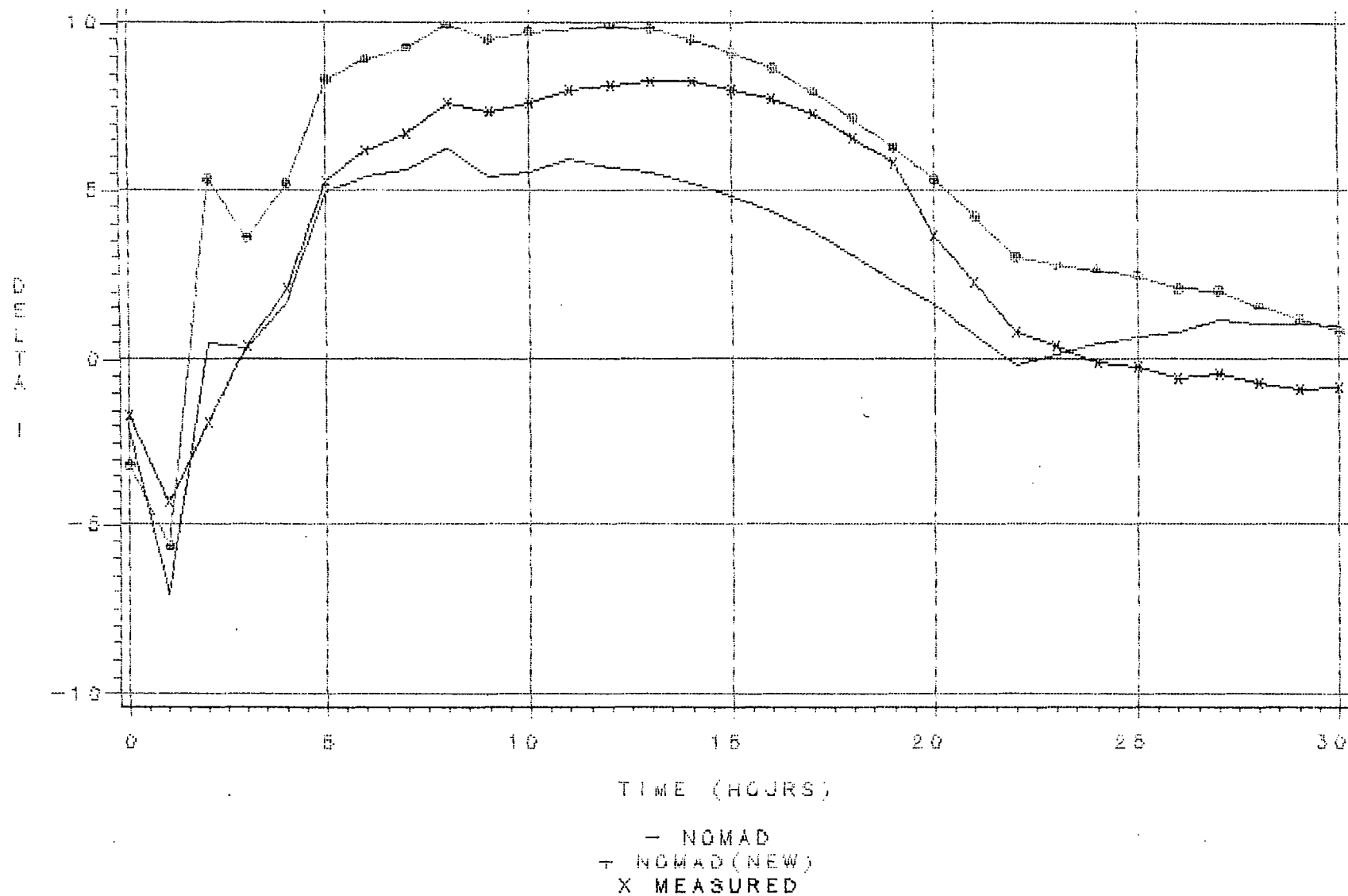


FIGURE 6.2

N1C2 70 LOAD REDUCTION TEST CRITICAL BORON CONCENTRATION

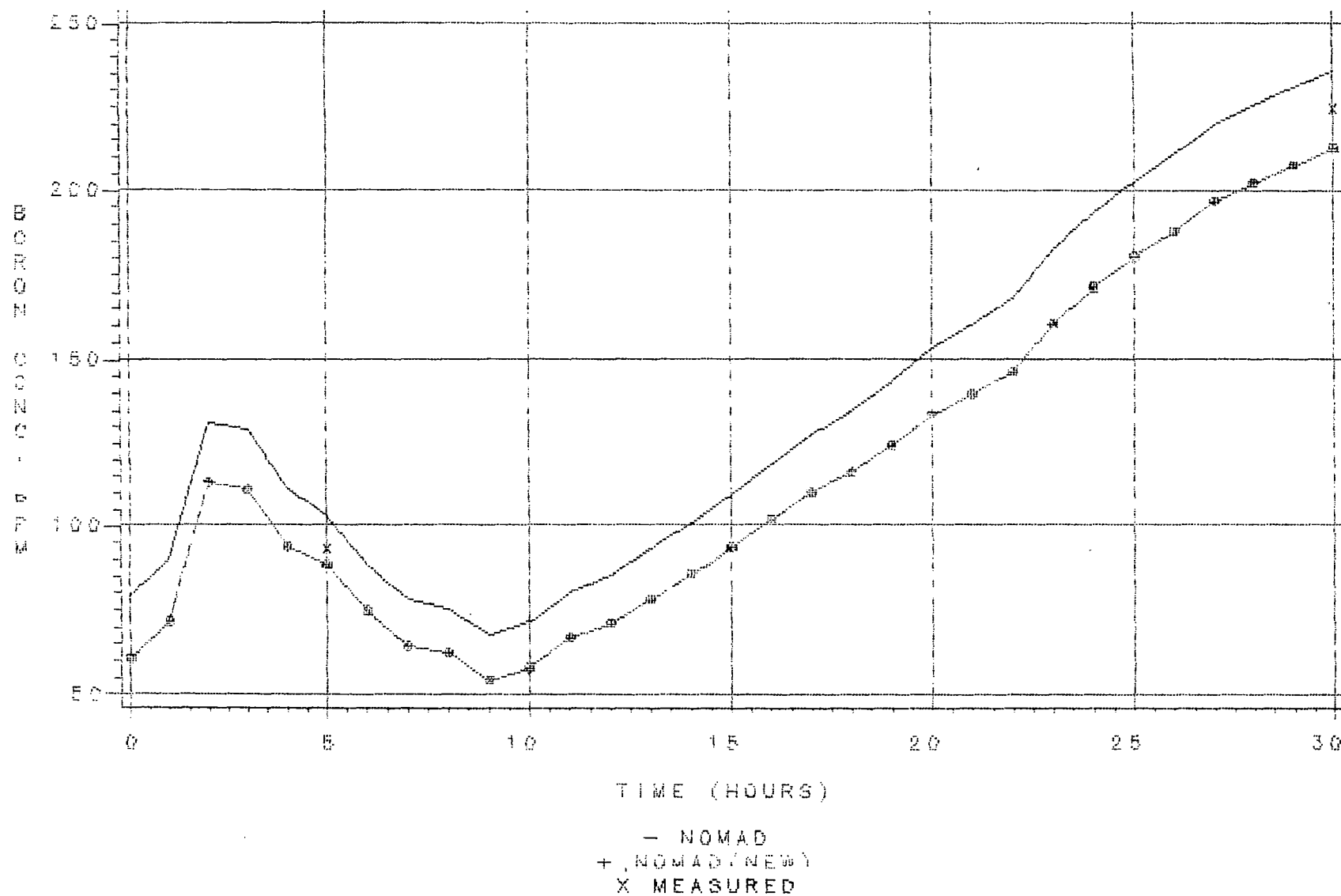


FIGURE 6.3

N1C3 SHUTDOWN/RETURN TO POWER (CASE 1) DELTA-I

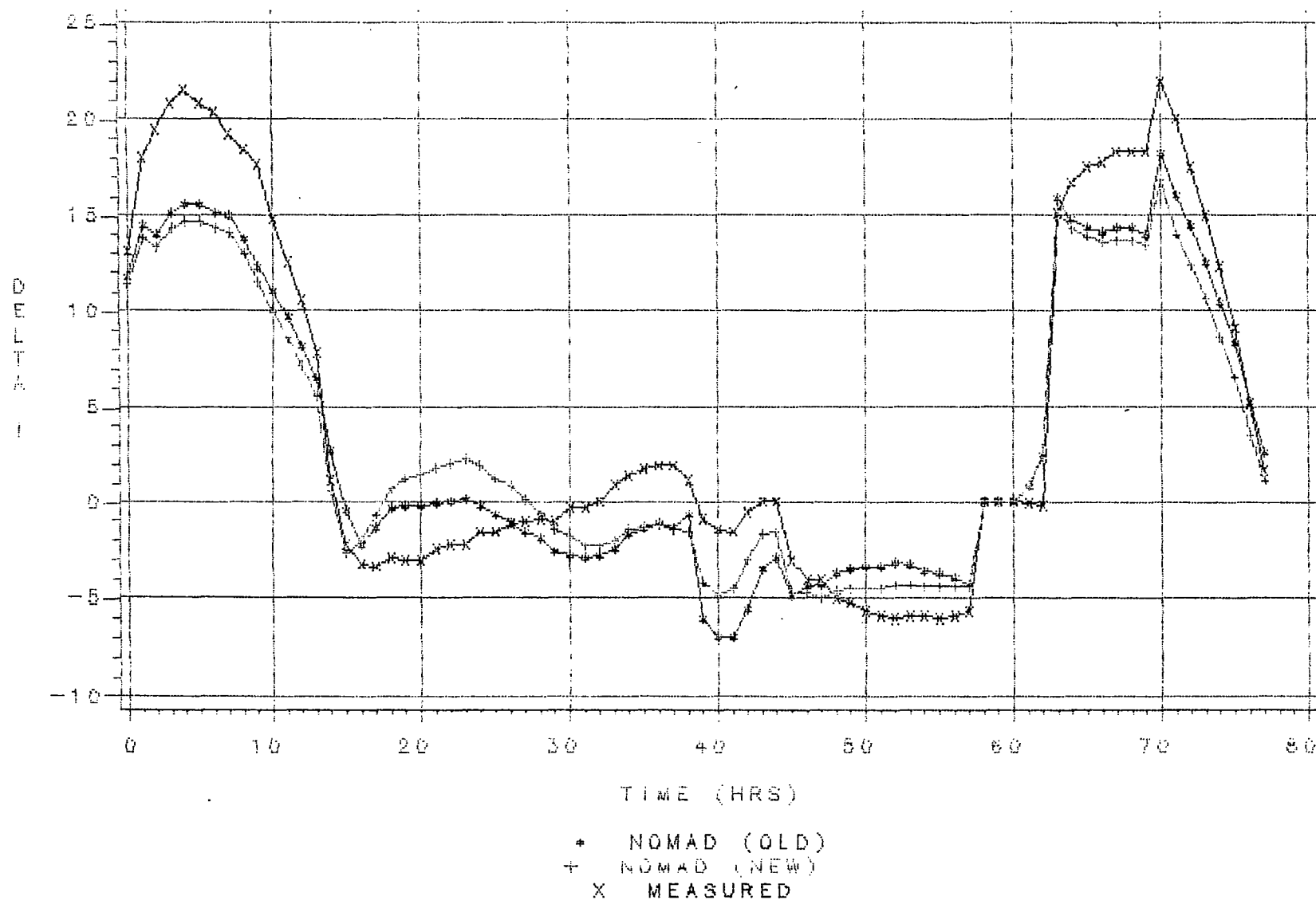


FIGURE 6.4

N1C3 SHUTDOWN/RETURN TO POWER (CASE 1) CRITICAL BORON CONCENTRATION

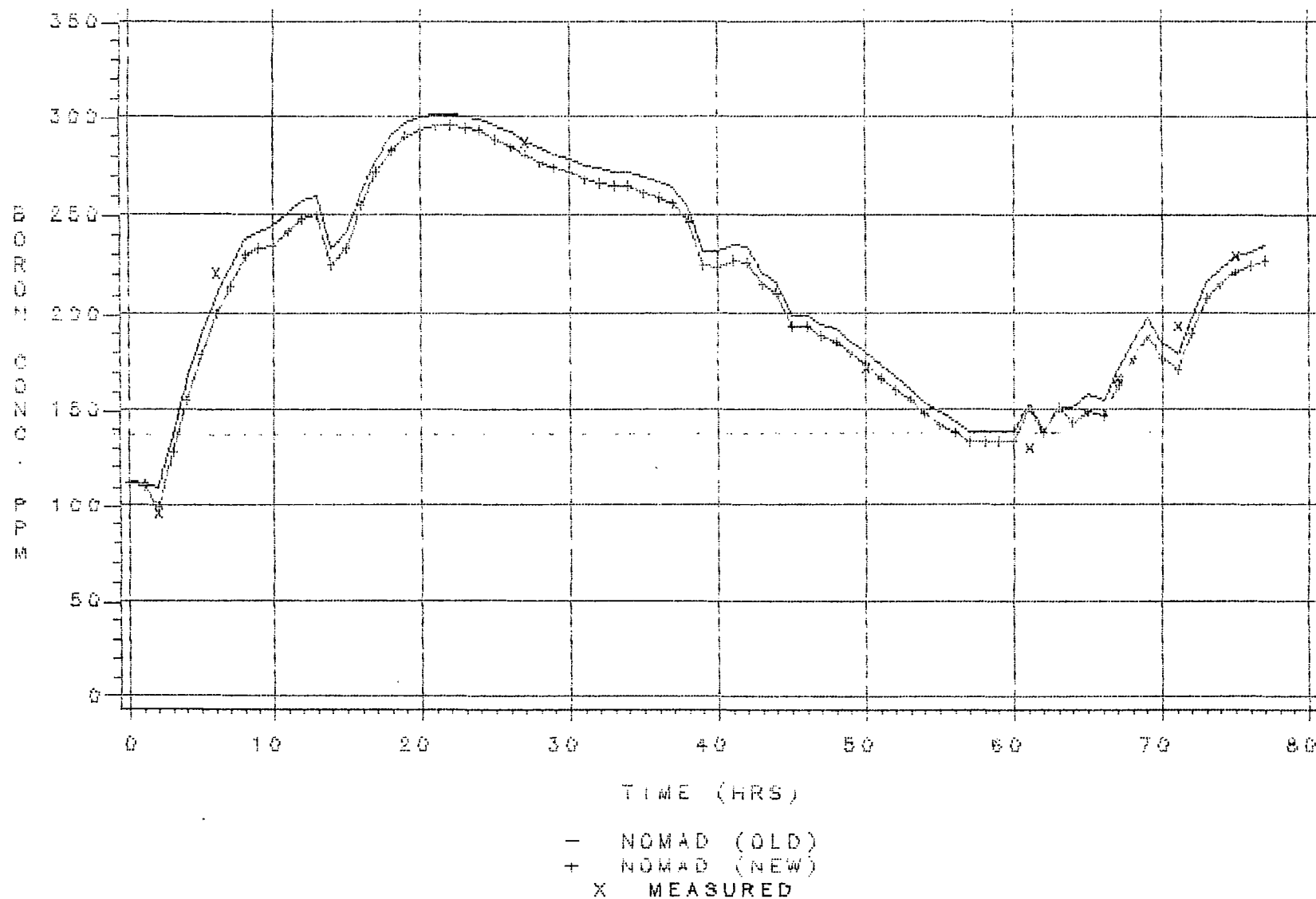


FIGURE 6.5

N1C3 SHUTDOWN/RETURN TO POWER (CASE 2) AXIAL OFFSET

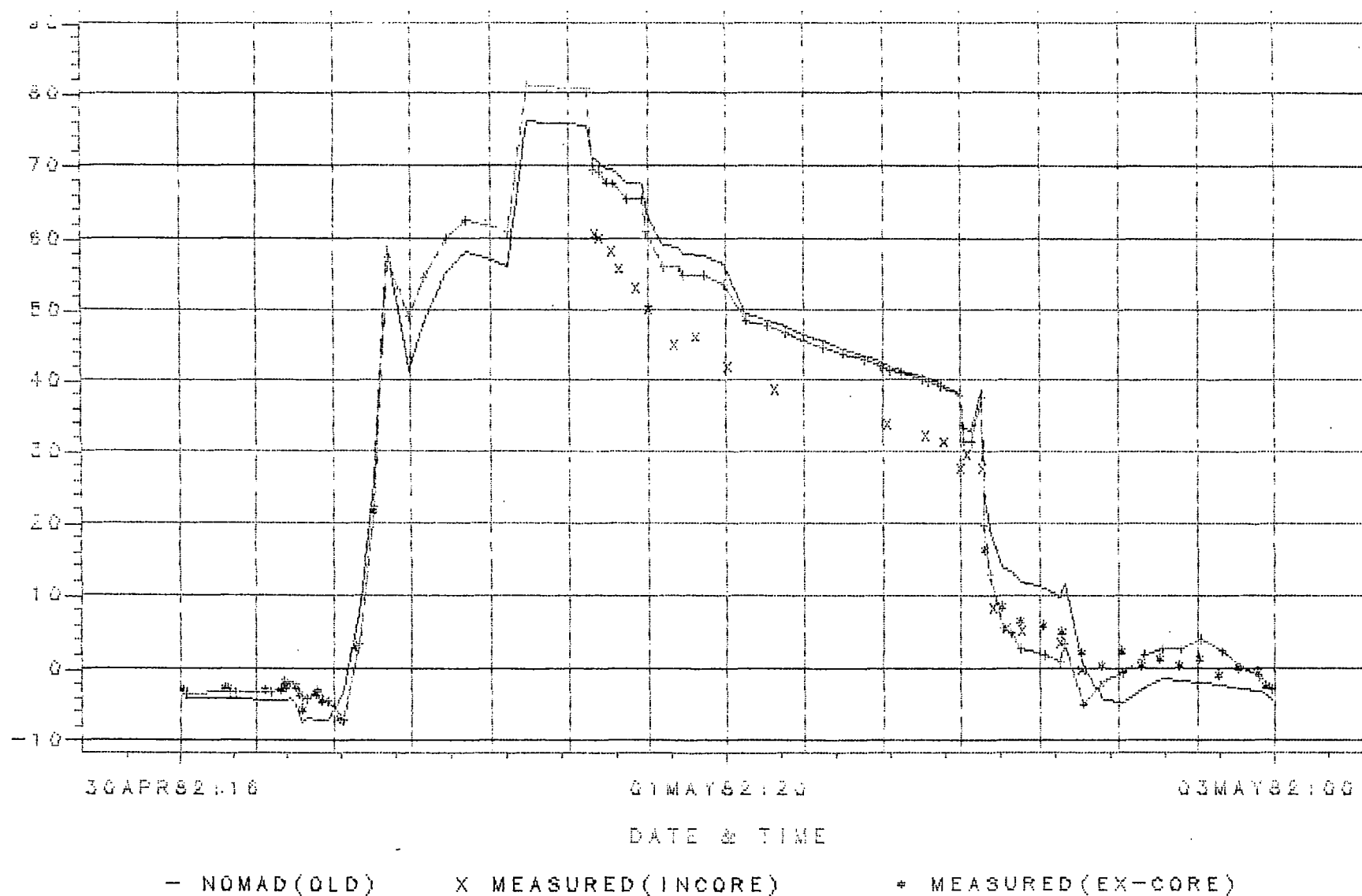


FIGURE 6.6

N103 SHUTDOWN/RETURN TO POWER (CASE 2) CRITICAL BORON CONCENTRATION

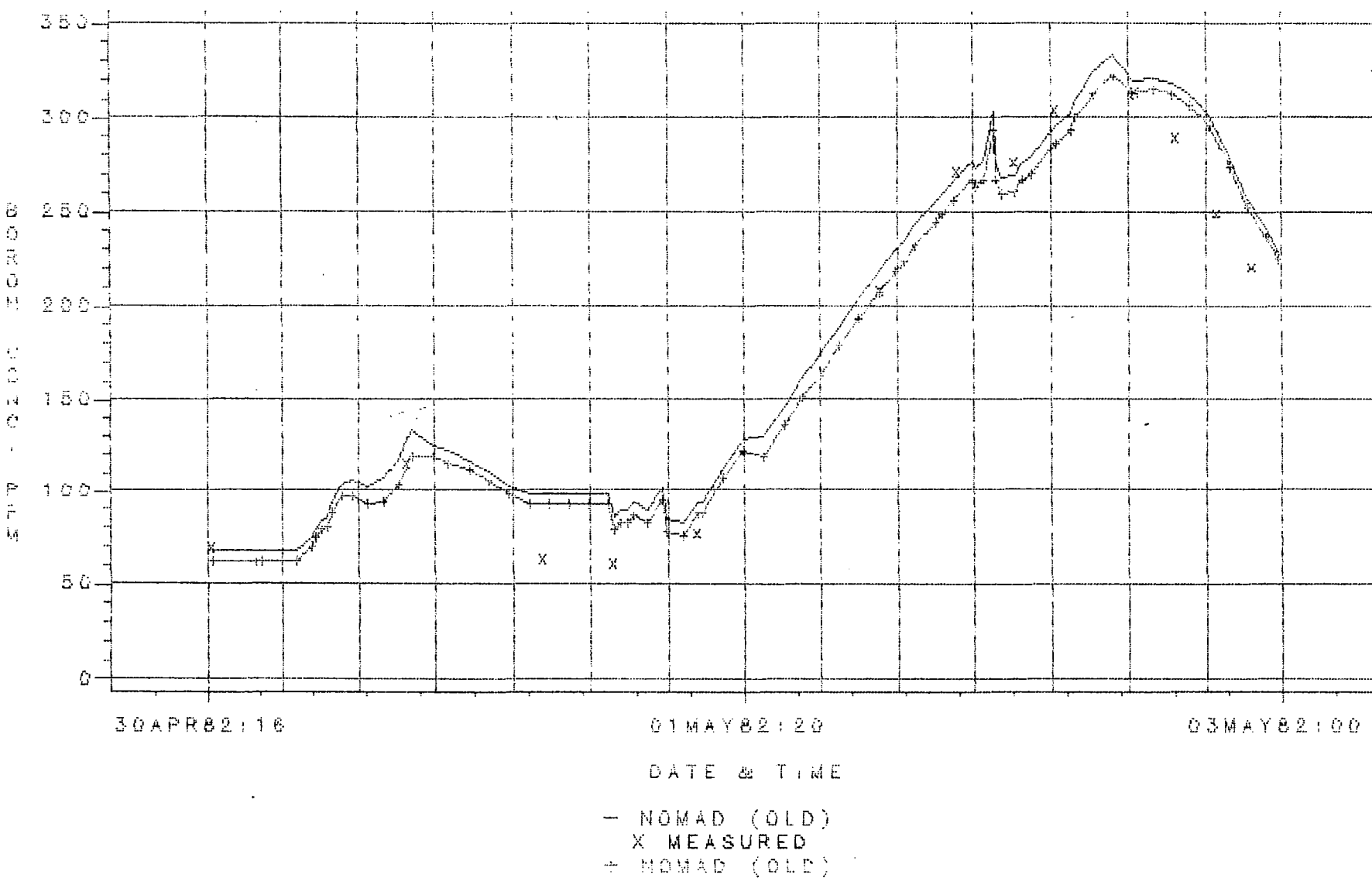


FIGURE 6.7

AXIAL POWER COMPARISON N1C3 5,000 MWD/MTU

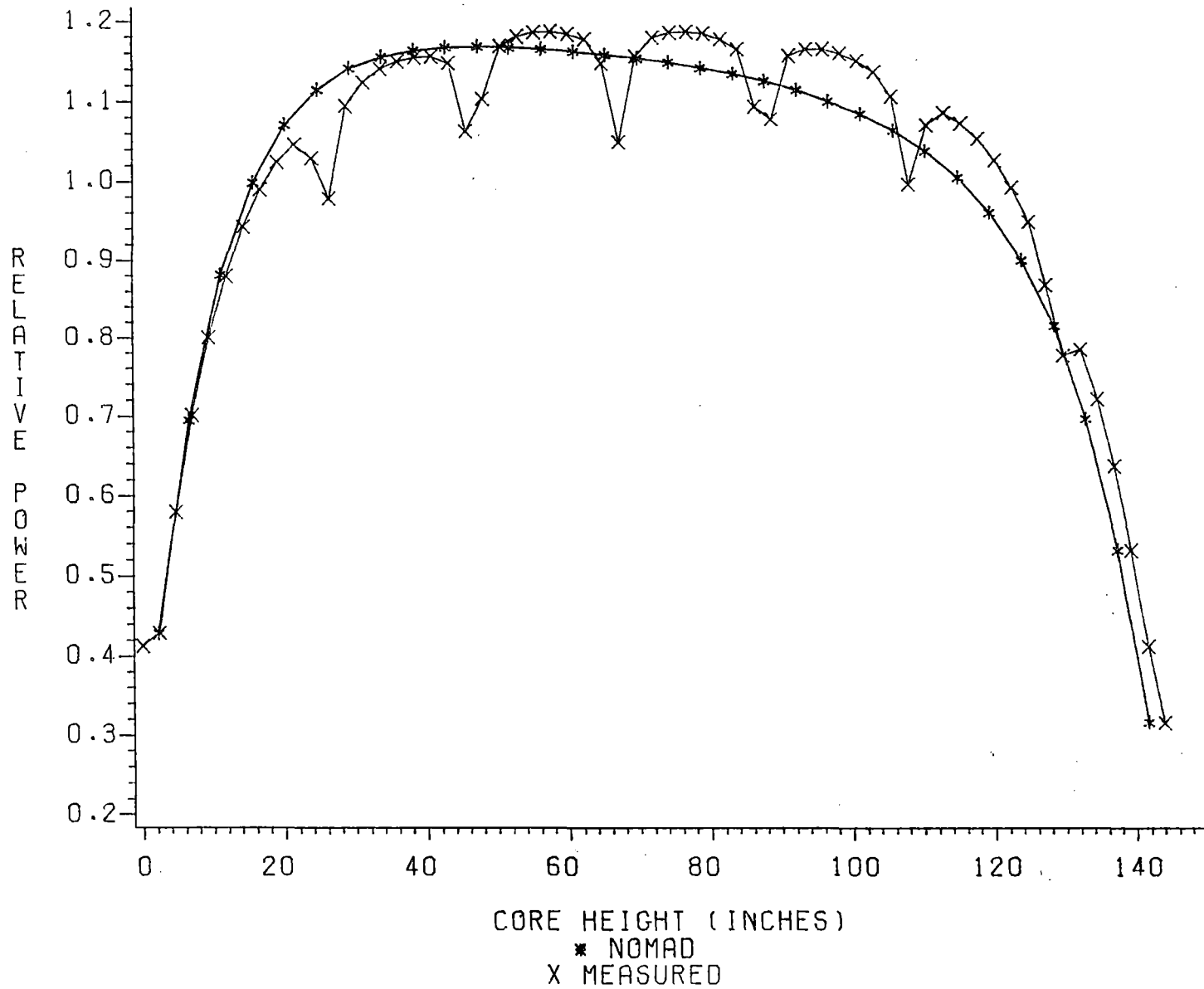


FIGURE 9.1

AXIAL POWER COMPARISON N1C3 11,000 MWD/MTU

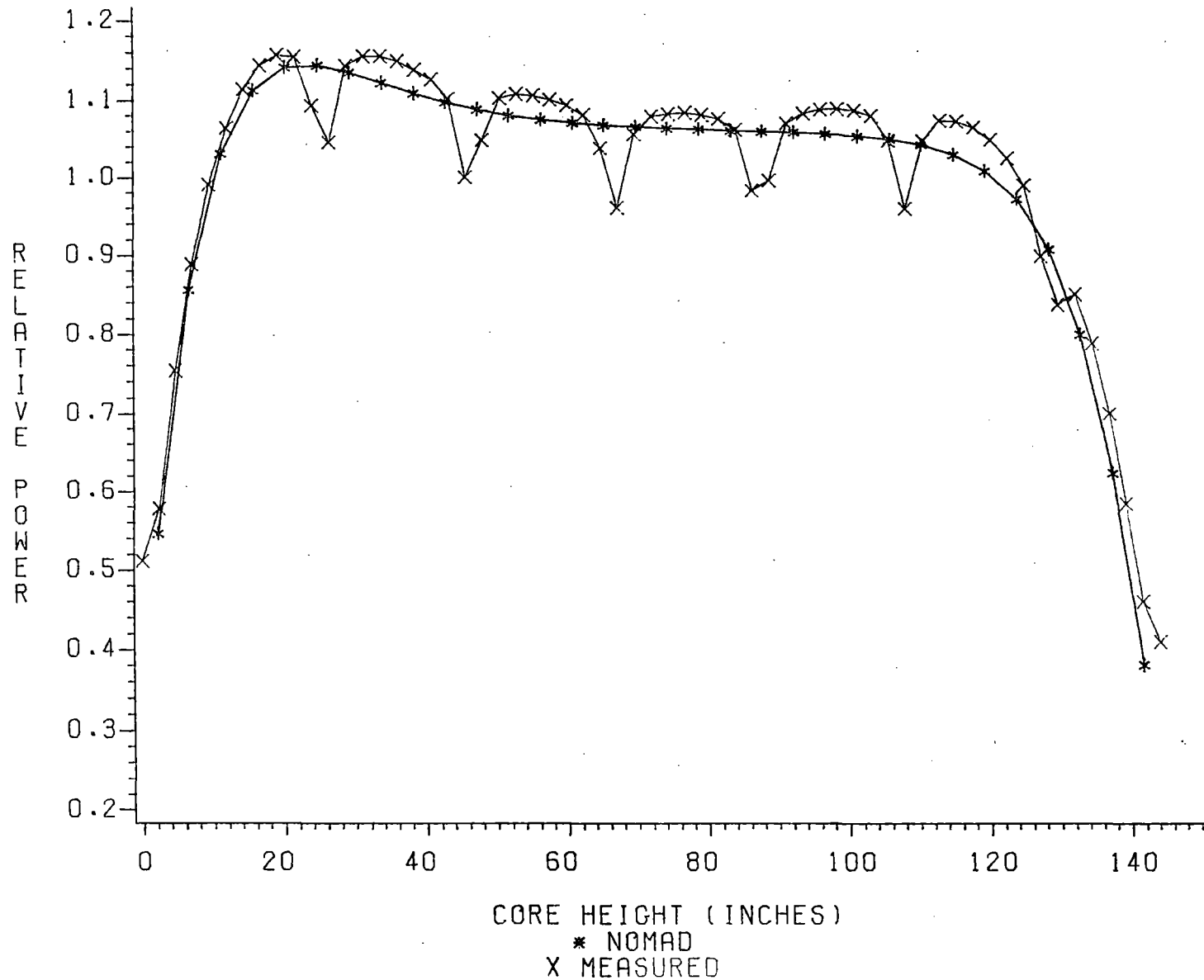


FIGURE 9.2

AXIAL POWER COMPARISON N1C4 4,000 MWD/MTU

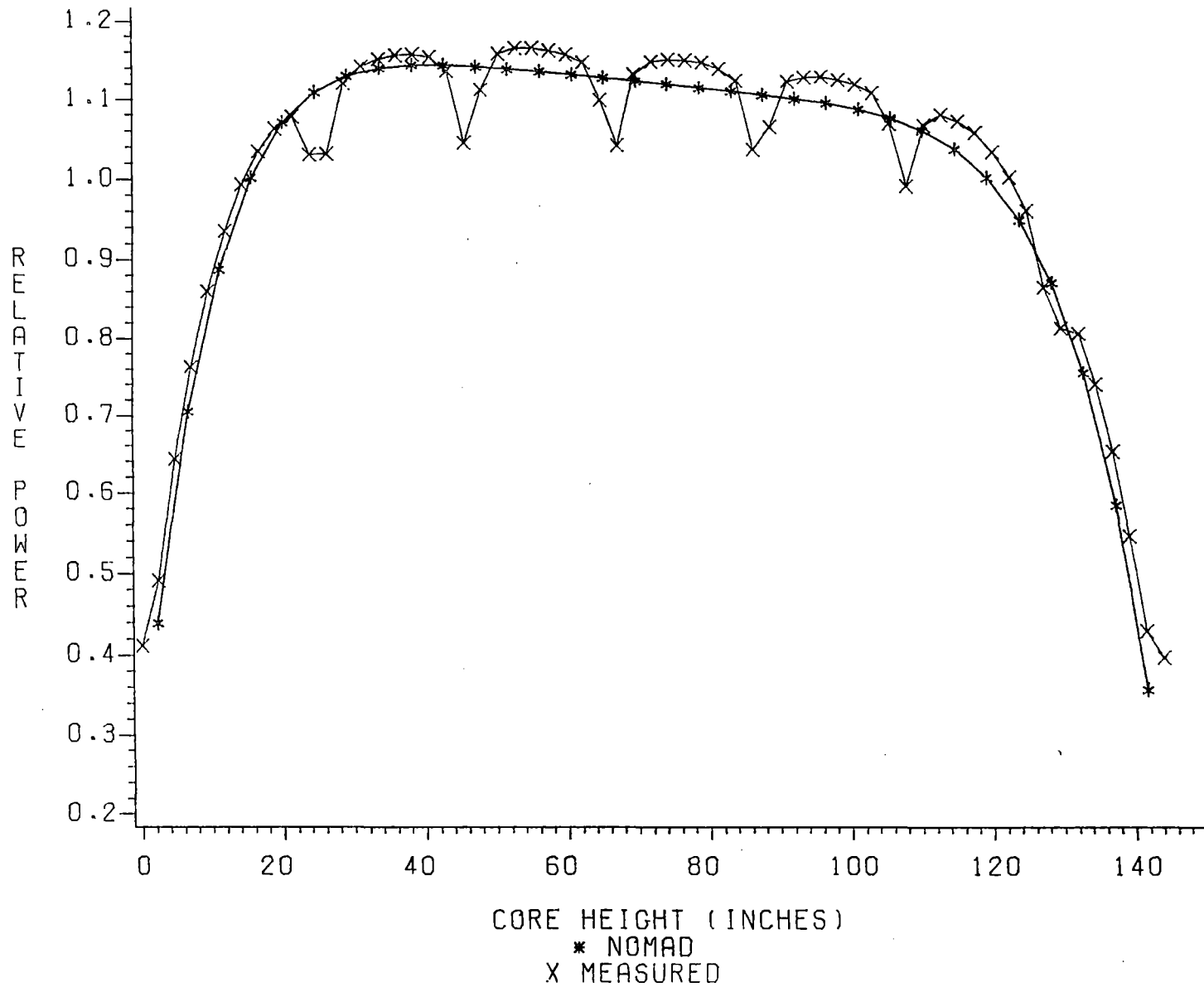


FIGURE 9.3

AXIAL POWER COMPARISON N1C4 9,000 MWD/MTU

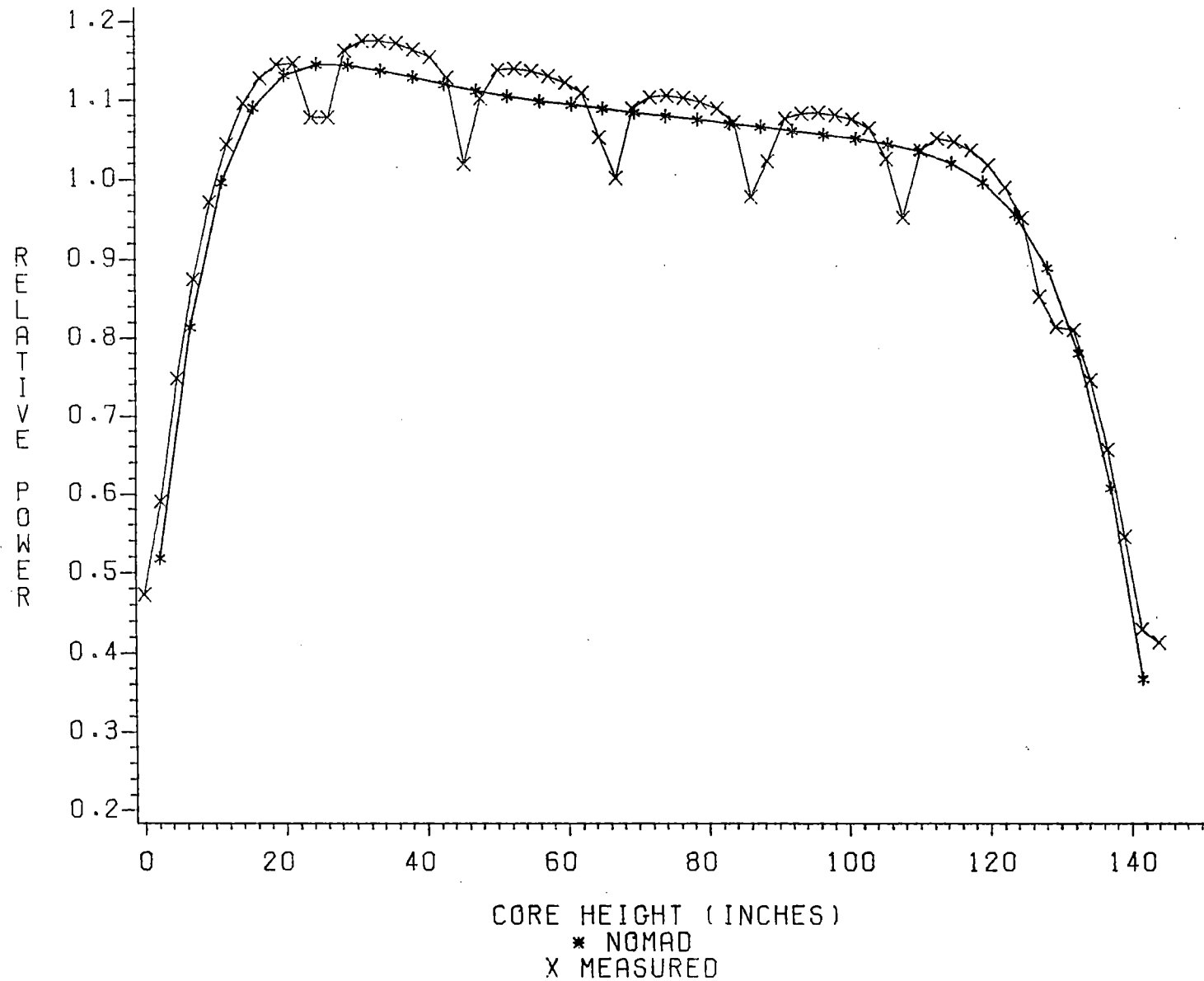


FIGURE 9.4

AXIAL POWER COMPARISON N2C2 4,000 MWD/MTU

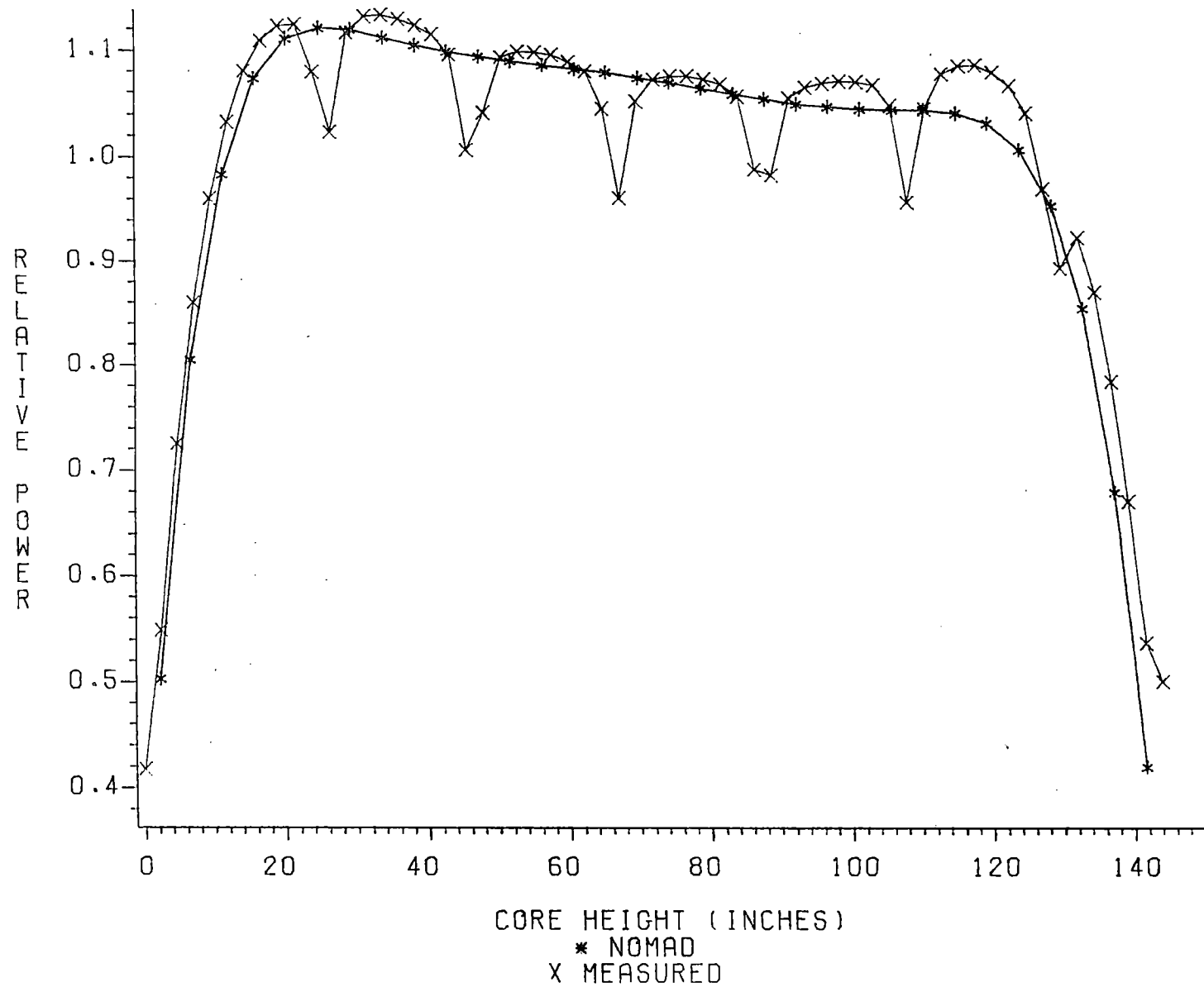


FIGURE 9.5

AXIAL POWER COMPARISON N2C2 8,000 MWD/MTU

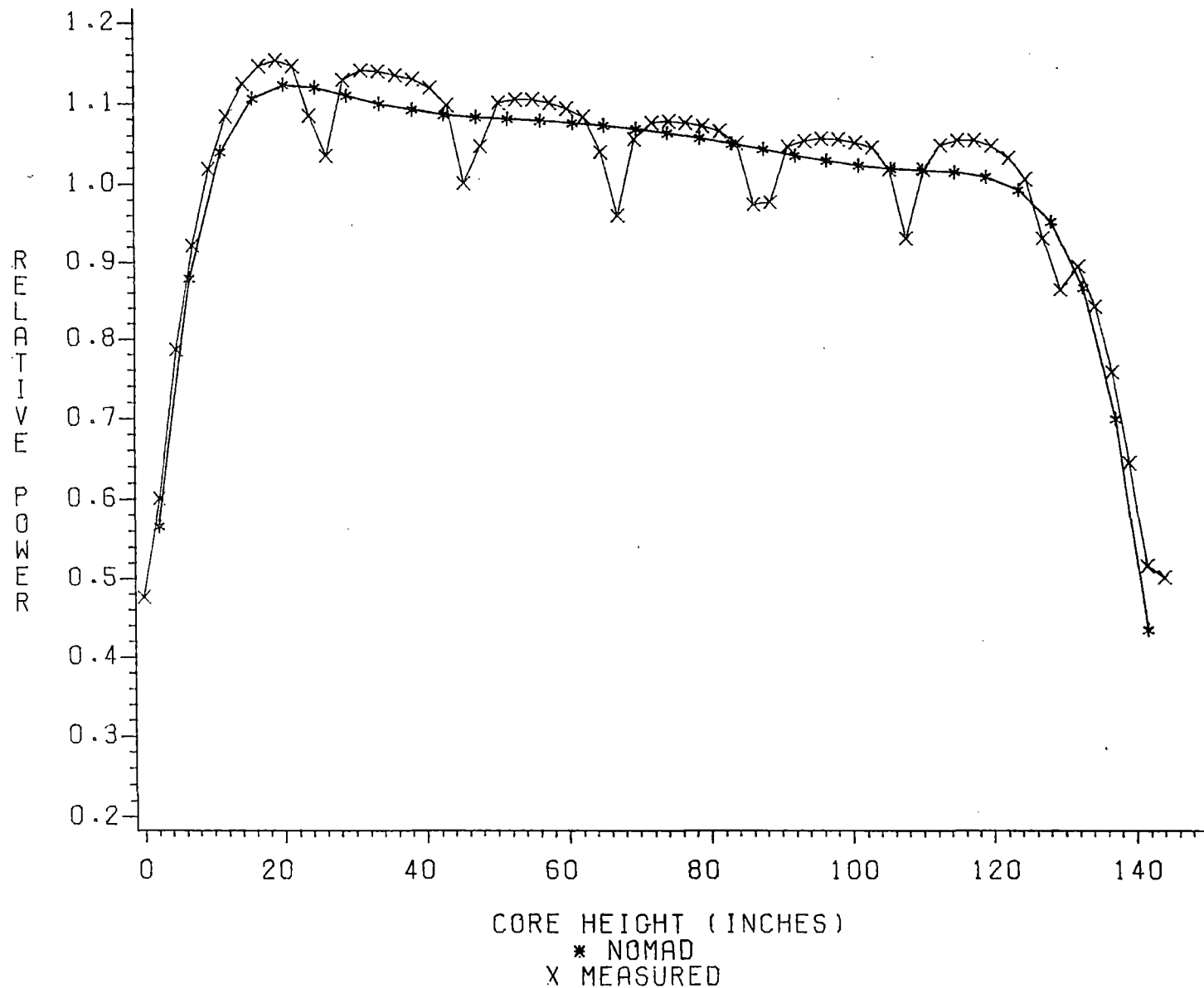


FIGURE 9.6

EOC AXIAL BURNUP COMPARISON N1C3 13,000 MWD/MTU

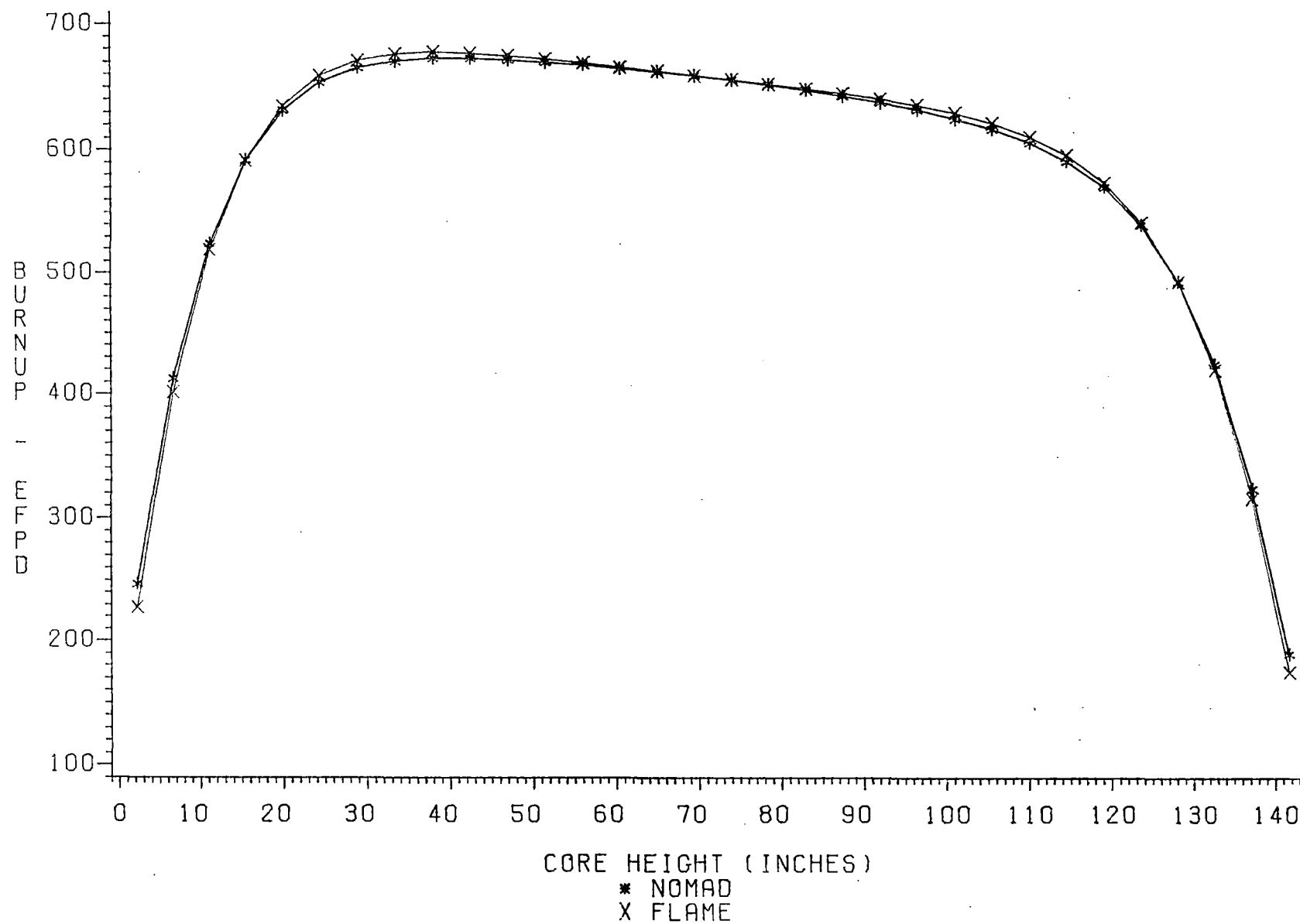


FIGURE 9.7

EOC AXIAL BURNUP COMPARISON N2C2 10,800 MWD/MTU

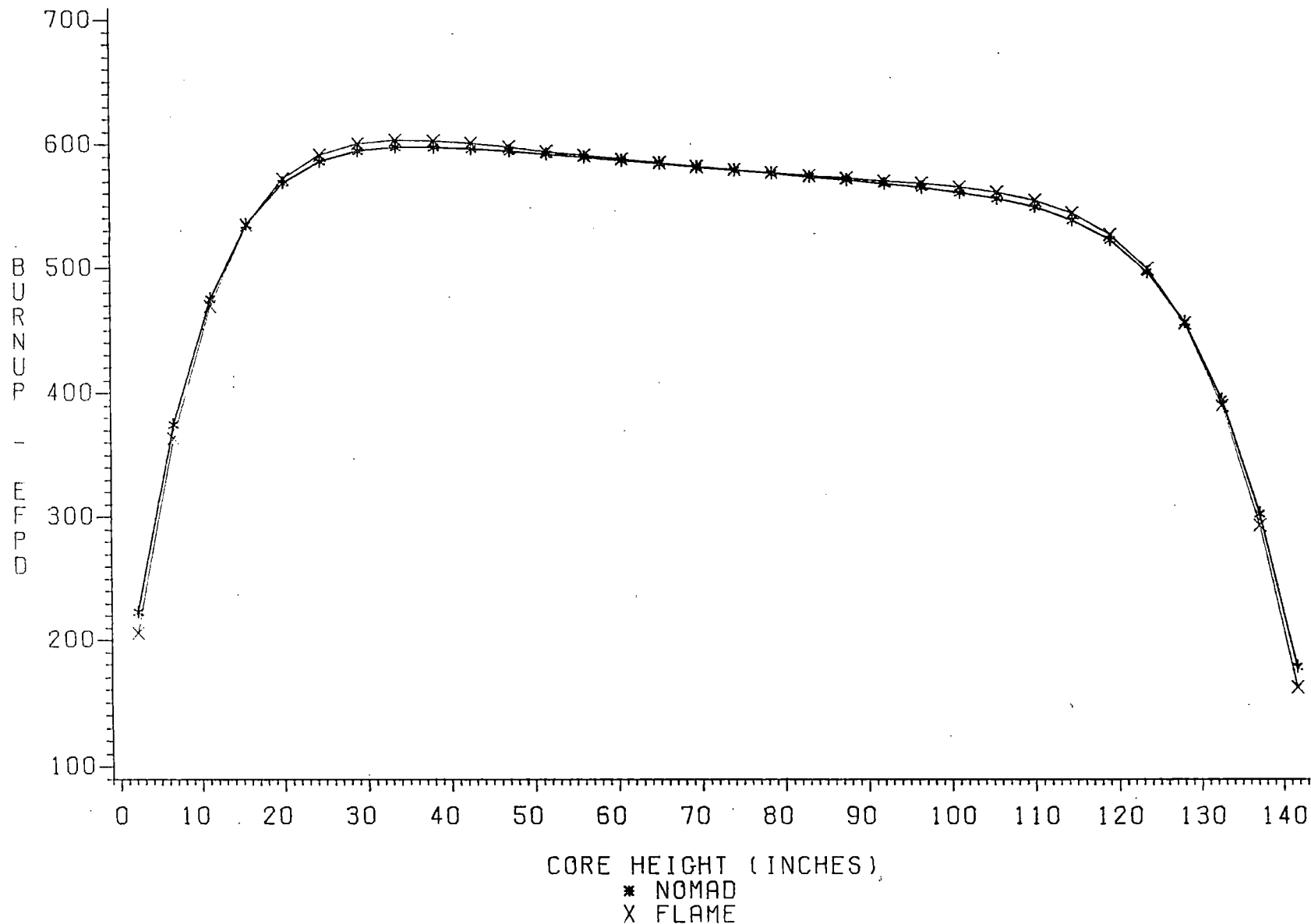
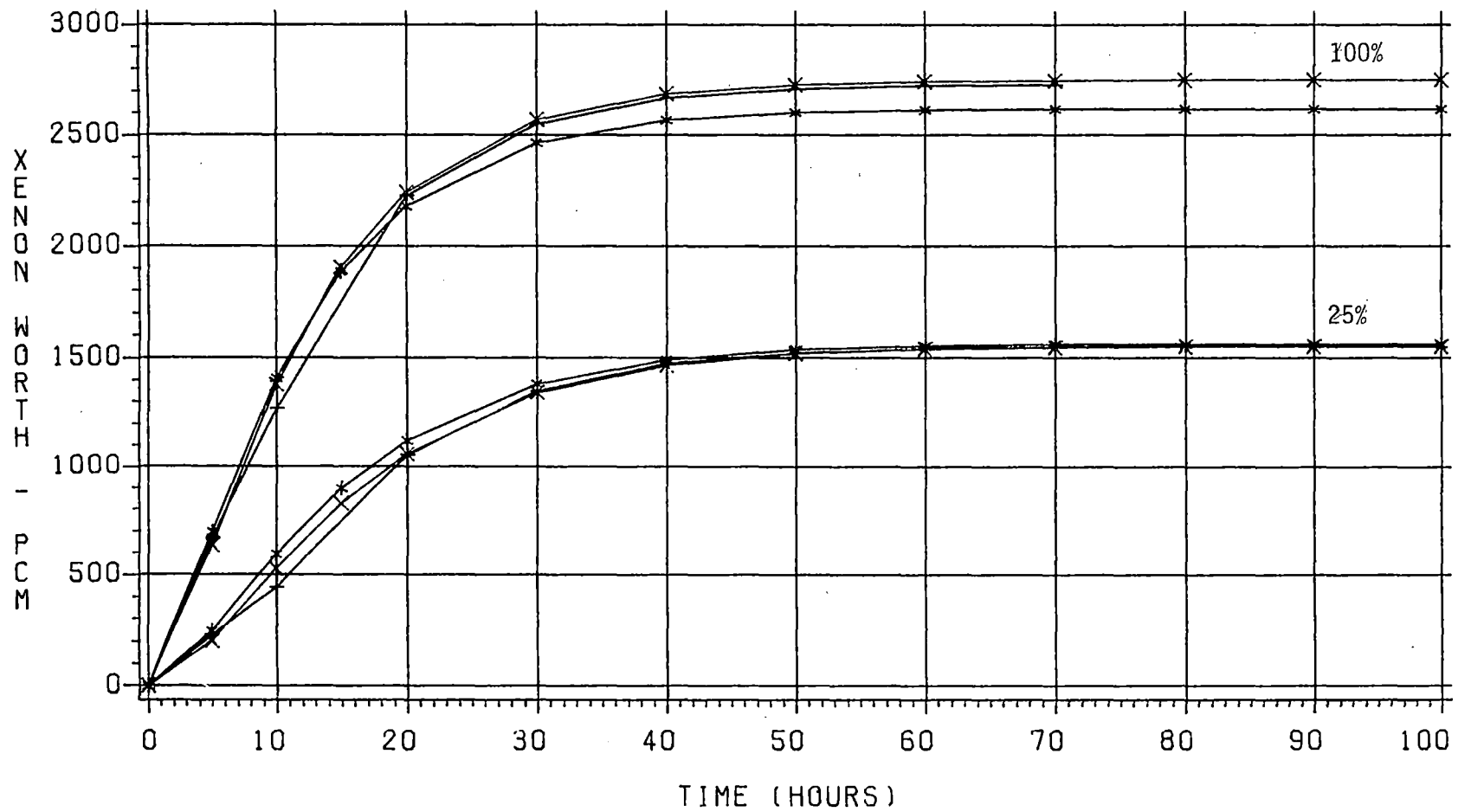


FIGURE 9.8

XENON WORTH AFTER STARTUP

NORTH ANNA UNIT 1 CYCLE 3



* NOMAD
X XETRAN
+ PDQ

FIGURE 10.1

XENON WORTH AFTER TRIP

NORTH ANNA UNIT 1 CYCLE 3

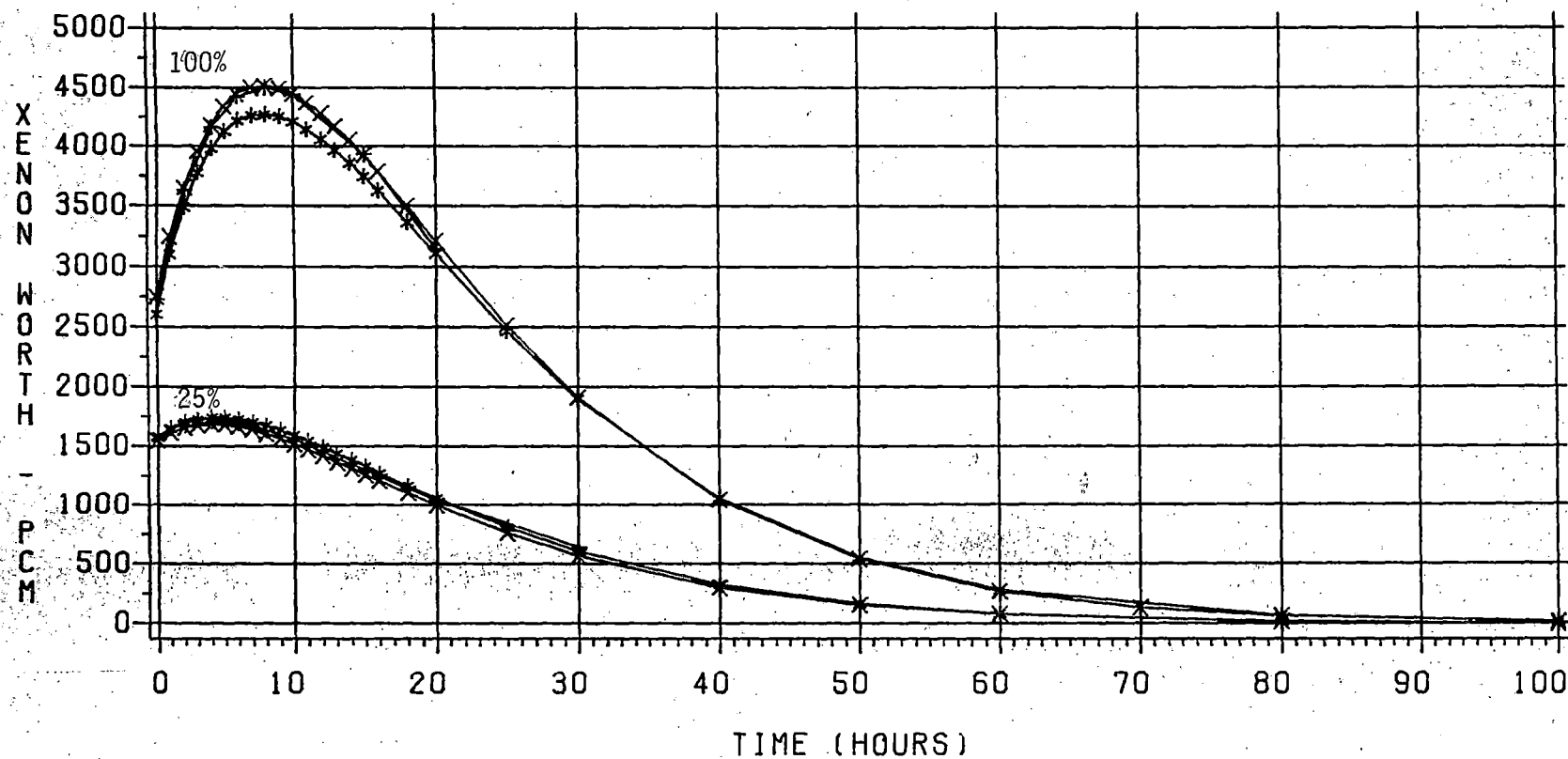


FIGURE 10.2

* NOMAD
X XETRAN
+ PDQ

XENON CONC. AFTER STARTUP

NORTH ANNA UNIT 1 CYCLE 3

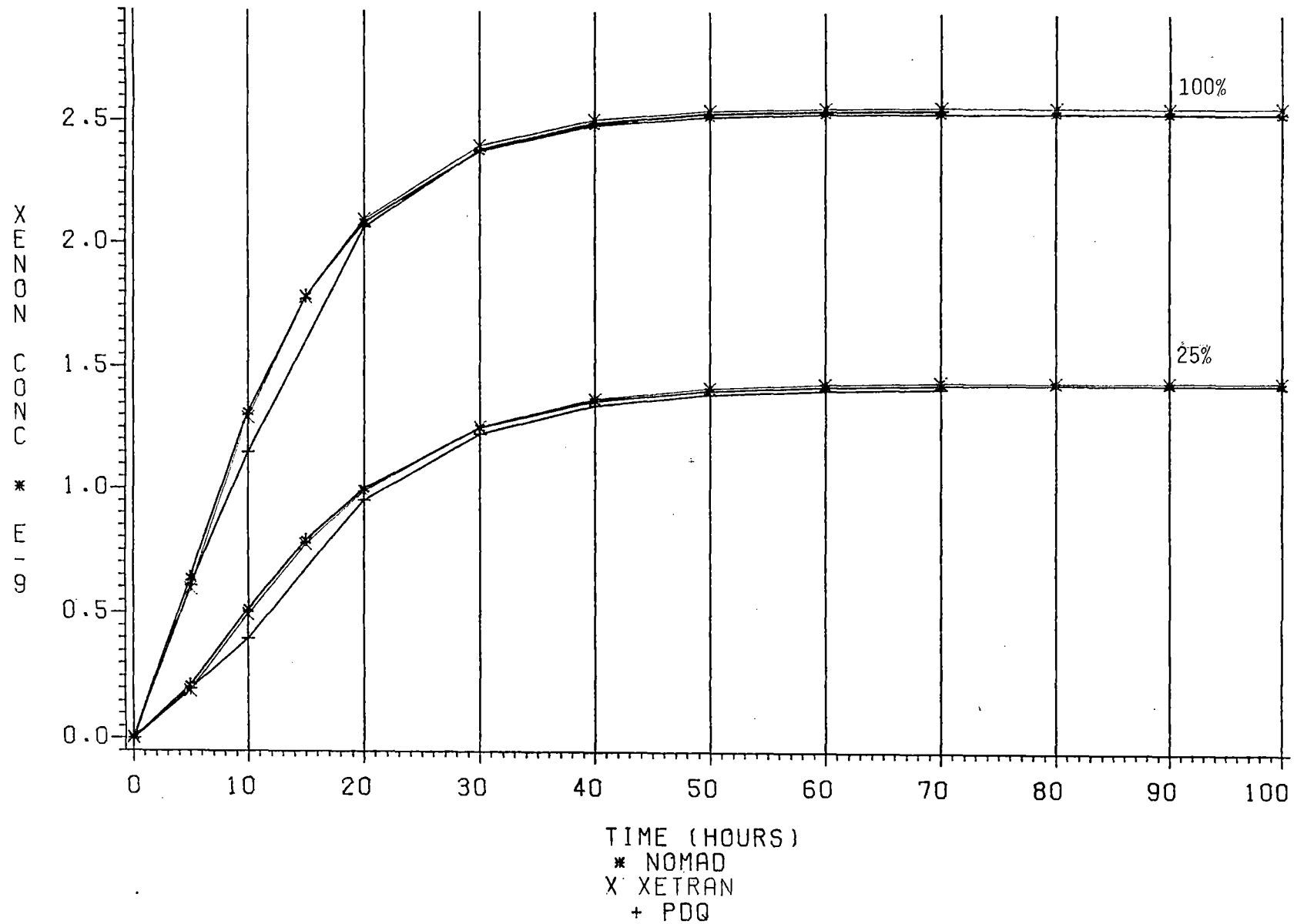
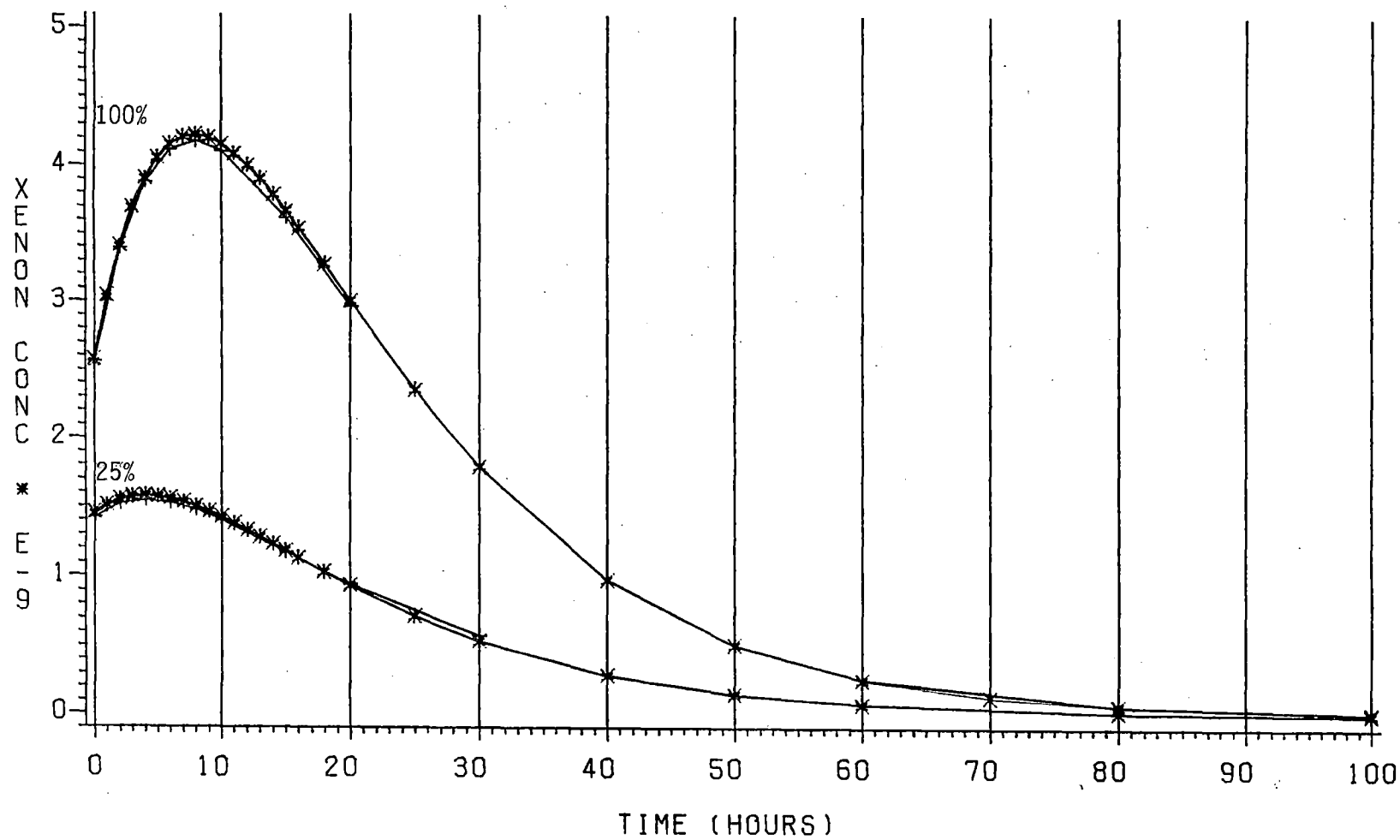


FIGURE 10.3

XENON CONC. AFTER TRIP

NORTH ANNA UNIT 1 CYCLE 3



* NOMAD
X XETRAN
+ PDQ

FIGURE 10.4

ATTACHMENT

ATTACHMENT 2
PROPOSED TEXT CHANGES TO THE NOMAD TOPICAL REPORT

1. VEPCO proposes to add a subsection to SECTION 2 entitled, "Control Rod Model". This subsection would contain the quoted material in Response to Question No. 2 contained in Attachment 1.
2. VEPCO proposes to modify the phrase following the equation in the middle of page 2-5 to read: "where M is a tridiagonal matrix."
3. VEPCO proposes to modify Equation 2.5-3 on page 2-12 as follows:

$$\begin{aligned} CZ(Z) &= \cos (BMID * PI * (Z - ZO) / HT) && \text{if } BMID > 0.05 \\ &= 1./(\cos(BMID * PI * (Z - ZO)/HT)) && \text{if } BMID < -0.05 \\ &= 1.0 && \text{otherwise} \quad (2.5-3) \end{aligned}$$

In addition, VEPCO would add the following paragraph to the end of Section 2.5:

"NOMAD automatically adjusts the buckling coefficients at power levels below 100% power to compensate for changes in the radial buckling as a function of core power. Since the dependence of the cross sections on moderator temperature are derived from a two-dimensional model, this adjustment is necessary to obtain consistent agreement between NOMAD and a three-dimensional model, where the moderator temperature varies in the axial direction."

4. VEPCO proposes to modify the first full paragraph on page 3-4 of

the Topical Report to read as follows:

"The variables upon which each macroscopic cross section have been found to be dependent are listed in Table 3-1. The XSFIT code analyzes the PDQ07 macroscopic cross sections and generates base macroscopic cross sections and polynomial coefficients which express these cross sections in terms of these variables:

$$\text{SIGt} = \text{SIGtbase} + (\text{IV1} * \text{COEFt1} + \dots + \text{IVx} * \text{COEFtx})$$

where

SIGt = macroscopic cross section type t for certain set of
independent variables

SIGtbase = base macroscopic cross section type t

IVx = value of independent variable x

COEFtx = coefficient for SIGt versus independent variable x
= delta SIGt/ delta IVx.

It then compares the PDQ07 cross sections to those calculated with the polynomial coefficients to verify the accuracy of the coefficients."

In addition, VEPCO proposes to correct Table 3-1 to show that NuSigf2 is also a function of xenon.

5. VEPCO proposes to delete Section 3.6 from the Topical Report.
6. VEPCO proposes to modify the description of the variable IWRITE(5) on page 4-2:

"Axial power sharing edit and flux squared edit (must =1 for 1-D/2-D synthesis)".

VEPCO also proposes to modify the comments on the power sharing edit and the flux squared edit on page 4-11 to read as follows:

"The axial power sharing edit gives the fraction of the axial power which exists in each axial segment with a different rodged configuration. This edit is necessary to perform 1-D/2-D synthesis. The flux squared sharing edit gives the fraction of the fast group flux squared which exists in each axial segment with a different rodged configuration. This edit is an importance weighting function which may be used in performing rod swap worth calculations."

Finally, VEPCO proposes to modify the first sentence of the third paragraph on page 5-3:

"Integral control rod bank worths were calculated for banks measured by rod swap using an importance weighting technique."

7. VEPCO proposes to delete the last two paragraphs of Section 5.6, table 5-8, and the final column of Tables 5-5 through 5-7.
8. VEPCO proposes to modify Section 5.7 as follows:

"Standard three case and eighteen case FAC (CAOC) analyses were performed with the VEPCO NOMAD model for North Anna 1 Cycle 4 and North Anna 2 Cycle 2. The VEPCO NOMAD model results were found to be consistent with the reload analysis results from an accepted and

verified vendor model which has been used in the design and licensing of the Surry and North Anna reactors. Both models indicated minor technical specification violations near the core bottom in the three case analyses and no violations in the eighteen case analyses."

"Figures 5-39 through 5-42 show the NOMAD results for the eighteen case analyses. The FQ(Z) plots in Figures 5-40 and 5-42 contain the radial xenon re-distribution factor and an uncertainty factor of 10.9%, which includes the engineering hot channel factor, the measurement uncertainty factor, and the grid correction factor."